UCLouvain

École polytechnique de Louvain

Influence of the mechanical properties of gelled culture media on the behavior of *S. epidermidis* bacteria

Author: **Julie GEORTAY**
Supervisors: **Karine GLINEL, Alain JONAS**
Readers: **David ALSTEENS, Louise DUPONT**
Academic year 2021–2022
Master [120] in Biomedical Engineering

Abstract

In recent years, the microbial population residing on the human skin has attracted a great deal of interest in the scientific community. Indeed, this organ, serving as barrier between the inner part of the host organism and its environment, hosts a myriad of microorganisms to form a rich niche, referred to as the "skin microbiota". Amongst resident skin bacteria, *Staphylococcus epidermis* (*S. epidermidis*) is one of the most prevalent microbes of this environment. Despite the fact that this bacterium was initially extensively studied for its opportunistic pathogenicity, which represents a challenge for patients exhibiting weak immune defenses, especially in the hospital sector, many benefits have been associated to its ubiquitous presence on human skin. Among others, *S. epidermidis* possesses an antimicrobial action against *Cutibacterium acnes* overgrowth from which acne vulgaris is believed to originate. To enjoy *S. epidermidis* beneficial action to its full potential in novel therapeutic solutions, encapsulation is mandatory to protect the user against the possible adverse effects related to this microbe. In this view, the design of a patch containing wells where *S. epidermidis* would be confined has been considered. In this context, optimization of the gelled growth medium used in the wells is necessary to support the growth and viability of the bacteria as well as to promote as much as possible their beneficial behavior.

With this aim, different agarose gels were prepared, aiming to cover a wide range of mechanical properties by means of concentration variation or agarose gel strength variation. In the first instance, the prepared gels were mechanically characterized either using shear dynamic mechanical analysis or rheology depending on the gel characteristics. The storage and loss moduli as well as the damping factor were measured during amplitude and frequency sweep tests and the steady viscosity was determined. An increase in either concentration or gel strength is shown to increase the moduli and the viscosity while the damping factor is globally the same in steady regime for all gels.

In the second instance, these gels were used as culture media for *S. epidermidis*, which was embedded in these matrices. The growth was assessed by measuring the fluorescence intensity related to fluorophore expression by the considered strain. The growth mode was observed by means of epifluorescence and confocal microscopy while the metabolic activity was tested using an alamarBlue assay test. An increase in either agarose concentration or gel strength was suggested to decrease the growth rate as well as to promote the transition to aggregate growth mode. The reduction of alamarBlue seems to be slowed down by an increase in agarose gel strength, which could or not be related to the metabolic activity of the bacterial population. However, no clear influence of the concentration was observed on the metabolic activity.

Since an increase in agarose concentration or gel strength causes an enhancement of the viscoelastic properties of the gel, the stiffer or more viscous the gel, the slower the growth and the more aggregates are favored over planktonic cells. Nevertheless, the change of viscoelastic properties does not seem to influence the metabolic activity of the bacteria. These results thus suggest that the mechanical properties of gelled media may be optimized to control bacterial growth, without significantly impacting metabolic activity, which offers an interesting possibility for the making of bacterial patches displaying long term activity.

Acknowlegements

First and foremost, I would like to express my deepest gratitude to my supervisors: Prof. Karine Glinel and Prof. Alain Jonas; who offered my the opportunity to be part of this fascinating project. I especially thank them for the time they dedicated to me and the valuable guidance they provided me throughout the project. Their help, incentive and wise advice helped greatly to complete this master thesis.

Then, I would like to express my most profound gratitude to a person without whom this endeavor would not have been possible: Louise Dupont. I would like to acknowledge her particularly for the planning of the work, for the pleasant work environment in which she allowed me to evolve as well as for her support all along the writing of this thesis. It was a real pleasure to work with her on the project and I wish her the best of success for the continuation of her PhD on the latter. Her accompaniment allowed me to gain confidence in my abilities and to discover a particular interest in research, and I cannot thank her enough for that.

I would also like to extend my sincere thanks to the experts that guided me throughout the realization of this work. They were all four competent, friendly, pedagogues and always ready to help me out. In particular, I thank Naïma Sallem for the training and help provided for rheological measurements, as well as Pascal Van Velthem for the training and help to perform DMA tests. I also acknowledge Marie-Christine Eloy for the confocal microscopy. Finally, I express my gratitude to Evelyne Van Ruymbeke for the help provided with the rheological measurements and the advices regarding the analysis of the results obtained from the latter. Their expertise allowed me to achieve a quality work that met my expectations.

Last but not least, I would like to express my further gratitude to my relatives. To my friends who supported me throughout this journey by accompanying me during my work moments, by showing me their support in the most difficult times and by sharing quality time with me to allow me to be in the best conditions to close this chapter of my life in the most beautiful way, by being proud of myself. Finally, special thanks go to my parents, Claire and Patrick, and my brother, Lucas, who have always supported me in my projects by offering me their time, by listening to me and reassuring me for so many years. Words cannot express how grateful I am for their unconditional support, patience and love.

List of Tables

List of Figures

List of Abbreviations

Aap: Accumulation-associated proteins

AB: AlamarBlue

AFM: Atomic Force Microscopy

AMP: Antimicrobial peptide

AS: Amplitude sweep

Bap: Biofilm-associated protein

Bhp: Homolog biofilm-associated protein

BSL1: Biosafety level 1

CCD: Charge coupled device

CLSM: Confocal laser scanning microscopy

CTC: 5-Cyano-2,3-ditolyl tetrazolium chloride

DEAE: Diethylaminoethyl

DMA: Dynamic Mechanical Analysis

DRI: Device related infection

ECM: Extracellular matrix

EEO: Electroendosmosis

EPS: Extracellular polymeric substances

FS: Frequency sweep

GFP: Green Fluorescent Protein

HEMA: Hydroxyethylmehacrylate

ICU: Intensive care unit

LED: Light-emitting diode

LVER: Linear Viscoelastic Region

NA: Nutrient Agar

NMR: Nuclear Magnetic Resonance

OD: Optical Density

ODRI: Orthopedic device related infection

PEG: Polyethylene glycol

PEGDA: Poly(ethylene glycol) diacrylate

PGA: Poly-γ-glutamic acid

PIA: Polysaccharide intercellular adhesin

PNAG: Poly-N-acetyl-glucosamine

PNIPAAM: Poly(N-isopropylacrylamide)

PSM: Phenol-soluble modulin

SEM: Scanning Electron Microscopy

TSA: Triptic Soy Agar

TSB: Triptic Soy Broth

TTS: Time-temperature superposition

Contents

Introduction

1 Context

In recent years, the symbiotic relationship that exists between microbes and the host that they colonize attracted a great deal of interest. The benefits as well as the adverse effects they can have on humans are indeed very broad and fascinating. More specifically, the interactions between some microbes colonizing the human skin, referred to as the human skin microbiota, are of great interest. Indeed, bacteria but also fungi, viruses and yeasts reside on the skin and live in a symbiotic way with their host as long as the homeostasis is maintained. However, once this balance is disturbed, so called dysbiosis can take place and cause skin diseases, such as rosacea, psoriasis but also acne vulgaris.[1–7]

Amongst the large number of bacteria residing on the human skin, *Staphylococcus epidermidis* (*S. epidermidis*) is one of the most prevalent microorganisms. It contributes to many benefits for the skin, whether it is to fight against pathogenic colonization or to maintain the balance between the skin commensals by interactions with other symbiotic bacteria. For instance, *S. epidermidis* has proved to regulate the overgrowth of *Cutibacterium acnes*, which is believed to be the cause for acne vulgaris pathogenesis.[8] Despite its pathogenic potential for special patient populations, *S. epidermidis* is thus studied as part of the development of novel therapeutic options to cure diseases such as acne vulgaris.[8–10] Its encapsulation in a patch for the skin as been proposed with this idea in mind. The patch currently developed in our laboratory is composed of a silicone support that is designed with cavities to serve as containers for the bacteria and the medium in which the latter grow. On top of the support, a semi-permeable barrier is grafted to allow for the diffusion of the metabolites of interest produced by the bacterial strain while preventing *S. epidermidis* escape. Two different barriers are considered: a polycarbonate membrane and a polyacrylamide-agarose hydrogel layer. As the medium should stay in place in the patch wells, the use of gelled medium is appropriate to prevent the nutrient-rich material containing the microorganisms to flow out of the construct. Encapsulation in the patch is critical on two aspects: it would on the one hand prevent any possible infection related to *S. epidermidis*, which is a well-known opportunistic pathogen in particular conditions, and it would on the other hand allow to get a better control on the growth kinetics of the bacteria, their viability as well as their metabolic activity.

Apart from the encapsulation method, other parameters are critical to ensure the good functioning of the above mentioned technology. In particular, it is well-known that the medium in which bacteria grow is tremendously im-

portant to optimize their growth, viability as well as their metabolic activity and gene expression. More specifically, the mechanical properties of hydrogel media have proved to impact the bacteria behavior, namely their viability, growth kinetics, growth mode and metabolic activity, in many ways for different combination of bacterium and polymers.[11–13]

2 Objective and strategy

In that regard, the optimization of the mechanical properties of the culture gelled medium used to grow bacteria is investigated in this work. In order to tune the mechanical properties of the agarose gelled media, two distinct parameters were played on: agarose concentration and agarose gel strength, using different agarose types which differed greatly in terms of gel strength. Agarose is a biocompatible and porous hydrogel that is inert to bacterial enzymatic degradation. Moreover, it keeps its gelled structure in the temperature range required for bacterial cell culture and, thanks to its high swelling capacity, allows for hydration maintenance of the microorganisms it hosts. In this view, its use is indicated to obtain appropriate gelled culture media.[11, 14] Aiming to elucidate the link between the medium viscoelastic properties and *S. epidermidis* behavior, we proceeded in two distinct steps. First, the mechanical properties of various agarose hydrogels used to culture bacteria were mechanically characterized using either rheology or dynamic mechanical analysis. Second, bacterial parameters were investigated in the prepared gels by different means to quantify growth and metabolic activity as well as to determine the growth mode of the microbe. Ultimately the results of both of those parts were merged to possibly establish the relationship between the mechanical properties of a gelled medium and the bacterial growth in this environment.

3 Report structure

The first chapter of this master thesis deals with a bibliographic study of skin microbiota with a particular focus on the bacterium used in this project: *S. epidermidis*. Moreover, an overview of the hydrogels, and more specifically agarose is proposed, as well as a state of the art on how bacteria behave in such hydrated polymer networks. Finally, the parameters used to characterize bacterial behavior and the way they are investigated are detailed.

In the second chapter, the global objective and strategy used to fulfill the latter are introduced in details.

In the third chapter, the mechanical characterization of the agarose gels is presented, beginning with objective and strategy used to this aim, followed by the protocols established to prepare the gels and measure their viscoelastic properties. Then the results obtained are introduced and a conclusion on this chapter ends this part of the report.

In the fourth chapter, the bacterial behavior in various agarose gels is investigated. First, the objective and strategy of this chapter are detailed. Second, the protocols to culture the bacteria, quantify their growth, observe their behavior in the gels and their metabolic activity are discussed. Third, the results obtained are presented, beginning with the influence of the agarose concentration on the investigated parameters and followed by the influence of the agarose type, namely its gel strength. Finally, the chapter ends up with a conclusion on the achieved results and deductions.

In the fifth chapter, the results of the two previous chapters are merged to establish the possible influence of

the mechanical properties of the gel media on *S. epidermidis*.

In the last chapter, improvements as well as prospects for future work are suggested to develop this topic further in the near future.

CHAPTER 1

State of the art

The objective of the first section of this chapter is to provide a description of the human skin microbiota, ranging from the organisms that compose it, its diversity and the influencing factors, to the symbiotic relationship it shows with its host as well as the problems that could emerge from microbiota imbalance. In the second section, a focus on one of the most prevalent skin microbiota bacterium, namely *S. epidermidis*, is provided to overview the benefits and drawbacks it can represent to the host as well as the reasons why it presents a challenge for the medical field. In the third section, hydrogels are discussed, first in a general way, then with a particular focus on their mechanical, i.e. viscoelastic, properties and the way they can be characterized. In the fourth section, a particular focus on the hydrogel used in this project is proposed, namely agarose, its origin, its structural characteristics, especially on the molecular and supramolecular scale, the way these structures are established as well as factors influencing the properties of this polymer. In the fifth section, a focus on bacterial growth in hydrogels is proposed, focusing on biofilm models as well as the impact the hydrogel properties can have on microbial behavior. Finally, the last section deals with the bacterial parameters that are used to characterize microorganism behavior and the techniques used to quantify them.

1 Skin microbiota

In recent years, the symbiotic relationship that exists between microbes and the host that they colonize attracted a great deal of interest. When referring to the human microbiota, one tends to think of the microbe population residing in the gut at first. However, not only the gut hosts an abounding number of microorganisms, but also other external organs, especially the human skin. A minor part of the human microbiota colonizes other epithelial surfaces such as the oral and vaginal mucosa as well as the respiratory tracts, comprising the upper and lower airways. The microorganisms composing the human microbiota can be as various as viruses, yeasts, fungi but the majority are bacteria. This wide range of living or dead microbes interact with each other. The trillions of microorganisms hosted by the human body outnumber human cells by a factor of 10 and the human genes by a factor of 100.[1–3]

The skin is the largest organ of the human body. This 2 m^2 large epithelial surface indeed represents 16%

of the total body weight. It serves as a physical barrier between the body itself and the environment, enabling to protect the inner part of the host organism from ambient conditions but also from harmful exposure from the environment, such as penetration of unfavorable substances like toxins but also microorganisms, thus serving as first line of defense against infections.[1, 3–5]
This organ hosts a myriad of different organisms that are able to overcome many challenges such as temperature shifts and moisture. The relative scarcity of microbes on the skin is due to the fact that the skin is a relatively unfavorable environment for them to grow. In addition to the previously mentioned conditions, the low pH of skin, the fact that it lacks nutrients but also the high levels of salts and antimicrobial molecules and the exposure to other external factors induce the relative low diversity of microbes on the skin.[1, 6]
The skin microbiota population can be divided in two distinct groups defined as the commensal and the transient residents. Commensal microbes play a role in the maintenance of a balanced skin homeostasis which enables the skin to stay in a healthy state while other bacteria only transiently reside on the skin, causing infection, which leads them to be considered as pathogenic microbes.[7] However, despite the fact that commensals do not usually infect healthy hosts, it is worth noting that some of them can switch to a pathogenic behavior in particular environmental conditions. These microbes are so-called opportunistic pathogens and are mostly inducing infections in hospitals for immunocompromised patients as well as sick patients presenting diseases that could favor subsequent infection.[15]

The human skin sites can either be sebaceous, moist or dry. All sites share the same microorganisms at the species level : *Cutibacterium*, *Corynebacterium* as well as *Staphylococcus* in terms of bacteria, *Malassezia* in terms of fungi are present on the whole skin surface, in different amount depending on the site nature and the individual hosting the niche. However, the species are distributed differently depending on the considered site. The skin microbiota is relatively stable over time for a given individual and its dynamics is site-specific: sebaceous as well as moist sites are very stable in terms of composition over time while dry skin sites exhibit more variability. It is challenging to define a core skin microbiota since inter- as well as intra-individual differences exist. These variations are due to various factors.[3, 6]
The most important factor influencing human microbiota variability seems to be the topography, due to specific skin-site characteristics such as pH, moisture, temperature or expression of antimicrobial peptides. Considering a particular skin site for different individuals, it exists less differences as it does when considering two different skin sites for a single individual: the inter-individual differences are less prevalent than intra-individual differences.[3]
However, not only topographical variability but also temporal variability - especially for dry sites -, host specific factors such as age, gender, ethnicity or genetics as well as environmental factors play a role in the population spectrum observed on human skin.[3]

The relationship between the microbes and their host is symbiotic. Indeed, the host provides a living habitat, nutrients and shelter to the microorganisms whereas the latter essentially contribute to the host metabolism, allow to maintain a balanced skin homeostasis, regulate inflammation and contribute to host immunity. The skin microbiota plays a major role in the immunity of the human host as it participates to the education of the innate immune system. Before birth, the infant is not yet colonized by those organisms. Depending on the delivery mode, the skin will acquire microorganisms: if the baby is vaginally born, it will acquire an initial population that is similar to the vagina flora of its mother while the primary microbiota of a baby born by caesarean section will be similar to the one of the stomach skin. This primary microbiota is relatively low in diversity. During early life, the microbiota develops and diversifies to become a proper microbiota through skin colonization when entering in contact with a microorganism.

Then its composition is surprisingly stable which brings to light the existence of a stable and mutually beneficial interaction between the symbiotic microorganisms and their host. A restructuring of the skin microbe species however takes place at the puberty. The encountered commensal microbes allow the host immune system to develop a tolerance to those resident bacteria, regulating the immune response and inflammation that could be caused by the presence of non-self cells. Apart from its educational role of the immune system, the microbial population also provides a protection against pathogens and breaks down natural products.[1, 4, 5, 7]

Thanks to novel technologies in terms of genetic sequencing, the scientific community can now have a more global look at the composition of the microbiota compared to the past, where we could only identify strains that were able to be cultured in a lab, which gave rise to a bias for years. Thanks to ribosome RNA sequencing and metagenomics shotgun, a direct identification of the microbes in a particular sample that was taken on the skin of a recipient is now possible. Unfortunately it cannot discriminate between live and dead organisms.[1, 4]

However, when the microbiota is unbalanced, it results in changes in terms of abundance and diversity of the commensal species. This condition is defined as dysbiosis and can lead to diseases that can either be skin or systemic diseases. Several exogenous and endogenous factors can lead to dysbiosis: infection, injury resulting in the breaking of the skin physical barrier or antimicrobial resistance but also host genetics and other environmental factors. This condition gives rise to the innate immune response and thus can be the origin of inflammatory skin diseases like atopic dermatitis, acne vulgaris, psoriasis or rosacea.[3, 6, 7]

2 *Staphylococcus epidermidis*

S. epidermidis is a facultative anaerobic Gram-positive *Staphylococcus*, belonging to the Micrococcaceae family. It is part of the group of coagulase-negative staphylococci, which are distinguished from coagulase-positive staphylococci such as *Staphylococcus aureus* (*S. aureus*) by their lack of coagulase enzyme. It is one of the most abundant skin colonizers, being one of the five significant organisms that are located on human skin and mucosal surfaces. It is thus a permanent member of the healthy human skin microbiota, predominant in moist skin sites such as armpits and nares but also present in sebaceous areas such as facial skin.[9, 16–18]
Thanks to its specific surface adhesins that enable it to anchor on the moieties of the tissue surface of the host, *S. epidermidis* establishes a lifelong commensal relationship with its host, beginning in early life. [17] However, *S. epidermidis* is a so-called opportunistic pathogen: usually, it has a symbiotic relationship with its host but in particular conditions, it can switch to a pathogenic behavior causing nosocomial infections.[9, 19]

2.1 Symbiotic relationship and benefits for the host

The symbiotic relationship with *S. epidermidis* provides many benefits to the human host. It helps with nutrition, enables to maintain homeostasis and provides a protection against pathogens in different ways. Different effects can be found depending on the *S. epidermidis* strain considered.[10, 17, 19]

Firstly, the bacterium is able to activate particular innate immune pathways in order for keratinocytes to produce antimicrobial peptides (AMPs) to a larger extent to kill pathogenic bacteria such as *S. aureus*. Secondly, *S. epidermidis* produces phenol-soluble modulins (PSMs) which are small α-helical peptides. PSMs are acting synergistically with host-derived AMPs in order to increase the killing capacity. They are believed to play a role in

inter-microorganism competition: PSM-δ and PSM-γ, naturally produced by *S. epidermidis*, have proved to provoke membrane leakage in pathogens such as *Streptococcus pyogenes* (*S. pyogenes*) and *S. aureus*. Thirdly, in addition to PSMs, many *S. epidermidis* strains secrete bacteriocins that act against other strains or species. Finally, the bacteria is believed to produce other factors that hinder the colonization capacity and/or the viability of *S. aureus* as well as to degrade *S. aureus* biofilms.
To sum up, all these secreted molecules aim to reach a same goal: fight against pathogenic colonization and further infection. [10, 17, 19]
Furthermore, *S. epidermidis* releases butyric acid, which allows differentiation of adipose-derived stem cells into adipocytes as well as lipid accumulation in the cytoplasm. This induces an increase in dermal thickness, providing an even better physical barrier for the host internal compartments.[10]
In addition, *S. epidermidis* plays a crucial role in the immune system education as well as in the way the host organism responds to external aggression from pathogens. *S. epidermidis* colonization in early life extensively contributes to the priming and development of the innate and adaptative defenses against more virulent pathogens. *S. epidermidis* also plays a regulation role for the immune system with which it is in constant crosstalk. It attenuates inflammatory responses in order to accelerate wound healing and modulates host innate immune response as part of the fight against pathogens.[10] Some strains also dampen the recruitment of neutrophils in the context of a *S. aureus* infection as well as the production of pro-inflammatory cytokines by the host cells, which potentially protects the organism against an aggravation of the infection due to extreme inflammation.[19]
Moreover, microbiota residents can interact with each other in order to maintain homeostasis. It is the case for *S. epidermidis* which has been shown to rein the overgrowth of another commensal bacterium *Cutibacterium acnes* (*C. acnes*), involved in the pathogenesis of acne vulgaris. Indeed, *S. epidermidis* possesses an antibacterial action against *C. acnes* through the release of succinic acid. It is one of the four short chain fatty acids that originate from the fermentation of glycerol by *S. epidermidis* in anaerobic conditions. These conditions are actually encountered in acne lesions where *C. acnes* overgrowth is facilitated. In addition to its antibacterial action to limit *C. acnes* overgrowth, succinic acid also dampens *C. acnes*-induced skin inflammation. That is to say that *S. epidermidis* aims to regulate skin homeostasis and suppress *C. acnes*-induced pathogenic inflammation.[8, 10, 17]

2.2 Opportunistic pathogenicity

As mentioned here above, *S. epidermidis* is an opportunistic pathogen. It indeed may adopt a pathogenic behavior in selected groups of patients such as immunocompromised patients and patients implanted with indwelling medical devices. The infection usually originates from the introduction of the bacteria from patient's or health care provider's skin during device insertion; it causes infections when breaching the skin surface and entering the bloodstream. It usually does not cause any infection in healthy populations.[9, 17]

Those *S. epidermidis*-induced infections are always device-related, following a surgical procedure, treatment or implantation of a medical device. Indeed, *S. epidermidis* strains exhibit a strong tendency to form biofilms on the surface of biomedical devices. When bacteria detach from the biofilms present on the surfaces of this device, they can cause so-called "bacteremia", which is the condition in which bacteria, in the case at hand *S. epidermidis*, are found in the bloodstream of the patient, possibly leading to sepsis or even death.[16]
In terms of device related infections (DRIs), *S. epidermidis* is a frequent cause of orthopedic DRIs (ODRIs) (for instance following prosthetic joints implantation), second only to *S. aureus*. It is believed that *S. epidermidis* causes as much as 20 to 30% of ODRIs, and even up to 50% when only considering late-developing ODRIs.[17] Vascular graft, central nervous shunt placement, cardiac devices implantation or other surgical interventions can also lead

to *S. epidermidis* infections. In particular, this *Staphylococcus* causes approximately 13% of prosthetic valve endocarditis infections leading in 38% of the cases to intracardiac abscesses and in 24% to mortality.[9] Following surgical interventions, other conditions such as mediastinitis, an inflammation of the space between the lungs, can take place due to *S. epidermidis* colonization at the surgical site.[18]
In addition, catheter use also leads to many *S. epidermidis* infections mainly in intensive care units (ICU) where the strains selected under pressure in the hospitalization conditions are often multi-resistant to antibiotics. *S. epidermidis* is indeed the major cause for central intravenous catheter infections: 22% of bloodstream infections in ICU are correlated to *S. epidermidis*.[9, 18]
Moreover, in neonatal ICU, invasive devices are also used to take care of the neonates which also leads to bacteremia and sepsis. As the immune system of those individuals is immature and their mucosal barriers are much more permeable than the ones of adults, their body fluids are readily accessed by *S. epidermidis* and other bacteria to cause nosocomial infections. As the strains show multi-resistance, it is very difficult to get rid of the infections which increases the hospitalization time and thus costs, but also the mortality in this particular population.[16]

S. epidermidis nosocomial infection therefore represents a huge challenge for the health care system. Its high prevalence is due to its ubiquitous presence on human skin and its ability to stick to tissues but also surfaces of implanted devices as well as to form biofilms.[9, 17] Unlike aggressive pathogen species such as *S. aureus*, *S. epidermidis* does not produce a large amount of enzymes and toxins. Only a paucity of virulence factors and toxin-associated genes are observed.[16, 17, 20] *S. epidermidis* is rather equipped with determinants that promote persistence over aggressiveness, the infections it induces are consequently subacute or chronic.[9] As infection is often indolent, it is difficult to detect and diagnose *S. epidermidis* infections. When collecting a blood or tissue sample from the patient and analyzing it to determine if the infection is due to *S. epidermidis*, it is more than probable that the presence of *S. epidermidis* could be due to contamination when sampling or analyzing, which makes it difficult to discriminate between a real infection or a sample contamination.[16, 18]

The pathogenesis of *S. epidermidis* mainly relies on the latter's ability to form thick multilayered biofilms on a broad variety of surfaces such as polymers, metals or host tissue. *S. epidermidis* also displays an ability to evade the host immune defenses.[9, 16, 17, 20] Moreover this microbe often is multi-resistant to antibiotics due to the selection pressure in the hospital environment or due to gene transfer between strains that enables it to acquire multiple resistance traits.[9, 16, 17, 20]

Many different molecules are secreted by various *S. epidermidis* strains and provide the microbe its virulence and subsequent pathogenicity. Biofilm formation is one of the main if not the main virulence factor of *S. epidermidis*. It is mediated by many molecules including for instance polysaccharide intercellular adhesin (PIA), also called poly-N-acetyl-glucosamine (PNAG), so-called biofilm-associated proteins (Bap) and their homolog protein (Bhp) as well as accumulation-associated proteins (Aap). Moreover, *S. epidermidis* exhibits an ability to evade from the host immune system thanks to the presence of biofilms and poly-γ-glutamic acid (PGA) which provide protection against phagocytosis but also thanks to inhibition of the host cells intervention as part of the immune response. In addition to this, an AMP sensing system enables the bacterium to detect AMPs and to up-regulate AMP-defensive mechanisms.
Notwithstanding, the virulence factors of *S. epidermidis* are not directly intended to pathogenicity. These factors actually have crucial roles in the commensal lifestyle of the bacterium. For instance, forming biofilm on skin is beneficial since it is an environment where a lot of mechanical stress is applied, PGA enables to live despite high

salt concentration and protection against AMPs makes sense in a commensal lifestyle. It can thus be considered as an *'accidental pathogen'*.[9, 16–18]

2.3 *S. epidermidis* as bacterial model

S. epidermidis is commonly used as a Gram-positive representative [11], probably for its culturing easiness and its availability due to its ubiquitous nature. Indeed, this microorganism is quite easy to culture using a large variety of commercially available media such as Triptic Soy Agar (TSA), Triptic Soy Broth (TSB) or Nutrient Agar (NA). The only additions it requires to a minimum culture medium are some amino acids, such as arginine, proline, isoleucine and valine, and a few vitamins, comprising nicotinic acid, pantothenic acids, biotin and thiamine. Accordingly, *S. epidermidis* can be considered as a not very demanding microorganism.[21]

More specifically, despite its opportunistic pathogenicity, *S. epidermidis* is of great interest in the field of probiotic therapeutics. Indeed, it is a relatively harmLess microbe for healthy human beings since it is categorized as biosafety level 1 (BSL1), which is the lowest possible level of this classification defining precautions to manipulate biological agents.[22]
Regarding its relative innocuousness, one could take advantage of the above mentioned beneficial effects to develop novel therapeutic approaches. For instance, *S. epidermidis* is already studied for the purpose of acne vulgaris treatment.[8] One could also imagine probiotics systems to fight against *S. aureus* or *S. pyogenes* colonization. These exciting possibilities to expand the biomedical field technologies are the major motives to study *S. epidermidis*.

3 Hydrogels

3.1 Overview

Hydrogels are defined as a class of polymeric three-dimensional (3D) networks formed by hydrophilic polymer chains that swell and do not dissolve in a water-rich environment. Indeed, these polymers are able to absorb water from 10% up to thousands of times their dry weight.[14, 23, 24]
The 3D structure of these hydrated polymer networks is achieved thanks to crosslinks between the chains which enable to form a matrix to hold the liquid together. In the absence of crosslinking points, the polymer chains would dissolve in water, since water is a good solvent for these polymer chains. Conversely, when crosslinking points are available, the solubility is counterbalanced by the entropic elasticity of the chains resulting from those crosslinks.
The swelling process is believed to occur in three steps. Firstly, the water molecules hydrate the more hydrophilic polar groups and the entrapped water at this stage is defined as *primary bound water*. Secondly, when the hydrophilic groups are hydrated, the network swells, exposing hydrophobic groups which in turn are hydrated, forming *secondary bound water*. Primary and secondary bound water are often considered as a whole and simply termed as *total bound water*. Thirdly, the osmotic pressure of water, which tends to force infinite dilution of the network, will lead to additional water absorption. However, the network elastic retraction force provided by crosslinked chain segments counterbalances the osmotic force: when expansion forces and contraction forces balance themselves, the hydrogel reaches an equilibrium swelling state.[14, 23]
The crosslinks can be of two types, either physical or chemical. On the one hand, chemically bound gels are gels in which crosslinks are covalent bonds that can be formed using different processes such as ultraviolet or high-energy irradiation, heating and various chemical reactions with crosslinkers including condensation reactions, radical polymerization reaction as well as click chemistry reactions.[14, 24] On the other hand, physically bound

gels are hydrogels in which the crosslinks are physical, i.e., they possess physical domains created by hydrogen bonding, hydrophobic interactions between the polymer chains, ionic complexation, physical entanglement of the chains and/or Van der Waals interactions.[14, 23–25] Some examples of crosslinks are schematically represented in Figure 1.1.

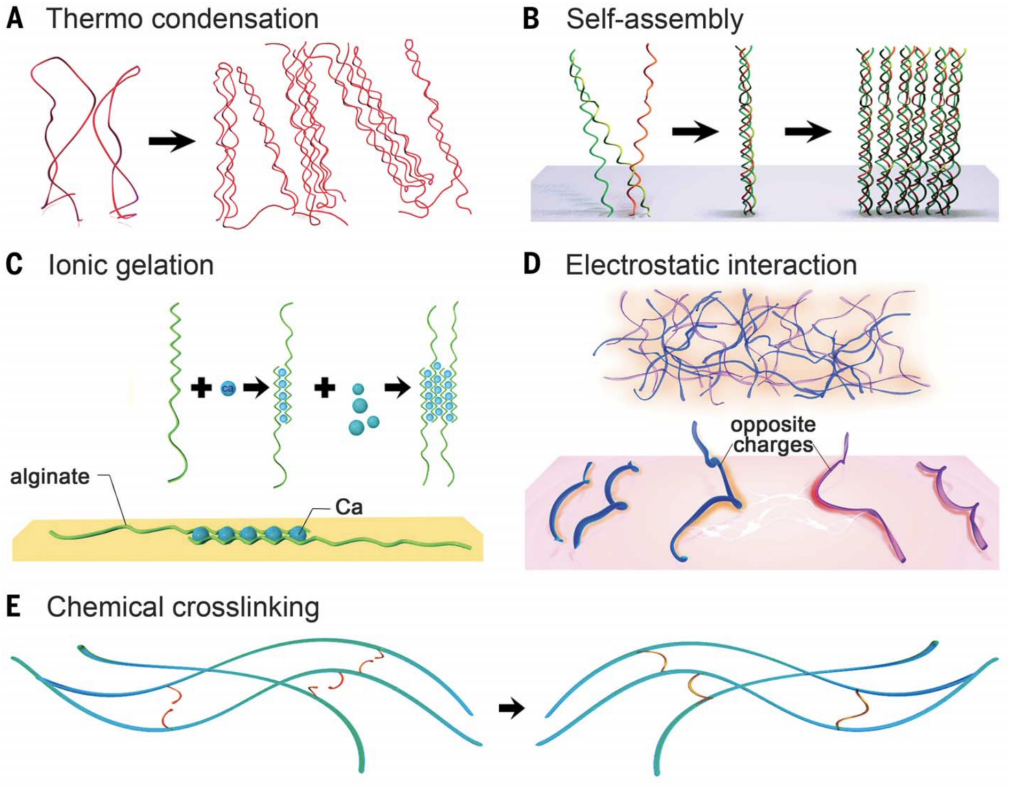

Figure 1.1: Cross-linking of hydrogels. (A to D) Physical cross-linking. (A) Thermally induced entanglement of polymer chains. (B) Molecular self-assembly. (C) Ionic gelation. (D) Electrostatic interaction. (E) Chemical cross-linking.[24]

Both chemical and physical crosslinks have their advantages and drawbacks. Indeed, chemically crosslinks better stabilize the hydrogel, improving flexibility and spatiotemporal precision in the crosslinking process in comparison to physical crosslinks.[24] However, physical crosslinked hydrogels allow solvent casting, post process bulk modification and are easier to produce and reshape. They can also be reversible contrary to chemically crosslinked polymers and often show no toxicity since no chemical crosslinking agents are necessary to obtain the 3D network, enhancing their biocompatibility. Although some physical crosslinks rely on the use of ions that can be toxic, physically crosslinked hydrogels are usually more biocompatible than most of the chemically crosslinked ones.[23] Nevertheless, physical crosslinking does not provide homogeneous networks since clusters are formed by the physical interaction domains.[14] Even though chemical crosslinks provide more control on the network structure, it is worth noting that some inhomogeneities are still present due to several non-idealities in gel formation which are mainly due to the distribution of reactive groups on the chains.[26]
Hence combining multiple components as well as crosslinking methods have attracted a great deal of interest to improve hydrogels properties further. The latter typically exhibit improved physicochemical properties: mechanical properties are enhanced, they can be injected and exhibit self-healing properties.[24]

In addition to the classification according to the nature of the crosslinks, one can also divide these materials on the basis of their origin that can either be natural or synthetic. Natural polymers can be as various as proteins, denatured proteins or polysaccharides.[27] A non-exhaustive summary of their advantages, drawbacks as well as examples of macromolecules is shown in Table 1.1. In relation to those characteristics, combining natural and synthetic hydrogels has been explored to optimize their properties. The classification thus extends to hybrid hydrogels and becomes more complex.[24, 27]

	Natural hydrogels	**Synthetic hydrogels**
Advantages	• biocompatibility; • biodegradability; • low toxicity; • physiologically-compatible structure.	• purity; • high absorption capacity; • well-defined microstructure; • well-defined functionality; • stability; • reproductibility; • tunable physicochemical and mechanical properties.
Drawbacks	• poor mechanical properties; • can provoke immune responses; • poor reproductibility; • batch-to-batch variability.	• toxicity due to crosslinking agents when chemically crosslinked; • lower biocompatibility.
Examples	• collagen; • gelatin; • agarose; • dextran; • starch; • glucan; • hyaluronic acid.	• poly(hydroxyethylmehacrylate) (PHEMA); • poly(ethyleneglycol) diacrylate; • poly(acrylamide); • poly(vinyl alcohol); • poly(N-isopropylacrylamide) (PNIPAAM).

Table 1.1: Comparison between hydrogels of natural and synthetic origins; advantages, drawbacks and examples.[14, 25, 28]

The mechanical properties of hydrogels vary according to several parameters, such as the crosslinking degree and/or the work temperature, and these materials can consequently be tuned to display properties that satisfy the needs in relation to their future purpose. For example, heating the material can increase or decrease its stiffness, depending on the nature of the polymer, whereas increasing its crosslinking degree results in greater stiffness. However not only these two but also a wide range of parameters play a role in the mechanical properties of hydrogels. Consequently, mechanical analysis has to be performed in order to define materials mechanical properties such as the storage and loss moduli, the damping factor and the viscosity. These can be evaluated by Dynamic Mechanical Analysis (DMA) devices or rheometers. The mechanical characterization of hydrogels will be discussed later in this report.[14]

Moreover, some hydrogels are able to respond to various stimuli that can be physical, chemical or even biochemi-

cal. eover, some hydrogels are able to respond to various stimuli that can be physical, chemical or even biochemical. These stimuli, whether they are physical, for instance light, pressure, electric field, temperature, magnetic field or mechanical stress, or chemical, for instance pH, ionic factors or chemical agents, can induce changes in terms of inter-segment interaction potentials or interactions between the chains and solvents and between the chains themselves at the molecular level. For instance groups on the polymer chains can become active or not depending on the context or the swelling capacity can be increased by partial decrosslinking of the network when exposed to a stimuli. Biochemical stimuli imply responses due to receptor-ligand interactions, antigen binding or recognition, enzymatic activity or other interactions with biochemical agents. These biochemical stimuli-responsive hydrogels are especially interesting in terms of use for the pharmaceutical, biomedical and biotechnological fields.[23, 25, 29]

3.2 Applications

In view of all the above cited characteristics, the hydrogel class is very versatile in terms of applications. It is used in many different hygiene products, such as diapers thanks to its tremendous absorption capacity, but also in a broad variety of other products such as soaps, shampoos, contact lenses or even toothpastes and cosmetics products, making the hydrogel class ubiquitous in our daily lives. More advanced industrial applications also take advantage of the swelling ability of hydrogels such as for oil recovery, water treatment and other separation techniques, textile, agriculture and pharmaceutical industries. However, hydrogels are above all appealing in the biomedical field. Indeed, due to their ability to retain large amounts of fluid under physiological conditions, their soft rubbery consistency comparable to the texture of tissues as well as their tunability regarding functionalization, biocompatibility and sterilization, they offer a myriad of possibilities. Among others, tissue engineering, drug delivery system, bacteria encapsulation, biosensors design, medical device coating or medical implant optimization are innovative disciplines into which hydrogels have successfully made their way. Hydrogels also offer great possibilities in the soft electronics field and organ-on-a-chip development.[14, 23–25]

3.3 Mechanical Characterization

Hydrogel characterization techniques include a broad range of different methods to determine various parameters. Nuclear Magnetic Resonance (NMR) and mass spectroscopy are for instance examples of techniques used to identify the composition of the polymer, while morphological characterization is achieved using microscopy equipment such as Atomic Force Microscopy (AFM), environmental Scanning Electron Microscopy (e-SEM) or even confocal microscopy. Among all hydrogel properties, thermo-mechanical characteristics are particularly important to control to be as suited as possible to the desired application.[30]

Just as any polymer, hydrogels are viscoelastic materials, meaning they exhibit both solid and liquid characteristics in their mechanical behavior. They consequently have a time-dependent behavior similar to any polymer due to their intrinsic viscoelasticity but also exhibit an additional time-dependent deformation component due to fluid flow in the polymer network.[31]
Hydrogel mechanical properties are relatively difficult to measure and to interpret for various reasons. First, the samples are usually not easy to fix in place so that they do not move during the test. Roughening fixtures are usually preconized to overcome this first challenge. Secondly, most of the available testing equipment is optimized to measure compressive moduli of the order of GigaPascals (GPa) or MegaPascals (MPa) whereas hydrogel's elastic moduli are in the range of kiloPascals (kPa). Specialized devices consequently need to be used. Finally, as hydrogels

are biphasic materials, containing a first phase defined as the polymeric network and a second one defined as the fluid absorbed in the mesh, interpreting the results is more difficult than it is for solid polymers.[27]

Still, different methods can be used to determine hydrogel mechanical properties: elongation tests, compression tests, local indentation with a probe and last but not least, frequency-based tests such as shear rheology and dynamic mechanical analysis (DMA).[27, 32] Moreover, it is possible to perform non-contact test to determine permeability, using pressure instead of direct contact with the sample.[27] We will focus below on the frequency-based tests, namely dynamic DMA and rheology measurements, which have been used in this work.

The principles behind the viscoelastic properties measured by means of these frequency-based methods are the following.
The deformation γ applied on the sample is oscillatory and thus follows a sinusoidal evolution. The subsequently measured shear stress τ is related to γ in the following way: $\tau(t) = |G^*| \cdot \gamma(t)$, where t is the time and G^*, the complex modulus, is an imaginary number such that: $G^* = G' + G'' \cdot i$. The obtained shear stress is thus also sinusoidal.
On the one hand the real part of G^*, which is defined as the storage modulus G', is in phase with the applied shear strain. It indeed corresponds to the amount of energy that is mechanically stored in the sample by means of elastic deformation. This modulus is related to the stiffness and the Young's modulus[1] of the material.[34, 35]
On the other hand, the imaginary part of the complex modulus, which is defined as the loss modulus, is 90° out of phase with the applied strain. It indeed corresponds to the amount of energy that is lost by viscous dissipation within the sample. This modulus is mainly associated with internal friction.[34, 35]
Moreover, the phase lag δ between the shear strain and shear stress and more particularly its tangent $\tan\delta$, called the damping factor, is a measure of the mechanical damping of the sample. Indeed, as $\tan\delta = \frac{G''}{G'}$, it allows to account for the dominance of elastic or viscous behavior depending on the value of $\tan\delta$: when $\tan\delta \geq 1$, the viscous component take precedence over the elastic one and inversely when $\tan\delta \leq 1$, the elastic component is dominant.[35]
An illustration of the shear strain and the resulting stress as well as the phase lag between these two is proposed in Figure 1.2.

Finally, the magnitude of the complex viscosity $|\eta^*|$, which can also simply be referred to as viscosity η, can be defined as a measure of the resistance to deformation of a material at a particular shear rate since $\tau = \eta \cdot \dot{\gamma}$ and can be expressed as a function of the moduli and the frequency f or angular frequency ω in the following way:

$$|\eta^*| = \frac{|G^*|}{\omega} = \frac{|G^*|}{2\pi f} = \frac{\sqrt{G'^2 + G''^2}}{\omega}$$

The so-called steady viscosity is usually the value used to describe the viscoelastic behavior of polymer melts and simply referred to as viscosity η in many cases. This steady viscosity is indeed the value of the viscosity at small enough deformation rate $\dot{\gamma}$ where the value of $|\eta^*|$ is constant.[36]

[1]The Young's modulus or the modulus of elasticity in tension or compression (i.e., negative tension), is a mechanical property that measures the tensile or compressive stiffness of a solid material when the force is applied lengthwise. It quantifies the relationship between tensile/compressive stress σ (force per unit area) and axial strain ε (proportional deformation) in the linear elastic region of a material.[33]

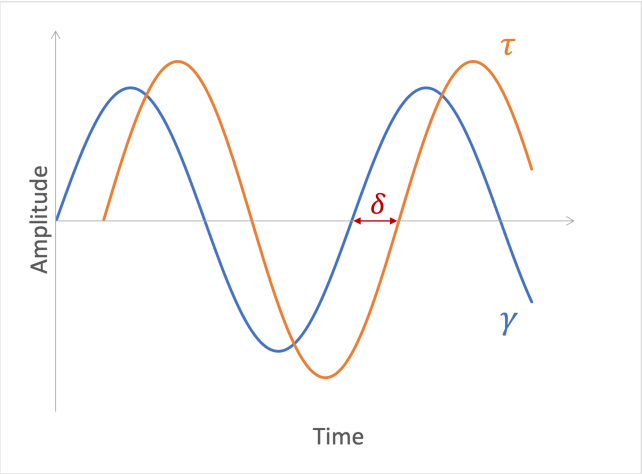

Figure 1.2: Phase lag δ between the applied shear strain γ and the resulting stress τ related to polymer viscoelasticity (as inspired from[35]).

In addition to these viscoelastic properties, thermal transition can also be characterized. For instance, the transition temperature T_g can be measured by DMA and rheology. T_g is defined as the temperature at which the mechanical properties of an elastomer change abruptly, marking the transition from rubbery to glassy state.[37]

Dynamic mechanical analysis

DMA involves imposing a cyclic deformation of small amplitude on a sample and measuring the resulting stress response or equivalently imposing a cyclic stress and measuring the resulting strain response of the sample.[31] Due to the difficulties related to hydrogel mechanical measurements, DMA is currently mostly used in combination with thermal analysis in order to determine changes in glass transition temperature depending on the material composition. Compressive DMA is widely used to characterize materials which are more rigid than hydrogels but in the present case, shear measurements are more appropriate.[32] However, bending and tensile tests are also possible.[27]

Oscillatory shear DMA provides information about different viscoelastic properties of the material such as the storage and loss moduli, respectively G' and G'', the damping factor $\tan\delta$ and the viscosity η but also the glass transition temperature T_g. Once the sample, which has a particular shape depending on the device geometry and type of test performed, is loaded, different so-called 'sweep' experiments can be performed. Two of popular sweep tests are amplitude sweep tests and frequency sweep tests, which respectively characterize the material behavior as a function of the shear amplitude and of the frequency. In each these cases, either a sinusoidal shear strain or stress is applied on the samples that are sandwiched between static plates and a mobile plate. A schematic depiction of this system is shown in Figure 1.3

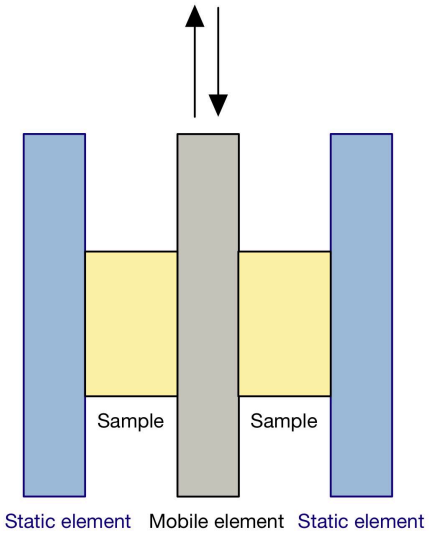

Figure 1.3: Schematic depiction of the shear DMA measurement.

DMA experiments to investigate the behavior of the polymers as a function of temperature do not only provide information on transition temperatures, for instance T_g , but also allow to extend the experimental data far beyond what is practicable thanks to the time-temperature superposition (TTS) principle. TTS stipulates that, by building a master curve of the modulus values at a reference temperature, it is possible to determine the behavior a material would have at very high or very low frequency, or equivalently after a very short or very long time. The curves of the moduli at different temperatures are used to build the master curve: as a change in temperature only implies a shift along the horizontal axis in the time domain, one can simply assemble the curves obtained from experiments at various temperatures to get a global view of the behavior as a function of time for time ranges far beyond the possible experimental time.[27, 35] An illustrative example of how the TTS principle is used in practice to extend the experimental window is shown in Figure 1.4.

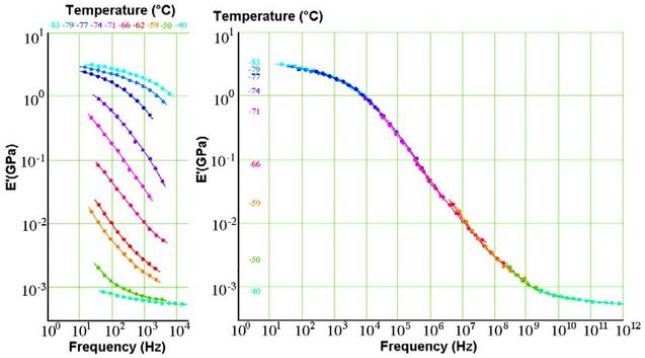

Figure 1.4: Example of application of the time-temperature superposition (TTS) principle; experiments are performed at different temperatures; results can be merged to determine the behavior outside the experimental window.[35]

Rheology

Rheology is very similar to shear DMA: indeed small amplitude oscillatory shear tests are performed in the same fashion except that the shear strain applied is angular and not linear. The same properties as for DMA are obtained from rheological measurements (G', G'', η, $\tan\delta$, T_g,...), establishing the relationship between deformation or flow of the hydrogel and the applied stress.[30, 39]
A rheometer is composed of two parts: the lower part is static while the upper part is mobile. The two main geometries used to measure the viscoelastic properties of the sample are either parallel disks are used on both parts (plane-plane geometry) or a cone on the mobile part and a disk on the static one (cone-plane geometry). Some more complex geometries also exist but are more complex and consequently less used and in more particular contexts.[39]

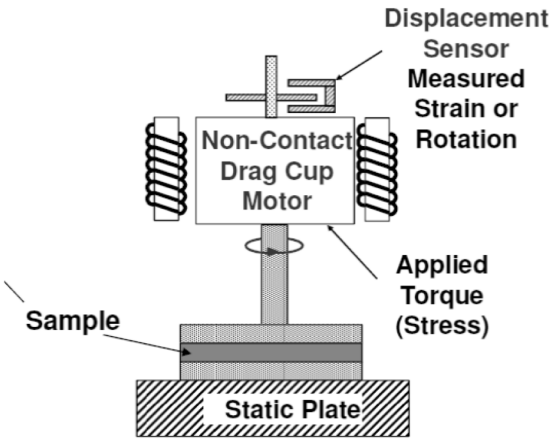

Figure 1.5: Oscillatory rheometer.[38]

Cone-plane geometries have the advantage to provide a constant deformation rate but require prior knowledge about the sample properties to place the sample in the right way using the appropriate amount of polymer. On the contrary, plane-plane geometry are easier to use but the shear strain is not constant, meaning the sample is essentially deformed at the border and not in the center due to the shear rate gradient.[36] The motor makes the upper part move in order to generate deformations of small amplitude on the sample loaded between the planes or the cone and the plane. A schematic representation of a rheometer is displayed in Figure 1.5.

Rheology measurements are appropriate mechanical characterization methods for hydrogels as they are quick, require small samples and are able to detect changes in terms of architecture of the polymeric network, such as the proximity to glass transition, structural heterogeneity or homogeneity or the degree of crosslinking.[39]

4 Agarose

Among hydrogels, polysaccharides meet many requirements needed when working in the biomedical field. Indeed, these natural polymers are non-toxic, compatible with bioactive compounds and are relatively cheap. Using ionic or other physical gelation methods, it is possible to avoid the use of chemical crosslinker which could potentially be toxic and to work in mild conditions.[40]

In particular, agarose is a linear and neutral polysaccharide composed of alternating repeating units of (1→3)-linked β-D-galactopyranose and (1→4)-linked 3,6-anhydro-α-L-galactopyranose. The repeating disaccharide unit composed of these two sugar cycles is called agarobiose; agarose is thus poly(agarobiose). Although agarose is considered a neutral polymer, some repeating units are substituted with charged groups, mainly pyruvate and sulfate but also methoxyl or glucoronate groups to a lesser extent.[41–44] The ideal molecular structure of agarose is presented in Figure 1.6, without any substituting groups.

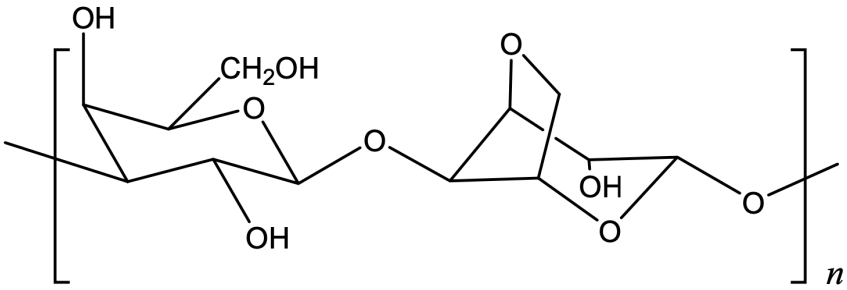

Figure 1.6: Agarose molecular structure.[45]

4.1 Origin

Agarose is one of the two fractions extracted from agar, next to agaropectin which is a charged sulfonated polysaccharide. Agarose is the subfraction of economic importance as it is the gelling component of agar and represents from 50 to 90% of the total agar mass.[44]
Agar is obtained by extraction from red algae of the *Rodophyceae* class denominated as agarophytes. The genera that are principally used are *Gellidium* (Figure 1.7(a)), *Gracilaria* (Figure 1.7(b)), *Acanthopeltis*, *Ceranium* (Figure

1.7(c)), *Pterocladia* or *Campylaephora* (Figure 1.7(d)). Actually agar is a constituent of the outermost portions of the cell wall of the algae cells or of their intercellular matrix. Isolation of agar is usually performed in several steps. First, the alga is boiled in water and then filtrated to get rid of particulates. Next, the filtered solution sets to a gel which is then purified by freeze-thawing to remove any water-soluble impurities. Finally, agar is precipitated with ethanol.
The final product is a polysaccharide complex, more precisely sulfonated galactan. The fractionation of agar into agarose and agaropectin can be performed by acetylation of agar and subsequent treatment with chloroform[46], polyethylene glycol (PEG) precipitation, diethylaminoethyl(DEAE)-cellulose chromatography, and PEG combined with DEAE-cellulose chromatography.[43, 47, 48]

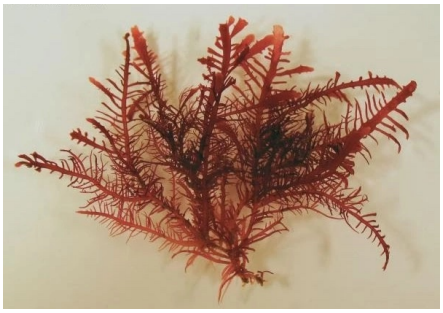

(a) *Gellidium*

(b) *Gracilaria*

(c) *Ceranium*

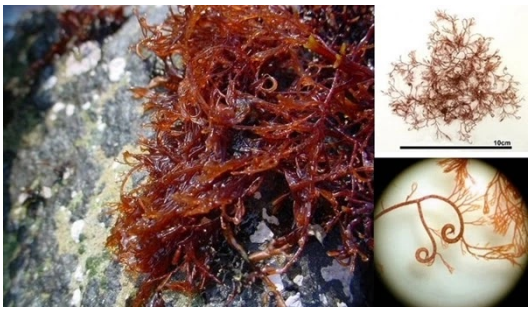

(d) *Campylaephora*

Figure 1.7: Agarophytes from which agar can be extracted.[49]

4.2 Molecular and supramolecular structures

At high temperature, the agarose molecules adopt a random and stiff coil conformation.[42] Upon cooling, the coils tend to order and form helices. They adopt a double helix conformation. When adopting this helicoidal conformation, a cavity is formed in-between the two molecular chains. It is large enough to accomodate small molecules such as water without steric hindrance. Hydrogen bonding with water molecules is made possible by the lining of the hydroxyl groups of the macromolecule in the cavity.[44] This conformation is only possible when the repeating units are not substituted with charged groups such as pyruvate or sulfate. At substitution location, it is not possible for the macromolecule to fold into an helical conformation owing to steric hindrance. Consequently, the chains segment near substituted repeating units remain flexible in solution and are named kink segments. Thus, agarose macromolecules are alternating chains of rigid helical segments and flexible kink segments, which makes them block copolymers of rigid and flexible segments.[41] The substitution degree depends on the washing and isolation procedures and is characterized by the electroendosmosis (EEO) which is a functional measure of the number of sulfate

and pyruvate substituting groups. EEO has a quite important influence on the gel properties and on its structure.[50]

Thereafter, the helical segments aggregate, forming thick fiber bundles and microgel domains that are held together thanks to hydrogen bonds between the helices, which makes agarose a physically crosslinked hydrogel. In view of the supramolecular structure of agarose, the obtained gel is rigid and opaque. However, this structure is very heterogeneous : large interstitial spaces are bonded by fibrous areas of variable density.[42, 51] Figure 1.8 shows a schematic representation of the arrangement detailed here above.

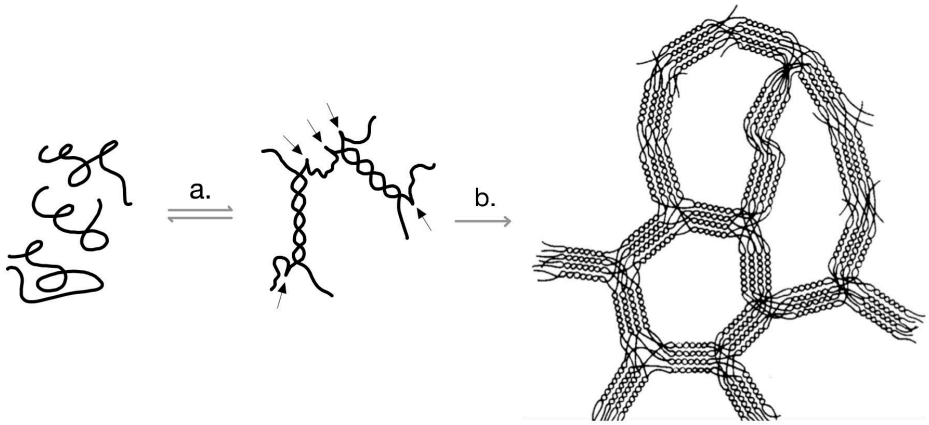

Figure 1.8: Formation of an agarose gel; transition a.: formation of double helices, strands exchange partners at kinks (arrows); transition b.: higher order aggregation into fiber bundles. (Adaptation from Figure 2 of [43])

However, it is worth noting that the double helical structure of agarose chains is a controversial topic. Indeed, it has been recently stated that the scattering diffraction patterns that were interpreted as a double helix conformation could also be representative of a simple helix conformation, leading to the conclusion that there possibly exists more simple helices than double helices in agarose gels. Moreover, some scientists state that there exists loose chains and dangling chains in the polymer that do not contribute to the elasticity of the network.[52, 53]

4.3 Sol-Gel transition

The so-called Sol-Gel transition, meaning the transition of agarose gels from liquid solution to solid gel, is a complex phenomenon. It is worth noting that agarose gels exhibit a significant degree of hysteresis between gelling on cooling and melting on heating.[42] In other words, gelling and melting temperatures are different.[54]

According to Indovina et al. [55], it is likely that this transition has to be regarded as a two-step transition mechanism. As explained above, one can look at the ordering of agarose at two different levels: the molecular level and the supra-molecular one. Indovina et al. suggest that supra-molecular and molecular level transitions, meaning order loss or reordering for each of those scales, are both thermally reversible processes but the supra-molecular transition does not exhibit any thermal hysteresis, just a slow kinetics whereas the molecular transition exhibit a large hysteresis and a fast kinetics. They worked with an agarose gel concentration of 2% w/v.
Consequently, when heating an agarose gel from its solid gel state to its liquid state, the loss of supra-molecular order begins around 50 °C and it takes quite some time to loosen up the bundles while heating. At a certain

temperature, usually around 80°C, the chains have enough energy to transition from helical to coil conformation. This process is much faster than supra-molecular loss of order. Around this particular temperature, the remaining supra-molecular order is lost and the molecular order is also quickly lost. The supra-molecular transition occurs through a temperature interval that is greater by an order of magnitude in comparison to the interval needed for molecular transition ($\Delta T_{molecular} \sim 5$°C as compared to $\Delta T_{supra-molecular} \sim 50$°C). This process can be identified as melting and the temperature at which the hydrogel flows, defined as the melting temperature T_m, is the temperature at which both orders are lost and the molecules adopt a random coil conformation.
Gelling upon cooling can also be explained following the same idea: first the helices are forming very fast when cooling the material below T_m, the molecular order is then recovered. Afterwards, the supra-molecular order takes time to establish upon cooling, even though the helices needed to form the bundles are available, due to its slower kinetics. The gelling temperature can thus be defined as the temperature at which both molecular and supra-molecular orders are recovered, which is around 50°C for 2% w/v agarose gels.
Since the double helical conformation of agarose molecules is a much-debated subject, this model has to be taken with caution. Actually, just as the structure of agarose molecule is a controversial topic, the Sol-Gel transition is a contentious issue.

More recently, Dai et al. [56] studied the gelation mechanism and the molecular interactions in agarose gels by means of Hydrogen NMR. They concluded that the helices formed by agarose, whether they would be single or double helices, aggregate progressively upon cooling. The setting temperature, which is an other term to name the gelling temperature, corresponds approximately to the moment when half of the agarose chains would form fibrous bundles so that the gel becomes rigid and turbid. The further one cools, the more the chains would aggregate. A schematic representation of this hypothetical process of Sol-Gel transition and the associated molecular interactions is represented in Figure 1.9.

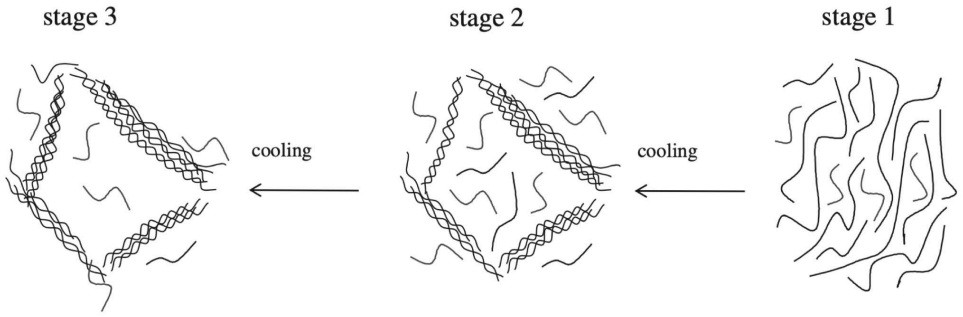

Figure 1.9: Schematic representation of the gellation mechanism of agarose gels at different stages upon cooling.[56]

4.4 Factors influencing agarose gel properties

Agarose gel properties are dependent on many different factors such as agarose concentration in solution, ageing influence [42, 50], cooling rate [57–59], EEO [43, 47, 50], solvent nature [59], the degree of methylation of the chains [50], as well as the shear rate applied upon gelation [58] which influence the viscoelastic and architectural properties of the gels. In this section, we will mainly focus on the influence of concentration and ageing.

Concentration

The concentration in agarose influences various properties of agarose gels.

To begin with, the gelling temperature as well as the melting temperature show a concentration dependence. Indeed both of these characteristic temperatures increase with concentration. For example, the setting of a 2% w/v agarose gel, which is associated to a sharp increase of viscosity upon cooling, occurs at 33°C while it occurs at 27°C for a 0.5% w/v gel. This faster gelation is attributable to the presence of a higher number of molecules in the most concentrated solution as compared to the lowest.[58] Considering melting, as the size of the organized regions is greater for higher concentrations and as the melting temperature T_m increases with the size of ordered regions in the polymer, T_m increases with concentration. The concentration dependence is most significant for concentrations below 1% w/v. Consequently, it is possible to take advantage of this influence to tune the setting and melting temperatures of a gel by simply varying agarose concentration.[50, 58]

In the second place, concentration variations change the viscoelastic properties of the gel. As a matter of fact, higher concentrations yield to higher viscosity as well as higher storage and loss moduli. The latter increase linearly with concentration, probably due to the enhancement of interactions induced by an increase in gel concentration.[58] Another viscoelastic property of agarose gel that is affected by the concentration is the gel strength. This property is defined as the force, expressed in $g.cm^{-2}$, that must be applied to an agarose gel to cause its fracture.[50, 54] It actually also increases with concentration.[60]

Finally, the porous structure which is a distinctive feature of agarose gels also varies with concentration. Indeed, the average pore size decreases when concentration increases. This is mainly due to the increase in packing density as well as in the degree of network in high concentration solution compared to lower concentrations. This density actually is related to the gel strength treated here above: the denser the packing, the higher the gel strength.[58] The resulting pore diameter distribution exhibits not only a mean shift but also a change in distribution width: in solutions of lower concentration, the pore diameters are much more variable than what they are in more concentrate solutions.[61] Illustrative SEM images of dried agarose gel microstructures and the distribution of pore size for different concentrations are presented in Figure 1.10 and 1.11 respectively. It also has to be mentioned that the swelling capacity of agarose increases with concentration. [58]

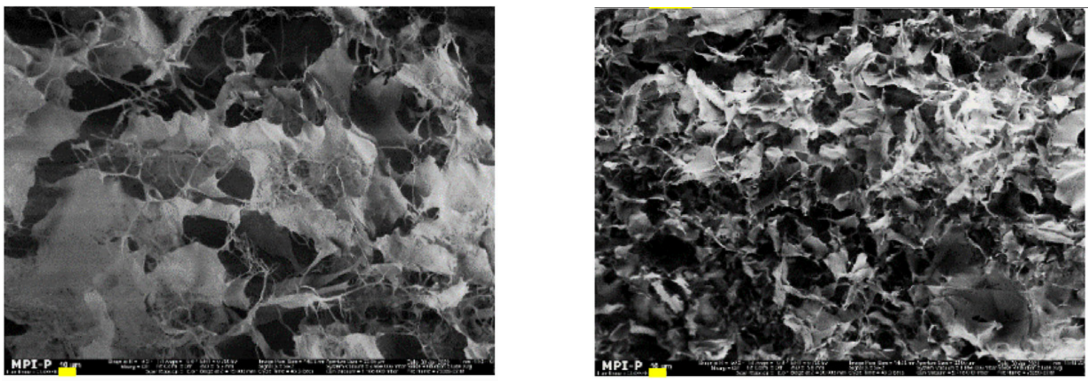

(a) agarose 0.5% w/v (b) agarose 2% w/v

Figure 1.10: SEM images of freeze dried fluid gels prepared with different agarose concentrations. Yellow scale bars are 10 μm.[58]

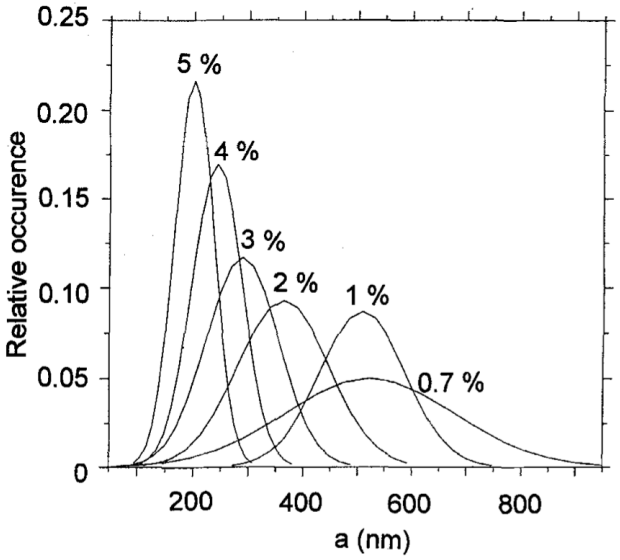

Figure 1.11: Pore diameter (a) evolution distributions for various agarose concentrations.[61]

Ageing

The changes due to ageing of the gel can be caused by different phenomena.

First of all, the gel strength of the gel decreases over storage time due to the spontaneous hydrolysis of the polysaccharide chains. This phenomenon is mainly observed after five years from manufacturing.[50]
Besides hydrolysis, changes in terms of microstructure in a much shorter period of time occur. Upon ageing, the extensive aggregation of the chains to the fibrous bundles is believed to considerably decrease the concentration of solute chains as well as the number of very loose aggregates.[42] This contraction of the network results in a larger mesh size. A schematic representation of this phenomenon is shown in Figure 1.12.

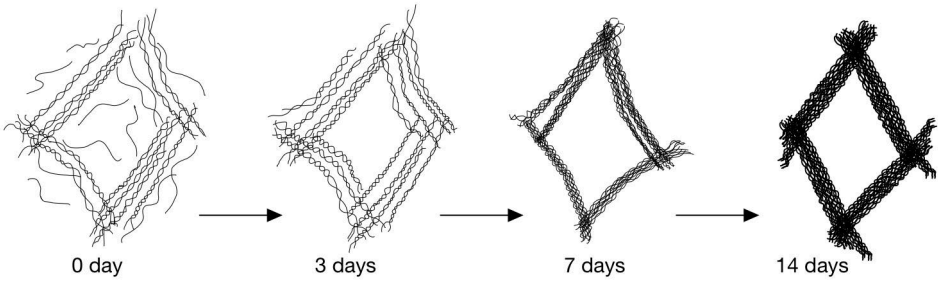

Figure 1.12: Schematic representation of the conformation evolution of agarose networks induced by ageing (Adaptation of Figure 9 of[42]).

4.5 Agarose use for bacterial culture

Agarose is widely used in the biomedical and biotechnology fields. From tissue engineering [14, 62] to separation techniques for DNA or for proteins [42, 56, 63, 64] to food industrial applications [58] and even drug delivery [65],

agarose is a quite commonly used hydrogel for various purposes.[66] Notwithstanding, agarose is the most frequent gelled substrate for bacterial culture. [14] Indeed, in addition to being biocompatible and porous, it is inert to bacterial enzymatic degradation (with rare exceptions), keeps its gelled structure in the temperature range used for bacterial cell culture and through its high water content, it allows to maintain hydration of the microorganisms it comes in contact with. [11] Moreover, agarose is sometimes preferred to agar as agarose is purified agar gelling component.
For these reasons, agarose will be used as gelled medium for bacterial cell culture in solid medium in the framework of this report.

5 Bacteria growth in hydrogels

5.1 Overview

As above mentioned, agar and its purified form agarose are hydrogels that are extensively used in the framework of bacterial cell cultures to obtain culture media prepared combining these hydrated polymeric network in combination with nutrient-rich liquid to allow for microbial culture. However, these materials are not the only hydrogels used in combination with bacteria. Hydrogel-bacteria systems can have purposes as various as treatment of infections by other microorganisms [67], wastewater treatment [68] or biofilm modelling [69–73]. In all those systems, the cells are usually encapsulated, entrapped or even immobilized in or on the hydrogels.

On the one hand, the most commonly used hydrogels are prepared from alginate [70, 74], agarose [11, 75–77] and polyacrylamides [78, 79], but some other polymeric gels such as hyaluronic acid [80], extracellular matrix (ECM) hydrogels from animal origin [81], chitosan [69, 71] or synthetic polymers such as waterborn polyurethane [68], poly(ethylene glycol) diacrylate (PEGDA) [82] and Pluronic F-127 (Poly(ethylene oxide)-poly(propylene oxide)-poly(ethylene oxide)) [67] can also serve as support for applications involving bacterial cells.
On the other hand, a large variety of bacteria were used in those systems, depending on the aim of the final product. Here is a non-exhaustive list of examples: *S. epidermidis* [69, 78, 83, 84], *S. aureus* [74], *Escherichia coli* (*E. Coli*) [13, 76, 78, 79, 84], *Bacillus subtilis* (*B. subtilis*) [67, 78], *Pseudomonas aeruginosa* (*P. aeruginosa*) [78, 82, 84], *Rhodobacter johrii* which are photosynthetic bacteria[81], *Lactobacillus* spp. [85] and many other bacteria.

Given the number of possible species and polymers combination that could be used for hydrogel-bacteria systems, only a few examples will be presented to give a global view of the versatility of such systems. First, Dong et al. [68] developed a system composed of nitrifying bacteria entrapped in a waterborn polyurethane gel for the purpose of waste water treatment to get rid of ammonia. Second, Zhao et al. [81] engineered a system composed of photosynthetic bacteria (*Rhodobacter johrii*) in a matrix of ECM hydrogel to facilitate the healing of wounds infected by other microorganisms. In the same perspective, Lufton et al. [67] had in mind to develop a thermoresponsive gel with *B. subtilis* in order to treat fungal infections related to the presence of *Candida albicans*. The gel containing the bacteria would in this case solidify when administrated on the skin to take advantage of bacterial antifungal properties. Finally, in the framework of research and understanding of bacterial biofilms, many combinations of hydrogels and bacteria are currently used to build artificial biofilm models. This particular application of hydrogel-bacteria systems will be discussed further in the following section.

It has to be noted that different techniques are used to engineer the products. In the recent years, bioprinting has aroused a tremendous interest in the biomedical and biotechnology fields in general. In this context, different

living systems have been produced using inks that contain both hydrogel and bacteria, referred to as bioinks.[13]

5.2 Biofilm models

Biofilm growth mode is the typical growth mode of bacteria in nature as it confers a plethora of advantages as already described above for *S. epidermidis* by way of example. For instance other bacterial strain and species such as *S. aureus* and *P. aeruginosa*, are able to form biofilms, which are defined as surface-attached microbial communities surrounded by a self-produced exopolymer matrix.[12] The latter are representing a challenge as already discussed for *S. epidermidis*. In order to overcome the problems caused by resistant infections caused by biofilms, it is necessary to understand the complex mechanisms underlying these biofilms, especially how this complex gelled environment allows bacteria survival, development and resistance for instance. In order to do so, an effort has been made to engineer artificial biofilm models to mimic the behavior of cells in a biofilm while precisely controlling the properties of the surrounding polymeric matrix and other environmental factors to assess their roles in biofilm formation and development.[73]

In that respect, several models have been conceived. For example, Strathmann et al. [73] proposed *P. aeruginosa* biofilm model utilizing agarose beads to replace the extracellular polymeric substances (EPS) normally produced by the microorganism itself upon biofilm formation. They manage to provide a protection similar to the one of EPS in natural biofilms. The construct cell viability was similar to the one of natural systems.
Another system was designed by Stewart et al. [86] in order to assess *Enterobacter aerogenes* (*E. aerogenes*) biofilm susceptibility to different biocides. In this framework, *E. aerogenes* were seeded in alginate gel beads, bringing to light the influence of initial cell density as well as bead size on biofilm resistance to biocide by means of a precise control of these parameters.

In general, bacteria in biofilm models are supplied with nutrients thanks to a continuous or intermittent liquid flow in closed flow cells systems or in open-surface fluid flow reactors. The attraction forces between bacteria and surfaces have to be greater than the shear forces exerted by the flow on the biofilm to ensure the survival of the cells. Flow cells are especially useful to study the mechanisms underlying biofilm formation as well as their morphology.[72, 87]

Apart from biofilm formation investigation, natural biofilms have exhibited great potential in other fields such as fuel cells for power generation and biocatalysis. In this view it is also of great interest to mimic natural biofilms and even optimize the obtained artificial system. Park et al. [71] for instance developed an artificial bioinspired biofilm that allows to overcome challenges in terms of bacterial immobilization while taking advantage of the properties of natural biofilms, without prejudice on cell viability.

5.3 Influence of the hydrogels properties on bacterial growth

As it has been widely acknowledged in the recent years, the properties of the substrate on which cells grow has a very important impact on growth, metabolism and gene expression, whether it is for eukaryotic or bacterial cells.[78] Many factors as diverse as hydrogel surface hydrophobicity and charge [88], the microstructure and composition of the gel [73], hydrogel viscosity [74] and stiffness [11, 76, 78, 82, 83] can have a broad range of effects on the behavior of bacterial cells.

Gel viscoelastic properties

The viscoelastic mechanical properties of hydrogels have aroused a great deal of interest in the recent years due to the changes in bacterial behavior they induce. Change in terms of stiffness, either obtained by variation of the hydrogel concentration or of its composition, for instance its molar mass [11, 82] thus enable to tune the bacterial growth, metabolism as well as their shape and material-cell and cell-to-cell interactions. For instance, viscosity has proved to influence *S. aureus* entrapped in both sodium alginate and methylcellulose matrices, inducing differences in terms of vancomycin resistance. The more viscous the matrix, the more resistant the colonies. This change in susceptibility is believed to be related to the diffusion limitation, in the medium as well as in the biofilm, induced by an increase in viscosity.[74]
Moreover, Blacutt et al. [82] highlighted that changes in gel stiffness could also have on influence on gene expression in *P. aeruginosa*. In particular, the populations seeded on softer PEGDA showed more heterogeneity in terms of adhesion while using stiffer gel, the population adhesion was quite homogeneous. Additionally, *P. aeruginosa* in stiffer PEGDA gels expressed more strongly and rapidly a substance related to the transition from planktonic to biofilm growth mode, strengthening the idea that hydrogel mechanics variation should induce changes in terms of biofilm development dynamics.

In brief, the effect of the stiffness and viscosity on different microorganisms has been investigated combining various hydrogels and bacteria. In the present report, efforts will be made to investigate the influence of the viscoelastic properties of agarose media on *S. epidermidis* viability, growth as well as its metabolic activity.

6 Bacterial parameters

Various bacterial parameters can be measured to characterize the behavior of the cells. Among others, kinetics of growth, growth mode, viability and metabolic activity are of particular interest.

6.1 Growth

Bacterial growth takes place in four successive phases.
First after the inoculation of the microorganisms in the medium, they need to adapt to the new conditions in which they will grow. During this so-called lag-phase, division does not occur and the bacterial density remains the same.
Second, when the microbes are used to their environment, they start to actively divide and reproduce. The so-called Log-phase or exponential phase is used to determine the growth rate of the microorganism μ and their doubling time t_d which is the time needed for the cell number to double, which is obviously related to the growth rate of the microorganism.
Third, the culture enters the so-called stationary phase. During a quite long period of time, bacterial density remains stable at high level. The reason why the density remains stable is related to the depletion in nutrients and/or the formation of inhibitory products. Consequently, the microorganisms do not divide anymore which explains the stability of the cell density.
Finally, since the lack of nutrients and the accumulation of eventual waste products get even worse with time, the population starts to die. This death phase is characterized by a drop in terms of cell density.[89, 90] This four stage growth is schematically represented in Figure 1.13.

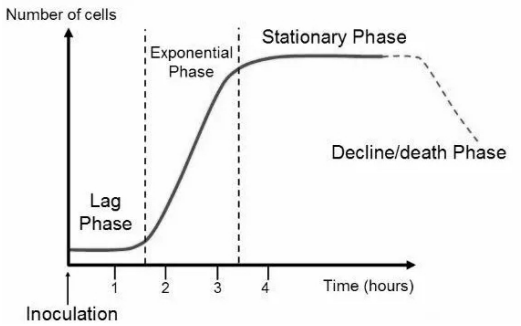

Figure 1.13: Phases in a bacterial culture (number of cells in logarithmic scale).[91]

Bacterial growth can be estimated using different measurements including Optical Density (OD) or nephelometry, although OD is the most commonly used technique. In the particular case of bacteria that stably express a fluorophore, the fluorescence intensity related to this fluorescent indicator is also used to get insight on their development.[89]

Optical density

OD measurement is the most common technique used to monitor bacterial growth. Indeed, OD measurements allow to get insight on bacteria concentration. Therefore, OD measurements over time allow to determine bacterial growth. These measurements are performed with a spectrophotometer and correspond to the amount of light that has been scattered when travelling through the sample. In the present case, the more microorganisms there are, the higher the light scattering and thus the OD. A schematic representation of the setting and light scattering is shown in Figure 1.14. Below a certain critical OD value, it exists a linear relationship between OD and the number of cells. Above this value, which is often around 0.4, the relationship is not proportional anymore and a correction is necessary to get a reliable information on bacterial growth. This proportionality and loss of proportionality is shown in Figure 1.15.[89, 90]

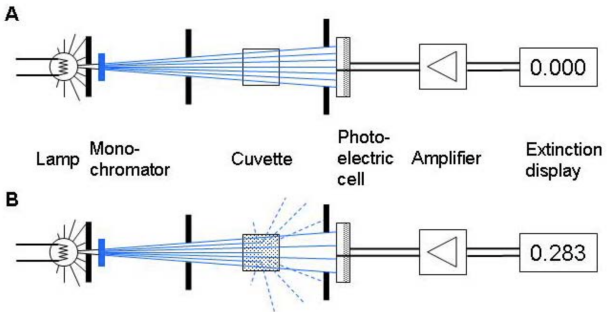

Figure 1.14: Schematic depiction of the spectrophotometer measurement principle to assess bacterial concentration.[90]

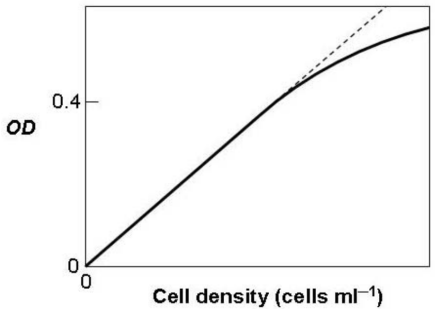

Figure 1.15: OD deviation from proportionality to the cell density above OD critical value.[90]

Nephelometry

Nepholometry is also based on the light scattering induced by the microorganisms, just as it is the case for OD measurements, they allow to follow the concentration of microorganism in the sample over time, which enables to follow its growth. However, instead of measuring the loss of transmission due to scattering as it is done in OD

measurement, nephelometric methods directly detect the scattered light.[89] The detector is collecting scattered light at a certain angle, which is usually 30 or 90°.[92, 93] Compared to OD measurement, this technique is more sensitive and is consequently more suitable to suspensions with low bacteria density.[89]

Fluorescence intensity

If the considered bacterium stably expresses a fluorophore, for instance green fluorescent protein (GFP), it is possible to rely on the measured fluorescence to report microbial growth. Indeed, the fluorophore concentration and the fluorescence intensity are proportional to one another, which allows to assess growth by measuring the fluorescence intensity at a wavelength specific to the expressed fluorophore.[89]

It is worth noting that OD and nephelometry measurements can give different read-outs compared to fluorescence intensity measurements. Indeed, all bacteria scatter light in a similar way, making OD and nephelometry suitable techniques to quantitatively measure bacterial growth. However, the fluorescence intensity depends not only on the number of bacteria in the sample but also on the ability of each cell to produce the fluorophore in a smaller or larger amount. Since this fluorophore production capacity can vary from one cell to another, the fluorescence intensity is not a quantitative measurement of the bacterial growth but rather of the bacterial growth as well as their ability to produce the fluorescent molecule.

6.2 Morphology and growth mode

On the one hand, bacteria can grow either planktonically in liquid or immobilized as colonies, in biofilm for instance. Biofilm growth mode is the typical growth mode of bacteria in nature as it confers a plethora of advantages as already described above for *S. epidermidis* by way of example. Indeed, except when in laboratory conditions, bacteria rarely find themselves in an environment that is as rich as a culture medium; in less-than-ideal conditions, biofilm growth mode is thus favored.[94] When immobilized, bacteria grow differently compared to free bacteria as they are physically constrained but also suffer from limitations in terms of nutrient diffusion in structured supports as compared to liquid culture environment. Their morphology as well as their gene expression vary depending on the growth mode they adopt.[95, 96] It is thus of critical importance to assess the growth mode to understand bacterial behavior. The techniques used to determine morphology as well as growth mode can be microscopy techniques to allow for visualization of the microbial populations. Among non-destructive analytical microscopic techniques, fluorescence microscopy techniques, namely epifluorescence microscopy and confocal laser scanning microscopy (CLSM), are widely used to observe bacterial populations. In addition SEM enables to observe fixed bacterial populations that are dead.[97, 98] In recent years, AFM also attracted a great deal of interest to image bacterial cells in a non-destructive way. These four imaging techniques are described in more detail in the sequel.

Epifluorescence microscopy

Fluorescence microscopy is an optical microscopy technique in which fluorescence emission is used to image a sample instead of or in combination with scattering, attenuation, absorption or reflection of light. In order to image a specimen using fluorescence, the object of interest has to fluoresce. Fluorescence is indeed defined as the emission of light that occurs extremely rapidly after absorption of light. The wavelengths of excitation and emission are different, which is a phenomenon known as the Stokes shift. The excitation energy is greater than the emission one as light energy is inevitably lost upon fluorescence process, the excitation wavelength is thus smaller than the emission one. The fluorescent molecules used in those imagery techniques are called fluorophores.[99–101]

Epifluorescence microscope is a quite simple set up that relies on fluorescence to generate an image. In this case, the illumination of the sample is called epi-illumination as the light that illuminates the sample and excites the fluorophores as well as the light emitted by the sample travel through the same objective lens, 'epi' indeed stands for 'same'. The objective thus does not only enable to image and magnify the specimen as it usually does but also serves as the condenser that illuminates the specimen. Fluorophore excitation and emitted fluorescence detection are done through the same light path. Typically, the epifluorescence microscopes are composed of a light source, excitation and emission filters, a dichroic beamsplitter and a charge coupled device (CCD) camera. The light source usually is a xenon arc or a mercury vapor lamp and more recently light emitting diodes (LEDs) which are more powerful light sources. Filters are intended to select the appropriate wavelengths for both illumination/excitation and emission, according to the considered fluorophore. Dichroic mirror or beamsplitter is used to reflect light beams of smaller wavelengths while it transmits beam with greater wavelengths. The excitation light is thus reflected by the mirror to illuminate the sample while the emission light is transmitted to the CCD camera, which in turn allows to detect the emitted light and to obtain an image after computer data treatment.[99–102]

CLSM

Unlike wide-field fluorescence microscopy methods such as epifluorescence microscopy, confocal microscopy relies on the use of pinholes to reject out-of-focus light and consequently improve the vertical resolution in comparison to other optical fluorescence techniques. Indeed, in fluorescence microscopy, any fluorophore in the field of view will be stimulated, even in the out-of-focus planes, which induces a blurring of the image if these data contribute to the image. Rejection of out-of-focus light is achieved using illumination- and detection-side pinhole apertures in the same conjugate image plane which is the reason why this technique is called 'confocal'. Furthermore, the illumination source is also different from the one used in wide-field techniques: in CLSM, lasers with precisely determined wavelengths are used as light sources and are scanned over the surface. Thanks to this laser point-illumination and the rejection of blurring effect related to out-of-focus light, CLSM is capable to get an even better vertical optical resolution as well as a better contrast in comparison to other fluorescence microscopy techniques. Moreover, as optical sectioning is provided by the confocal configuration, it allows for 3D reconstruction of the sample based on high-resolution images stacks.[103–105]

SEM

Unlike the two previous imaging techniques, SEM does not rely on fluorescence but uses electrons to obtain an image of the sample. Indeed a focused electron beam is used to scan the surface of the sample. By interactions with the atoms of the sample, particular signals are produced and provide information on the sample composition (thanks to the electronic contrast) and topography. Unlike CLSM and epifluorescence microscopy, SEM is a destructive imaging technique. Indeed, the object to observe first require to be fixed, for instance by dehydration and even sometimes metalliza-

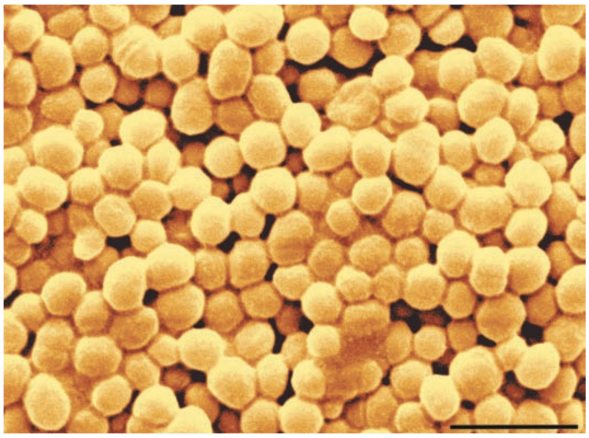

Figure 1.16: *S. epidermidis* biofilm on the plastic wall of a transfusion bag; bar: 5 μm.[106]

tion or cryogenization (cryo-SEM).[107] This technique is thus especially suited to visualize the external morphology of bacterial cells, showing the specimen as a 3D object. Many different techniques can be used when considering SEM imaging. For instance, conventional SEM for which the bacteria are fixed, dehydrated and dried before imaging, but also cryo-SEM for which bacteria are cryofixed and observed at very low temperatures, are widely used techniques. Cryogenization or drying prevent the release of volatile compounds in the high vacuum chamber of the SEM. According to the specimen at hand, the preparation technique is adapted to obtain the images of interest whether it is to visualize external or internal compounds of the bacterial population.[106] On Figure 1.16, a SEM image of a *S. epidermidis* biofilm is shown as way of example.

AFM

AFM is a powerful imaging technique that can be used on biological samples to obtain images at the nanometer to micrometer scale under nondestructive conditions. The operating principle of AFM is the following: a very sharp probe (tip) is mounted at one extremity of a cantilever with a precisely determined flexibility, the analyzed sample surface is scanned with this tip and the deflections of the cantilever caused by the interaction between the probe and the sample are detected by an optical detector. The detection is performed thanks to a laser beam that reflects on the upper surface of the cantilever (that is coated with a reflecting material such as gold) and the changes of the reflected beam are detected by means of a photodiode.[108, 109] A schematic depiction of this microscope is shown in Figure 1.17.

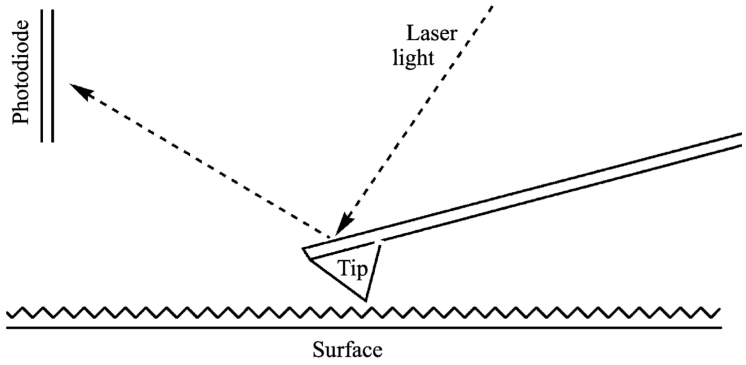

Figure 1.17: Scheme of the atomic force microscope. A sharp tip is scanned across a surface, and small deflections in that tip are used to generate an image of the shape and contours of the sample. The laser does not penetrate the sample and is used to detect deflections in the tip.[109]

In Figure 1.18, an example of topography image obtained by AFM is shown for *E. Coli*, the achieved resolution is incredibly high and allows to visualize nanometric features of the bacteria, for instance pili and flagella of the latter. Nevertheless, AFM does not only allow to get insight on the topography of a bacterial surface but also to detect some component of the surface thanks to specific interactions between the latter and the tip, which can be coated with a molecule showing a particular affinity for the component of interest. The resulting interaction force between the tip and the cell can be measured to obtain so-called force-maps.[110]

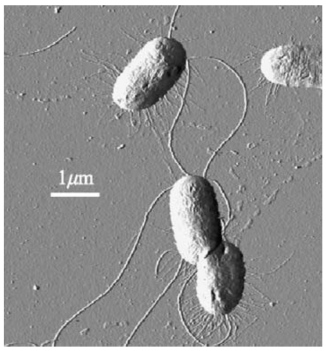

Figure 1.18: AFM image of *E. coli* strain ZK1056 grown on a glass surface.[109]

6.3 Viability and metabolic activity

Bacterial viability can be defined as the proportion of the cells that are capable to multiply after incubation in standard microbiological conditions. Therefore, plate count techniques can be used to determine this bacterial parameter. However, limitations to this definition and technique exist as some microorganisms are unculturable under usual culture conditions while other are culturable in general but can be in a particular physiological state in which they are viable or even active but nonculturable. To overcome these limitations, a number of methods have been proposed to determine bacteria viability without any culturing step. Viability can be assessed relying on various metabolic activities or on membrane integrity.[111]

Bacterial viability measured via Live/Dead kit:

Live/Dead viability kits contain two nucleic acid stains, SYTO-9 and propidium iodide, that have different spectral characteristics, being respectively green- and red-fluorescent, as well as different bacteria cell penetration abilities. Their use to assess bacteria viability consequently relies on membrane integrity. Indeed, the bacteria with an intact cytoplasmic membrane appear green as SYTO-9 is able to penetrate the membrane, while the damaged one appear fluorescent red, because propidium acid penetrates only these cells and SYTO-9 fluorescence is reduced by the presence of both stains.[111, 112]

Bacterial respiration measured by 5-Cyano-2,3-ditolyl tetrazolium chloride reduction:

5-Cyano-2,3-ditolyl tetrazolium chloride (CTC) is reduced into insoluble red fluorescent formazan via the electron transport chain related to bacterial respiration. Consequently, the respiring cells contain red deposits and the more rapidly they respire, the more formazan is formed, enabling to get a semi-quantitative estimate of the number of respiring bacteria and to which extent they respire.[111, 113]

Bacterial viability measured by ChemChrome staining:

ChemChrome is a nonfluorescent dye that penetrates the bacterium and is cleaved by nonspecific esterases in the cytoplasm, resulting in the release of a green fluorescent product: fluorescein. This stain is used in combination with a red counterstain so that when dead cells with permeable membranes still contain active esterase they are labelled by both dyes. As energy transfer increases the red fluorescence signal by transfer from fluorescein to counterstain, the living cells are stained green only when esterase activity is normal and the membrane is not damaged. Otherwise they appear red by counterstaining.[111, 114]

Metabolic activity measured by alamarBlue reduction:

AlamarBlue (AB) assay aims to quantitatively measure the proliferation of cells including bacteria. AB is the commercial name under which the reagent used for so-called 'resazurin reduction tests' is sold to assess cell growth and metabolic activity. Resazurin is a blue nonfluorescent dye which is reduced to a pink and highly fluorescent dye named resozurin when exposed to cellular activity. Unfortunately it is not known whether this reduction occurs intracellularly, at the plasma membrane of even in the medium as a chemical reaction. AB assays have many different benefits as compared to other techniques used to assess for growth and metabolic activity, may they be conventional or radioactively-labelled incorporation assays. For instance, AB exhibits change in both color

and fluorescence intensity upon reduction, so it is possible to chose between colorimetric or fluorescent detection methods. Moreover, it is a water soluble molecule, which allows to get rid of any extraction step. Furthermore, the reagent is stable and non-toxic to cells, which ensures minimal interference with bacterial metabolic pathways, but it is also non-toxic to the technician, who will be able to work in a safer environment with less regulation.[115, 116]

CHAPTER 2

Global Objective and Strategy

In light of the important role the human microbiota plays on the health of its host, new therapeutic strategies have emerged in recent years. Different products have been designed to take advantage of the beneficial effects of microorganisms to regulate the commensal population, whether it is aiming to regulate gut, skin or mucosal microbiota compositions. As part of the development of these novel therapeutic options to cure diseases such as acne vulgaris, the encapsulation of *S. epidermidis* in a patch for the skin has been proposed. The patch currently developed in our laboratory is composed of a silicone support that is designed with cavities to serve as containers for the bacteria and the medium in which the latter grow. On top of the support, a semi-permeable barrier is grafted to allow for the diffusion of the metabolites of interest produced by the bacterial strain while preventing *S. epidermidis* escape. Two different barriers are considered: a polycarbonate membrane and a polyacrylamide-agarose hydrogel layer. A schematic presentation of this construct and a picture of a prototype are presented in Figure 2.1.

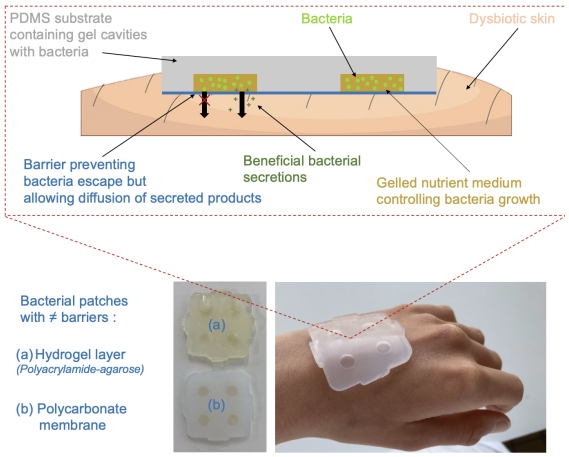

Figure 2.1: Schematic depiction of the patch designed to heal dermatological diseases related to skin dysbiosis, allowing for the diffusion of secreted molecules of interest while preventing bacteria escape thanks to a semi-permeable membrane (polyacrylamide-agarose hydrogel layer or polycarbonate membrane).

As the medium should stay in place in the patch wells, the use of gelled medium is appropriate to prevent the nutrient-rich material containing the microorganisms to flow out of the construct. Encapsulation in the patch is critical on two aspects: it would on the one hand prevent any possible infection related to *S. epidermidis*, for which some strains are well-known opportunistic pathogens in particular conditions, and it would on the other hand allow to get a better control on the growth kinetics of the bacteria, their viability as well as their metabolic activity. Such a construct would ideally maintain cellular growth in a closed system to prevent uncontrolled bacteria proliferation

while taking advantage of the benefits offered by the agents secreted by the microorganism.
In order to maintain the viability of cells over the time as well as their metabolic activity of interest, one should provide nutrients and a proper environment to the microorganism. Indeed, as mentioned in the previous section, environmental factors, including medium characteristics, can have diverse effects on the behavior of the bacteria, including growth, viability as well as metabolic activity.

In that respect, it is critical to optimize the medium in which the microorganisms grow in the construct. Since the mechanical properties of the medium in which bacteria grow has been demonstrated to have an important influence on the bacterial behavior, the optimization of the latter to maintain the bacterial activity of interest is critical. However, the influence of these material properties on the general behavior of the cells, namely growth and metabolic activity, should be investigated first. In this view, we will investigate the influence of the mechanical properties of gelled media on the latter, using agarose as gelled medium, in the present report. In order to obtain gels with different mechanical properties, we decided to play on two parameters. On the one hand, the variation in terms of agarose concentration was used to tune the stiffness and the viscosity. On the other hand, various gelled media with different agarose types were studied. These agarose differed greatly in gel strength. Aiming to elucidate the link between the medium viscoelastic properties and *S. epidermidis* behavior, we proceeded in two distinct steps.

First, we need to determine the mechanical properties of the agarose hydrogels that we plan to use as media for *S. epidermidis* in the patch. As mentioned in Chapter 1, different parameters exist to characterize the viscoelastic properties of hydrogels such as the storage and loss moduli, the damping factor as well as the viscosity of each employed gel. In this master thesis, two characterization techniques have been selected to investigate these materials properties: DMA and rheology. One or the other technique has been used depending on the characteristics of the tested gel sample.

Second, we need to assess different bacteria behavior parameters such as growth, growth mode and metabolic activity when bacteria are seeded and grown in the previously characterized gelled media. It is worth noting that the bacteria are embedded in the gels and not on their surface. As explained earlier, different techniques allow to get measurements related to different properties of a bacterial culture. In the case at hand, the bacteria we used were modified by genetic engineering to express plasmidic genes and subsequently produce GFP. Thanks to this feature, fluorescence measurements will be used to quantify cell growth and viability in a 96-well microplate for periods of 24 h. Moreover, epifluorescence microscopy as well as confocal microscopy are useful tools to assess the growth mode. Additionally, metabolic activity was quantified by measuring the fluorescence related to AB reduction.

Lastly, the information obtained in the materials characterization and in the bacterial parameters measurements are combined so as to endeavor to establish the possible trends connecting agarose gel mechanical properties and the subsequent bacterial activity in the medium or possibly related to other parameters.

CHAPTER 3

Characterization of agarose hydrogels

This chapter aims to describe in details the preparation of culture media containing agarose as gelling agent as well as their mechanical characterization. The prepared gels contain various amounts and types of agarose. Two characterization techniques were used to determine the viscoelastic properties of the gels. One or the other was selected depending on the characteristics of the gelled sample at hand.

1 Objective and strategy

As a reminder, the aim of this master thesis is to investigate the influence of the mechanical properties of the gelled culture medium on growth and activity of a bacterial population of *S. epidermidis*.
For this purpose gelled media with various mechanical properties must be prepared in the first instance. In order for the hydrogel properties to vary, two distinct parameters influencing the latter were played with: agarose concentration and agarose gel strength.

On the one hand, agarose concentration is known to influence the mechanical properties of the material[58] (cfr. Section 4.4 of Chapter 1). Therefore, gels with various concentrations of the same agarose type where prepared to tune the mechanical properties.
On the other hand, the gel strength of a gel is defined as the *"force that must be applied to a gel to cause it to fracture"*[54], actually corresponding to the yield stress to be more accurate; it is therefore a mechanical property in itself. Hence, using agarose with different gel strengths enables to prepare agarose gels with variable mechanical properties.

In the second instance, the prepared media have to be characterized. The most relevant properties to determine for agarose gels are viscoelastic properties such as the storage and loss moduli, respectively G' and G'', the damping factor $\tan\delta$ as well as the viscosity η. These data enable to identify the moduli related to either the elastic energy component of the polymer or its viscous energy component but also to quantify the prevalence of one or the other previously mentioned energies and the resistance to flow the gel exhibits.

To perform this characterization, different techniques are available as described in Section 3.3 of Chapter 1. In the framework of this report, DMA as well as rheology were used depending on the characteristics of the tested sample. The most rigid gel was tested using DMA as this technique is more suited to gels exhibiting a more or less solid-like behavior while the softer ones were tested using rheology as they were more "liquid" and thus more prone to be tested using a rheometer as compared to DMA. In both cases, amplitude as well as frequency sweep tests were performed to determine the evolution of the above-mentioned properties as a function of the applied shear strain as well as a function of the frequency at which the oscillatory deformation is applied.

2 Materials

Agaroses: Four different agaroses were purchased from Sigma-Aldrich, their characteristics are summarized in Table 3.1.

Reference	**Description**	**Sulfate content**	**Gel strength ($g.cm^{-2}$)**	**Gel point (°C)**	**Melting point (°C)**	**EEO**
A0576	Agarose Type I-B Low EEO	$\leq$ 0.12%	$\geq$ 1800 at 1.0% $\geq$ 3200 at 1.5%	36±1.5 at 1.5%	86±2.0	$\leq$ 0.12
A9918	Agarose Type II-A Medium EEO	<0.25%	>1000 at 1.0%	36±1.5 at 1.5%	87±1.5	0.16-0.19
A4018	Agarose Type VII Low Gelling Temperature	$\leq$ 0.10%	$\geq$ 200 at 1.0%	26-30 at 1.5%	$\leq$ 65	$\leq$ 0.10
A5030	Agarose Type IX Ultra-low Gelling Temperature	$\leq$ 0.10%	$\geq$ 75 at 2.0%	8-17 at 0.8%	$\leq$ 50	$\leq$ 0.05

Table 3.1: Characteristics of the agaroses used in this experiment.[54]

Broth: Dehydrated Nutrient Broth (BD234000) was purchased from BD Bioscience.

Water: Milli-Q water, also known as ultrapure water, was obtained from a Merck Millipore system. It was characterized by a resistivity of 18.2 MΩ·cm.

3 Protocols

3.1 Gel preparation

Eleven different 25 mL agarose solutions were prepared. First, following manufacturer's specifications, 0.2 g of dehydrated broth was put in each of the eleven 25 mL glass bottles used to contain the solutions. Thereafter, the appropriate amount and type of agarose powder was poured into the appropriate bottle (cfr. Table 3.2).
The nomenclature used to name agarose solutions and gels in this work is defined as: '**x**%_GS**y**'; with **x** the concentration w/v of agarose in the solution and **y** representing the gel strength ordered by decreasing order. GS1 gel thus exhibits the highest gel strength whereas GS4 exhibits the lowest gel strength.

Solution name	Description	Agarose type	Weight (g) for 25 mL of gel
3.0%_GS2	Agarose A9918 3.0%	A9918	0.75
1.0%_GS1	Agarose A0576 1.0%	A0576	0.25
1.0%_GS2	Agarose A9918 1.0%	A9918	0.25
1.0%_GS3	Agarose A4018 1.0%	A4018	0.25
1.0%_GS4	Agarose A5030 1.0%	A5030	0.25
0.5%_GS1	Agarose A0576 0.5%	A0576	0.125
0.5%_GS2	Agarose A9918 0.5%	A9918	0.125
0.5%_GS3	Agarose A4018 0.5%	A4018	0.125
0.5%_GS4	Agarose A5030 0.5%	A5030	0.125
0.3%_GS2	Agarose A9918 0.3%	A9918	0.075

Table 3.2: Summary table of the agarose amount and type used to prepare the gels.

In each bottle, 25 mL of MilliQ water was then added.

Since the tested gels are intended for bacteria culture, to work in the same conditions as the ones they will be prepared for further experimentation, the solutions were autoclaved. During the autoclave cycle, the agarose powder solubilized in water thanks to the high temperature required for sterilization. Afterward, 8 mL of each of the solution was casted in round Petri dishes and once the gels were solid, the Petri dish was closed, sealed with Parafilm and placed upside down in the refrigerator at 4 °C, preventing dehydration of the sample as well as condensation at its free surface. However, solutions 0.5%_GS4 and 0.3%_GS2 should not be turned upside down since the gels are not rigid enough to adhere on the Petri dish and subsequently flow. They still required to be sealed to avoid dehydration.

It is worth noting that not all gels were prepared on the same day. Indeed, the mechanical characterization of the gels was performed on fresh samples, meaning from just after gelation up to one day later. The preparation of the gels was planned according to the time needed to perform the tests while ensuring sample freshness during characterization.

3.2 Mechanical characterization

Even if rheology and shear DMA are different characterization techniques, the types of test performed in this work rely on the same principles for both of them. As a first step, the viscoelastic response of the gel is measured as a function of shear strain amplitude during a so-called amplitude sweep (AS) test and as a second step as a function of the deformation frequency during a so-called frequency sweep (FS) test.

Firstly, AS tests were performed by imposing shear strain or stress to scan a defined amplitude range while the frequency of deformation was kept constant throughout the test. The principal aim of AS tests is to determine where the linear viscoelastic region (LVER) takes place. LVER is defined as the shear amplitude range during which the storage and loss moduli, G' and G'', are strain-independent.[60] It was important to determine this region as it is mandatory to perform FS tests in the LVER.

Secondly, FS tests were performed at a fixed shear strain amplitude, which was selected according to the previous

test's results to be in the LVER. This time, it is a frequency range that is scanned throughout the test. This kind of test allows to get an insight on the evolution of the moduli or the viscosity as a function of deformation frequency and consequently as a function of time since time is directly related to the frequency.

Rheology

The rheological tests were performed using a Kinexus Pro rheometer and the associated software Kinexus rSpace (Malvern Instruments GmbH; Herrenberg, Germany) using a plane-plane geometry. Indeed a cone-plane geometry would require prior knowledge of many properties of the sample which are not available per se for the ones at hand. Rheology measurements are particularly suited to the characterization of soft gels. As a result, most of the gels were tested using rheology with the exception of 3%_GS2 gel which was too solid to be tested using a rheometer: the water released from the agarose gel when compressed formed a lubrication layer, resulting in the sliding of the sample between the plates and consequently in the inability to measure the viscoelastic properties.[117]

First and foremost, the rheometer was connected to an air supply, switched on and it performed its calibration without any loaded geometry or sample. Once the calibration was done, the upper plate was loaded (plane circular plate, ∅ 25 mm), identified by the rheometer and the zero gap was performed to define the exact distance between the upper and bottom plates for the following measurements. Once all calibrations were done, the sample was loaded between the two plates. The sample was cut using a circular piece cutter (∅ 25 mm) and placed in the center of the bottom plate. The upper plate was lowered gently until the sample was sandwiched between the plates and the contact force became non zero ($\sim$ 4-6 N), which usually corresponds to a gap between 1 mm and 1.5 mm. To allow force relaxation before performing the tests, one waited until the contact force was smaller than 1N. In the meantime, the excess gel was removed using a brass spatula and the gutter was filled with water to avoid sample dehydration during measurement. Once relaxation was achieved, the oven of the rheometer was closed: the setting was ready to launch an experiment. The placement of the sample is critical and must be done with the utmost care.

In the first instance, AS tests were performed with the parameters listed in Table 3.3. Two successive AS tests were performed going from the smallest strain to the largest and then in the other way around. This process allows to spot possible hysteresis which would account for the destruction of the (micro)structure of the sample, rendering further measurements on the latter erroneous.

	Mode	**Frequency (rad/s)**	**Initial shear deformation (%)**	**Final shear deformation (%)**	**Temperature (°C)**
AS1	Strain control	1	0.001	5	25
AS2	Strain control	1	5	0.001	25

Table 3.3: Parameters of the amplitude sweep (AS) tests performed with Kinexus Pro.

Based on the results of the AS test, if no hysteresis was observed, the upper limit of the LVER was determined for further characterization.

In the second instance, FS tests were performed with parameters listed in Table 3.4. The strain amplitude had been determined thanks to previous AS testing and was for each gel in the LVER.

	Mode	Initial frequency (rad/s)	Final frequency (rad/s)	Shear deformation (%)	Temperature (°C)
FS	Strain control	100	0.1	0.1	25

Table 3.4: Parameters of the frequency sweep (FS) tests performed with Kinexus Pro.

Once both tests were completed, the oven was opened, the gap was set to 10 cm and the sample was removed. The plates were cleaned with Kimtech tissues and water and subsequently dried with acetone.

This procedure, including sample placement, AS test, FS test and sample removal was repeated 2 to 3 times for each agarose gel. The data obtained from these tests were analyzed using Excel, determining the mean and standard deviation for each test type (AS or FS). The steady viscosity was determined by calculation of the average of the viscosity values in LVER for AS tests.

Shear DMA

The DMA tests were performed using a DMA/SDTA861^e (Mettler Toledo GmbH; Schwerzenbach, Switzerland) in combination with the STAR^e software in shear liquid mode. Since DMA shear tests are suitable for gels that are almost solid, only 3%_GS2 gel was tested using DMA. The clamp used in this case was a special shear clamp for low-viscosity liquids, which is shown in Figure 3.1(a). The names of the different parts of the clamp will be referred to thereafter for sample placement description. The clamp loaded with the sample was placed in the system already described in Chapter 1 and is represented on Figure 3.1(b), where the central clamp holder is mobile while the external ones are fixed.

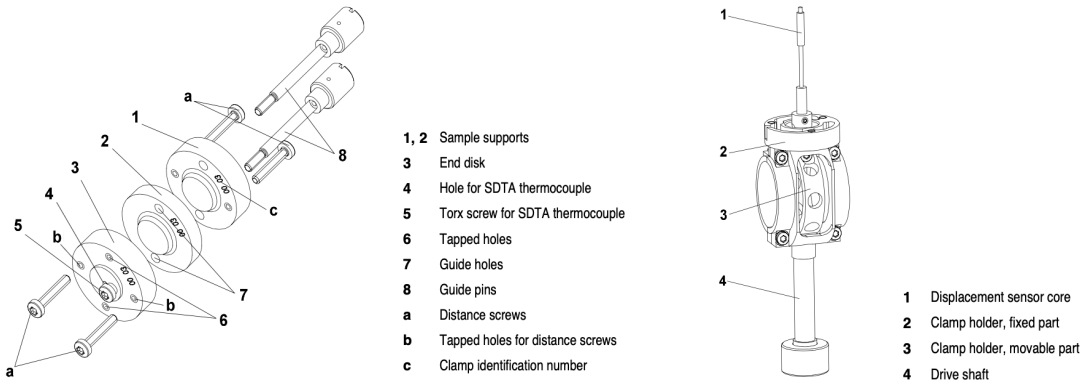

(a) Special shear clamp for low-viscosity liquids.

(b) Assembled small clamping assembly.

Figure 3.1: Shear liquid system elements.[118]

The samples were cut into circles of 8 mm diameter using a piece cutter. In the case of shear DMA, the sample dimensions had to be exactly known as the measurement of the viscoelastic properties relies on a geometric factor which obviously depends on the sample dimensions, namely the circle diameter and the sample thickness.
Just as for rheological measurements, AS were performed to determine the LVER and consequently chose the parameters for the FS test. In this case, the measurements were controlled using the force and not the strain, which ensured that an erroneous measurement in strain amplitude does not end up in sample destruction. The shear strain amplitude and the force associated to it were usually determined on the basis of a plot of the force as a

function of deformation obtained during the AS test. The strain limit of the LVER was assessed to be the value above which the relationship between the force and the deformation was not linear anymore. The associated force value was slightly decreased and used to perform FS tests in LVER, while ensuring force control mode.

First and foremost, two samples of the same gel were cut and placed on the clamp. For this purpose, the clamp was split open: the external sample support, maintained by the guided pins pointing upwards, was loaded with one sample. The sample was placed as precisely as possible in the center of the support. The central sample support was then placed on top of the assembly using the guide holes to place the guide pins. The other sample was placed in the center of the latter. The end disk was then put on top of the assembly and the screws were tightened. Unfortunately, it was not possible to tighten the screw exactly the same way for each test as the minimal couple of the dynamometric screwdriver was too large to ensure sample integrity. The screws were tightened enough to hold the sample but not to squeeze it too much, at the risk of having the mechanical properties altered. Once the clamp was screwed in place, the exact thickness of the sample was measured using a caliper and the clamp was placed in the DMA chamber on the support. The central sample support was aligned with the mobile holder and then the four corner screws as well as one on the mobile element of the support tightened with a dynamometric screwdriver to allow for guide pins removal. An example of a step-by-step guide for sample placement is shown in Figure 3.2 (note that in our case the gels were already solidified compared to the one used in the example).

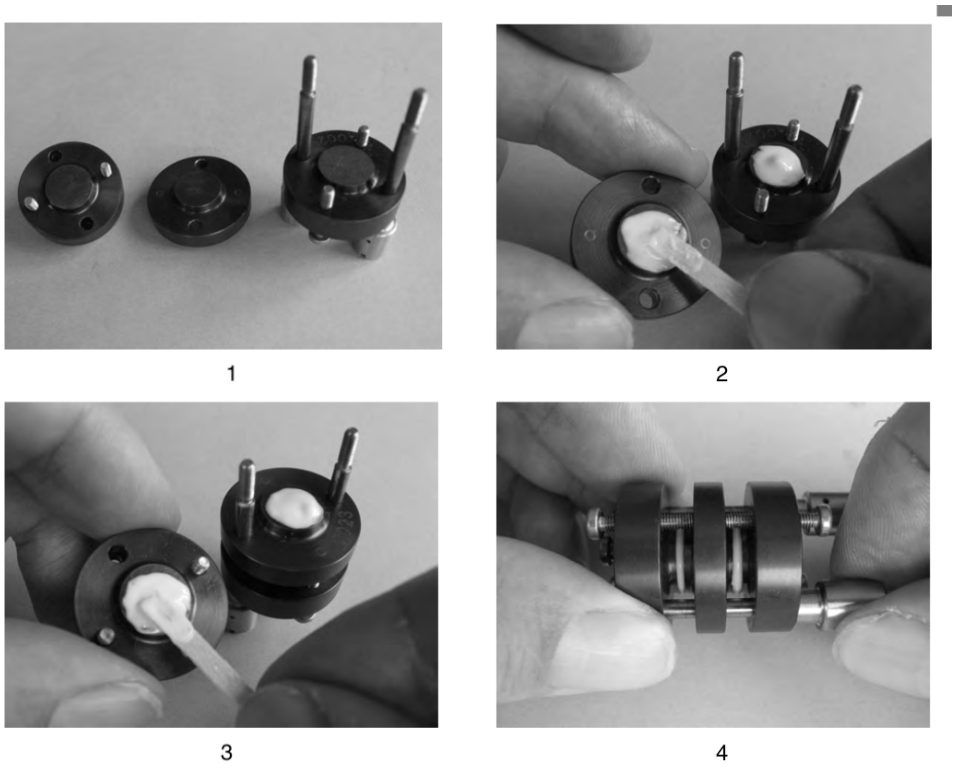

Figure 3.2: Sample placement on the shear clamp used for DMA measurements.[118]

Once the sample was set in place, AS was performed in the first instance. The parameters used to perform the AS test are summarized in Table 3.5. When using DMA, one had to specify the linear deformation quantitatively (in μm) instead of relatively (in %). The relative strain was thus defined as: shear strain [%] $= \frac{\text{shear deformation } [\mu\text{m}]}{\text{sample diameter } [\mu\text{m}]}$.

In view of that, the initial and final shear strain were respectively 0.001% and 1%.

	Mode	Initial shear deformation (μm)	Final shear deformation (μm)	Frequency (Hz)	Temperature (°C)
AS	Force control	0.08	80	1	25

Table 3.5: Parameters of the amplitude sweep tests performed with DMA/SDTA861^e.

According to the results of the AS test, the force to apply during the FS test was determined following the principle explained here above.

In the second instance FS tests were performed using parameters summarized in Table 3.6.

	Mode	Maximal shear deformation (μm)	Maximal force (N)	Initial frequency (Hz)	Final frequency (Hz)	Temperature (°C)
FS	Force control	20	0.15	120	0.1	25

Table 3.6: Parameters of the frequency sweep tests performed with DMA/SDTA861^e.

Once the tests had been successfully performed, the clamp was removed: the guide pins were inserted in the guide holes, the screws on the support were loosened and the clamp was gently removed from the clamp holder system. The clamp was then split open and the sample was removed from the sample support. The surfaces in contact with the sample were cleaned with water and dried using acetone.

This protocol was repeated three times for the gel.

4 Results and discussion

In this section, a focus on different viscoelastic properties of the agarose gels is proposed. In particular, the storage and loss moduli, respectively G' and G'', the damping factor $\tan\delta$ and the viscosity η are compared among gels with variable concentrations and properties to identify the differences between those gels as a function of their agarose composition. As a reminder, the principles laying behind these viscoelastic properties were introduced in Section 3.3 of Chapter 1.

The measurements obtained either by DMA or rheology were globally reproducible, giving values in the same order of magnitude for each test and property that was measured multiple times. However, the measurements using the rheometer with very small deformation amplitudes were very noisy due to the fact that the minimal torque of the Kinexus is greater than the torque it should measure at such small deformation. The data for very small deformations in rheological measurements were consequently not reliable.

4.1 Influence of the concentration on the viscoelastic properties

In this part of the report, the results of the comparison between gels prepared with different concentrations in agarose A9918 (GS2) are presented.

Moduli G′ and G″

In the first instance, AS tests were performed to determine the LVER and to assess for any possible destruction of the (micro)structure of the material for samples tested using the rheometer. For each of these gels, no hysteresis is observed following the first AS test, the integrity of material is thus conserved during the rheological tests. A representative example of the results is shown in Figure 3.3. The selected shear strain amplitude used to perform the subsequent FS tests is 0.1% since every gel that was rheologically tested was in LVER for this strain value. As already mentioned above, measurements for very small deformation amplitude were very noisy as it can be seen in the figure, making them unreliable.

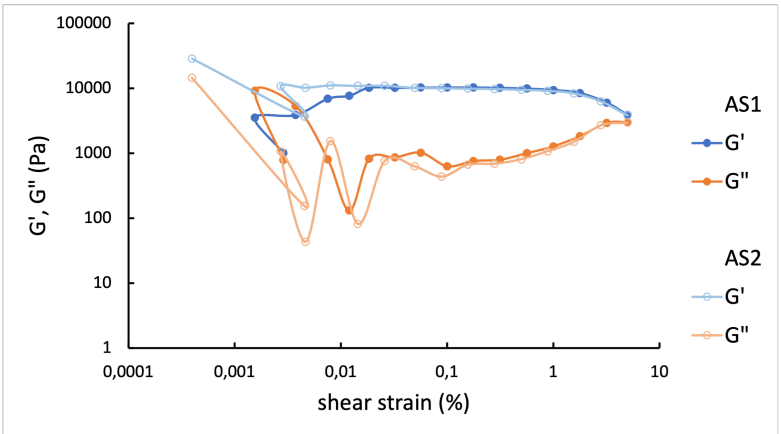

Figure 3.3: Results of two successive AS tests for a 1%_GS2 gel.

Based on the graphs shown in Figure 3.4, one sees that the higher the agarose concentration, the greater the value of both the storage and loss moduli in the LVER, which highlights the fact that an increase in G^* occurs when increasing agarose concentration. In addition to that, the strain at which the material enters the non-linear viscoelastic regime, called the LVER limit, gets smaller as the concentration increases as it can be observed when comparing the results obtained by rheology. Indeed, the drop of G' occurs at a lower strain amplitude for a 1.0% concentration as compared to a 0.5% and this difference is also encountered when comparing concentrations of 0.5% and 0.3% although it is less marked than for the previous ones. It is worth noting that the comparison of the LVER limit between DMA and rheology results would not make any sense as the shear strains, respectively linear and angular, are different. Finally, the yield strain, which is defined as the critical strain value at which G' and G'' cross-over, thus representing the transition from elastic to viscous dominance, follows the same trend as the LVER limit: an increase in concentration induces a decrease in terms of yield strain.
These trends were already observed in other works, for instance, Bertasa et al. [60] also deduced that for agar gels, when increasing concentration, the moduli increase while the LVER strain limit as well as the yield strain decrease. The increase in terms of moduli is probably related to the increase in crosslinking density related to concentration influence, as already mentioned in Section 4.4 of Chapter 1. This change in terms of ordering in the network would confer enhanced mechanical properties, making it more stiff. The mean and standard deviation of the modulus values G' and G'' are computed in the LVER for all concentrations and presented in Figure 3.5. The modulus enhancement along concentration increase is confirmed by this histogram representation of the mean moduli in LVER.

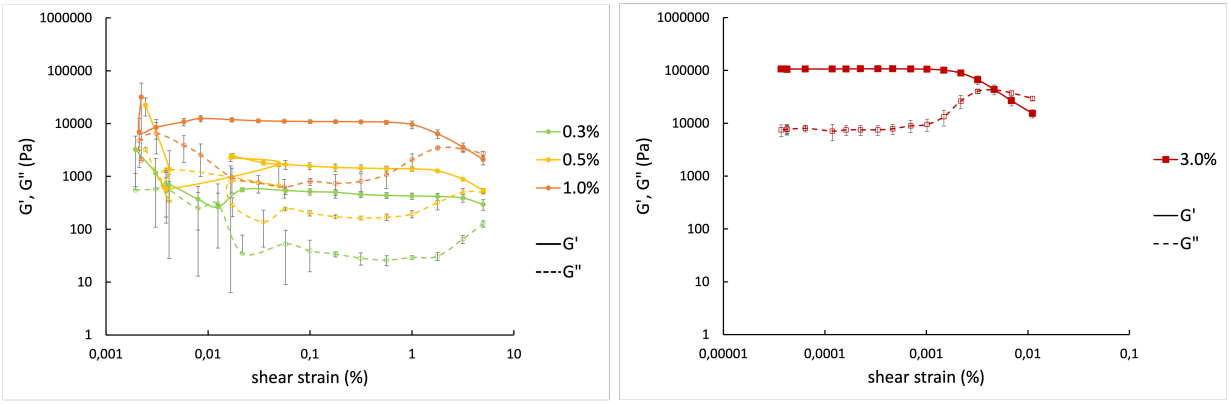

Figure 3.4: Storage and loss moduli obtained from AS tests for agarose gels prepared at various agarose concentrations, either by DMA (right) or rheology (left) measurements. *Note that the strain for DMA and rheology experiments is different so only the general behavior of the red curve should be compared to rheology measurements.*

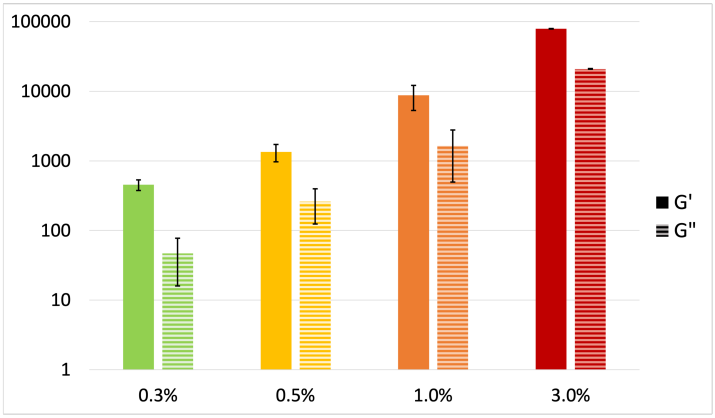

Figure 3.5: Mean storage and loss moduli computed based on the results from amplitude sweep (AS) tests in the linear viscoelastic region (LVER) for agarose gels prepared at various concentrations.

In the second instance, FS tests were performed to determine the frequency dependence of the moduli. The results are presented in Figure 3.6. Globally, the higher the agarose concentration, the greater the value of both the storage and loss moduli, just as it was already mentioned for the modulus values in LVER in AS tests. Furthermore, the storage moduli are consistently superior to their associated loss moduli, which once again accounts for the elastic dominance in the LVER for each of the tested gels. Additionally, the moduli do not exhibit any dependence on frequency except for the gel at 3% and tested by DMA, which shows a moderate influence of the frequency in the low frequency domain. Therefore the lower concentration gels exhibit a typical gel-like behavior, since G' is superior to G'' and since both modulus curves are constant when considered as a function of frequency. Although G' and G'' are not constant for the more concentrated gel (3.0%), the sample still exhibits a gel-like behavior. Indeed, the storage modulus remains invariably superior to the loss modulus even though the values do not stay perfectly constant over the frequency range. The slight changes in modulus values are due to dissipative modes that are only discernible at low frequencies since the time required to relax is sufficient in these conditions only. Increasing the concentration most probably implies that in some parts of the microstructure, local relaxation processes can take place, whereas those dissipative areas are not present in low concentration gels since the number of molecules required to form those independent network parts is not sufficiently high. As shown in Figure 3.7, a gel-like behavior

is characterized by a frequency (quasi-)independence of the moduli while exhibiting elastic dominance in the whole frequency domain, which corresponds to the behavior observed for the agarose gels at hand.

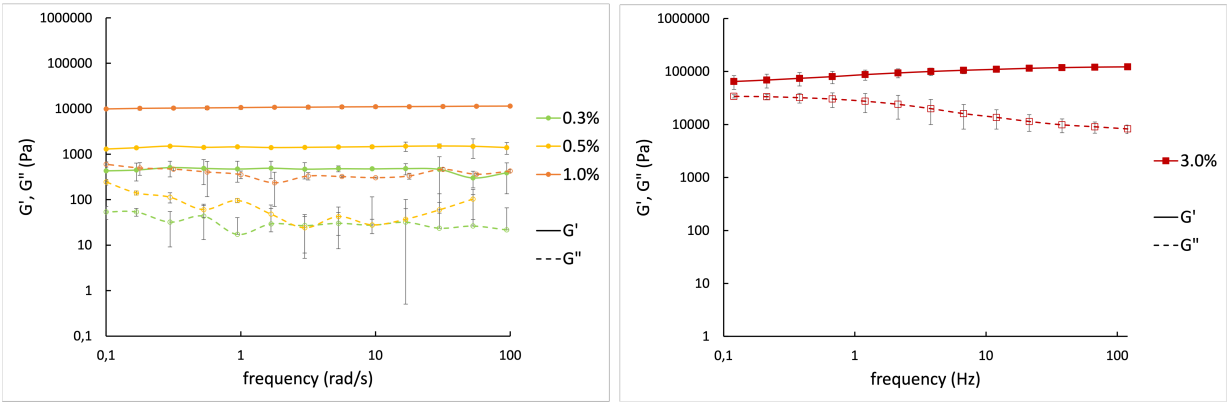

Figure 3.6: Storage and loss moduli obtained from AS tests for agarose gels prepared at various concentrations, either by DMA (right) or rheology (left). *Note that the frequency for DMA and rheology experiments is different (f vs ω) so only the general behavior of the red curve should be compared to rheology measurements.*

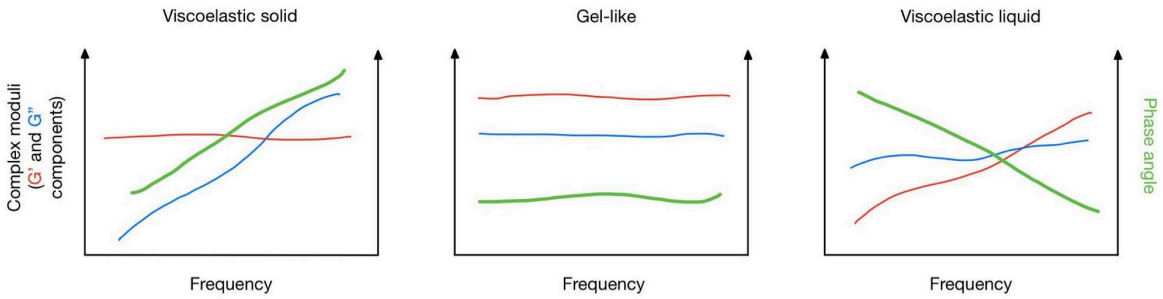

Figure 3.7: Responses of viscoelastic solid, gel-like and viscoelastic liquid materials (as inspired from Figure 6.5 of [11]).

Damping factor $\tan\delta$

The damping factor evolution obtained by means of AS tests is shown in Figure 3.8 and provides results in accordance with the ones deduced from the analysis of G' and G'': for small amplitude deformations, the elastic component is greatly dominant as the value of $\tan\delta$ is well below 1. Moreover, when comparing the results obtained from rheological measurements with one another, the LVER limit as well as the yield strain decrease with increasing agarose concentrations: the more concentrated the gel, the sooner the rise of $\tan\delta$ occurs upon deformation amplitude increase and the sooner it reaches 1, meaning the behavior switches from elasticity dominance to liquid-like dominance. As already mentioned for moduli interpretation, the results obtained by means of DMA should only be compared in terms of trend with the ones obtained by means of rheology as the shear is performed in a different fashion. However, it is important to note that the value of the damping factor in the LVER is very similar for every tested gels, meaning the importance of the elastic component as compared to the viscous one is similar for each one of them regardless of the agarose concentration in the steady regime.

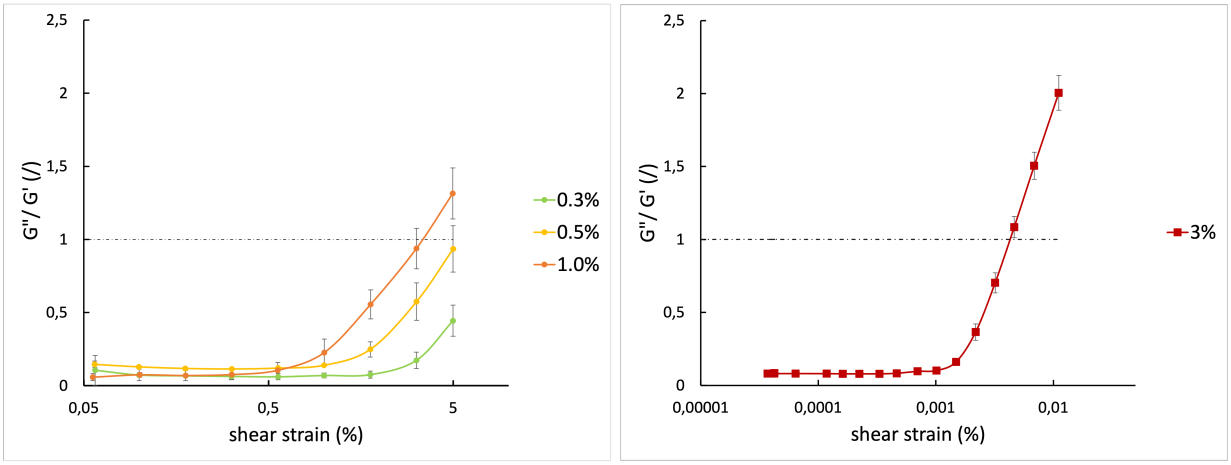

Figure 3.8: Damping factor obtained from AS tests for agarose gels prepared at various agarose concentrations, either by DMA (right) or rheology (left).*Note that the strain for DMA and rheology experiments is different so only the general behavior of the red curve should be compared to rheology measurements.*

The damping factor evolution as a function of shear strain frequency obtained by means of FS tests is depicted in Figure 3.9 and also provides results in accordance with the ones drawn from moduli analysis. Indeed, the value of $\tan\delta$ is stable for the lower concentration gels while the damping factor of the 3% concentrated gel becomes greater when the deformation frequency is very small. Despite this increase, $\tan\delta$ value never becomes greater than one, so the elastic behavior still remains dominant despite the local relaxation that can take place in the low frequency range. In this view all gels exhibit a gel-like behavior. It is worth noting that the obtained oscillations of $\tan\delta$ are probably due to the lack of sensitivity of the rheometer when measuring G'' at low frequency since the torque is very small.

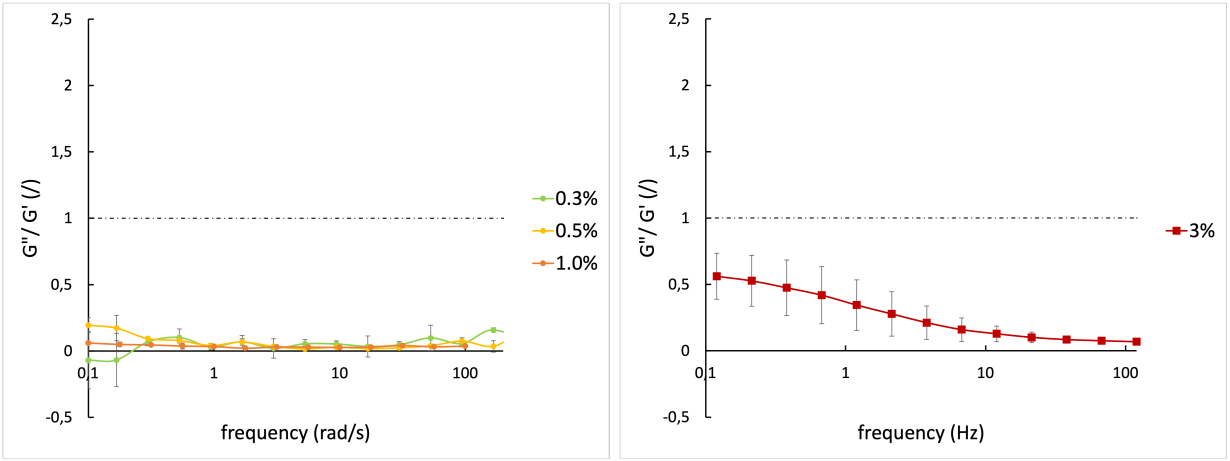

Figure 3.9: Damping factor obtained from FS tests for agarose gels prepared at various agarose concentrations, either by DMA (right) or rheology (left). *Note that the frequency for DMA and rheology experiments is different (f vs ω) so only the general behavior of the red curve should be compared to rheology measurements.*

Viscosity η

The viscosity of the gels was determined using data of the LVER of AS tests only, to obtain the steady viscosity. In the case at hand, as the frequency is fixed in AS tests, when the strain amplitude γ is increased, it corresponds to an increase in strain rate $\dot{\gamma}$, which is the reason why it is consistent to determine the steady viscosity using the LVER during AS tests as it corresponds to the steady regime. A bar chart representing the mean values of the viscosity along AS tests in the LVER for the different gels is shown in Figure 3.10. A clear tendency can be drawn: the viscosity of an agarose gel increases with the concentration. This effect was already determined in other works as it was described in Section 4.4 of Chapter 1, probably originating from the increase of crosslinking points density which in turn increases the resistance of the network to strain and consequently strain rate in the case of AS tests, which is the definition of η.

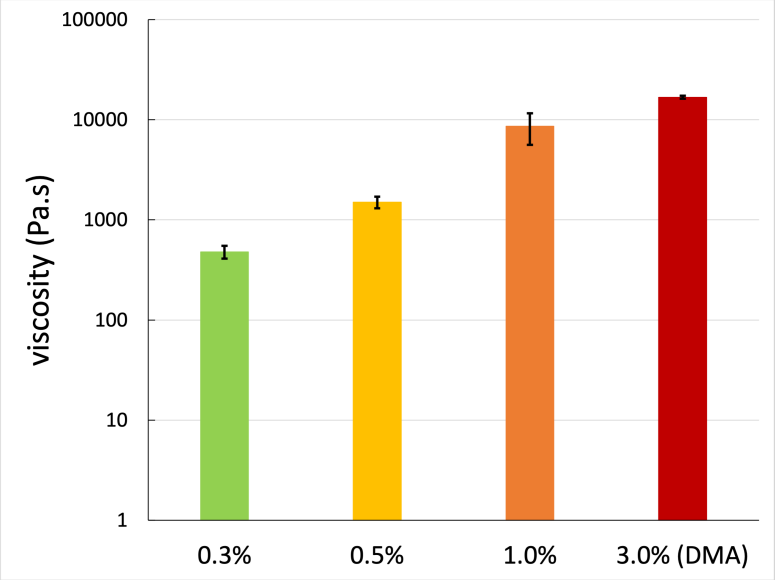

Figure 3.10: LVER mean viscosity obtained during oscillatory AS tests for agarose gels prepared at agarose various concentrations, either by DMA (red) or rheology (orange, yellow, green).

The viscosity means and the associated standard deviations are summarized in Table 3.7. It is worth noting that a quite large variability was obtained for the results obtained by means of rheology (0.3 and 1.0%) especially for the most concentrated gel, with a standard deviation value of almost 35% of the calculated mean value. This could be due to either an erroneous calculation or an erroneous measurement. On the one hand, as the 1% gel is quite rigid, the slippage problem which was already mentioned earlier in this work could have had an influence on the measurement of the viscoelastic properties of this gel. On the other hand, the measurement variability of the less concentrated gel could originate from the difficulty to place the sample in a reproducible way between the plates. Indeed, the 0.3% gel was very soft and could not be easily taken out of the Petri dish as it was viscous. Moreover, the gap was set as carefully as possible to avoid sample destruction while still maintaining contact between the plates and the gel, which was not an easy task.

Agarose (GS2) concentration	Viscosity (Pa.s)
0.3%	481 ±71
0.5%	1507 ± 201
1.0%	8601± 3000
3.0%	16779 ± 581

Table 3.7: Summary of the steady viscosity obtained for agarose gels prepared at various agarose concentrations, calculated using the data obtained from AS tests in the LVER.

4.2 Influence of the gel strength on the viscoelastic properties

In this part of the chapter, the results of the comparison between gels with different properties, namely gel strengths, at 0.5% and 1% w/v concentration are presented. As a reminder, the nomenclature '**x**%_GS**y**' is used, where **x** is the concentration w/v of agarose in the gel and **y** represents the gel strength ordered by decreasing order. The measurements were all obtained by means of a rheometer.

Moduli G′ and G″

In the first instance, AS tests were performed to determine the LVER and its upper limit but also for the possible destruction of the sample's (micro)structure. As it was the already the case for gels at various concentrations, no hysteresis was observed following the first AS test, meaning that the sample structure remained intact during the two successive AS tests in the selected deformation range. The selected shear strain amplitude used to perform the subsequent FS tests is 0.1% since this amplitude is in the LVER for each of the tested gels.

Based on the graphs presented in Figure 3.11, one can first make a general comment: for both agarose concentrations (left and right graphs on the Figure), the modulus values of gels containing agarose with higher gel strength are systematically higher than the ones prepared with an agarose power of lower gel strength, whether it is G' or G''. This result is in accordance with the manufacturer documentation as a higher gel strength means the force we can apply on the gel before it fractures is greater, which is related to the modulus values. Moreover, for each gel, G' is always greater than G'' for small amplitude deformations, accounting for the dominance of the elastic behavior over the viscous one.
Focusing on the moduli for 1% w/v gels, results similar to the ones obtained for concentration influence are observed in terms of gel strength. Indeed, the LVER limit as well as the yield strain are decreasing as the gel strength increases. Though GS2 and GS1 have rather different gel strengths (from simple to almost double), the gap between their LVER limits is not pronounced. However, the same trend is not completely true for agarose gels 0.5%. In fact, the GS1 storage modulus drop occurs after the one of GS2 gels and evolves almost like the curve of GS3 gels. Nevertheless, except for GS1, the trend observed for the 0.5% are similar to the ones of 1%. This divergence between the more and less concentrated samples are probably due to the fact that the torques are easier to measure for stronger and thus more concentrated gels as compared to softer gels for which the response torque can be very small. Once again, it is worth noting that the measurements for very small amplitude deformations exhibit a very high variability.

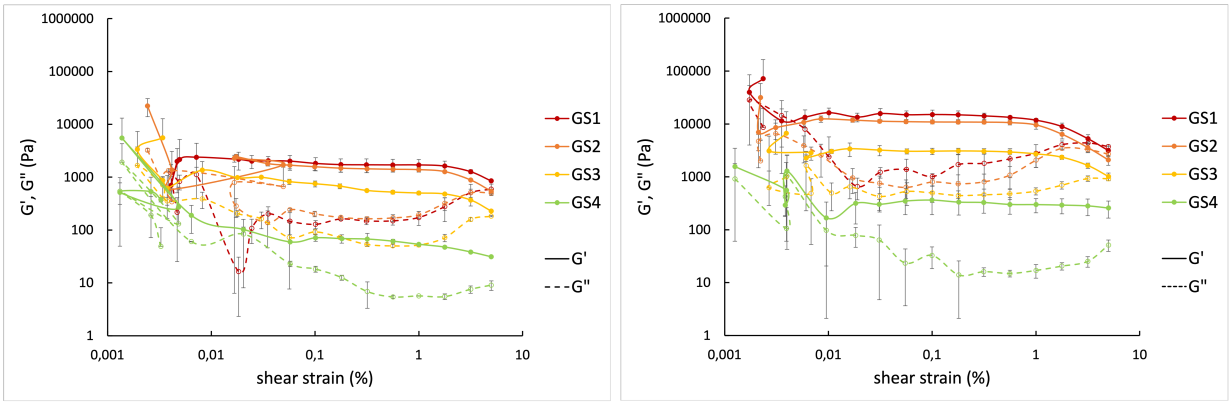

Figure 3.11: Storage and loss moduli obtained from AS tests using a rheometer for agarose gels prepared with agarose of different gel strengths at concentrations of 0.5% (left) and 1.0% (right)

In the second instance, FS tests were performed to determine the influence of deformation frequency on the gels. The results are presented in Figure 3.12. As already observed for AS, the moduli are systematically higher for stronger gels, except for G'' for the lowest concentration, which was discussed here above. Regardless of the concentration, the moduli do not exhibit any frequency dependence, meaning all agarose gels exhibit a gel-like behavior (cfr. Figure 3.7). It is worth noting that the variations observed for G'' are probably once again originating from the lack of torque sensitivity of the rheometer: the behavior of the storage modulus and the loss modulus are related to one another and when one of them is stable, the other should also be constant in theory. This phenomenon is more marked for gels at 0.5%, which have smaller moduli. This observation reinforces the previously stated hypothesis. The loss moduli measured for gels at 0.5% concentration are probably not consistent with the reality.

Furthermore, the storage moduli are consistently superior to their associated loss moduli regardless of the gel strength, which highlights the elastic dominance in the LVER for each of the tested gels over the whole frequency range.

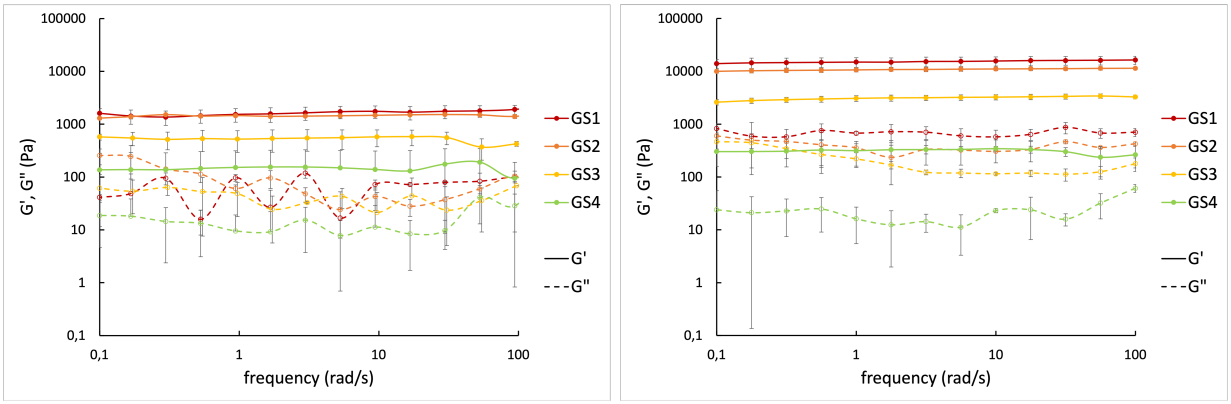

Figure 3.12: Storage and loss moduli obtained from FS tests using a rheometer for agarose gels prepared with agarose of different gel strengths at concentrations of 0.5% (left) and 1.0% (right)

Damping factor tan δ

The damping factor evolution obtained by means AS tests is shown in Figure 3.13 and the observations agree with the moduli analysis on some points but not on others. First, for both concentrations, the elastic dominance is confirmed for small amplitude deformations, since $\tan\delta$ is significantly smaller than 1 over this strain range. However, the LVER limit as well as the yield strain are not exactly following the trend established in the previous analysis: indeed, for gels at 1% the rise of $\tan\delta$ occurs at a smaller amplitude for GS2 compared to GS1 meaning the LVER is smaller for the less strong of these two gels. Moreover, the yield strain, which is the strain value at which $\tan\delta$ is equal to 1, is also larger for GS1 as compared to GS2 while the opposite was observed during moduli analysis. Focusing on the 0.5% gels, the deduced information is the same as the one drawn from the moduli: except for GS1, the LVER limit as well as the yield strain decrease when the agarose gel strength increases.
Besides this, the value of $\tan\delta$ is very similar for every gels in the LVER, independently of both the concentration or gel strength, ranging around 0.1 to 0.2. This means that the importance of the elastic behavior over the viscous one is the same, no matter the composition of the agarose gel, whether the agarose type or concentration changes.

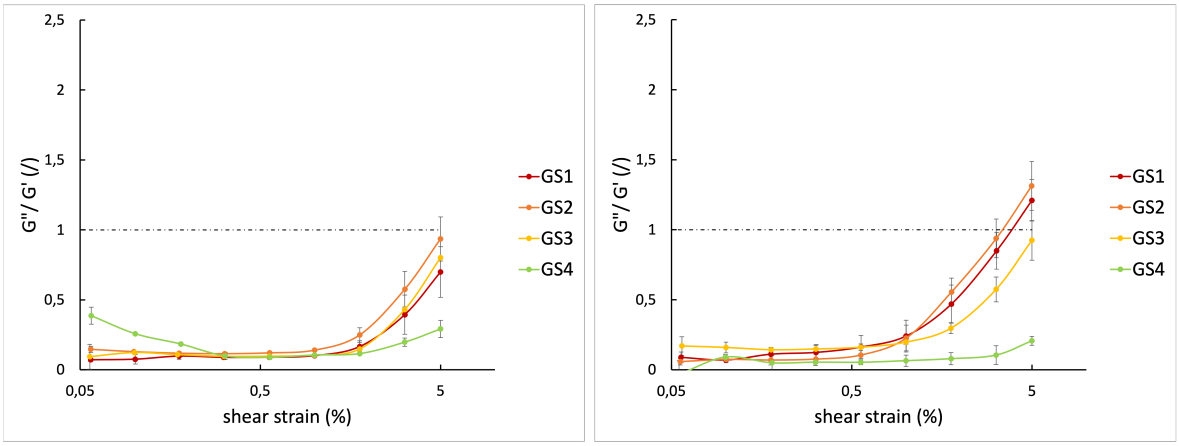

Figure 3.13: Damping factor obtained from AS tests for agarose gels prepared with agarose of different gel strengths at concentrations of 0.5% (left) and 1.0% (right)

The damping factor evolution as a function of shear strain frequency obtained by means of FS tests is depicted in Figure 3.14 and provides the following information: regardless of the agarose gel composition, whether it is its concentration or the used agarose type, the damping factor is frequency independent. This result is in accordance with the one obtained from the moduli: all the gels exhibit a gel-like behavior (cfr. Figure 3.7) and the elastic behavior is dominant over the viscous one. Furthermore, as already mentioned above for small amplitude deformations, the value of $\tan\delta$ is the same regardless of the gel strength and concentration, meaning the importance of the elastic component is the same for all gels. The oscillations could once again be due to the torque sensitivity of the rheometer, making the data noisy and less reliable.

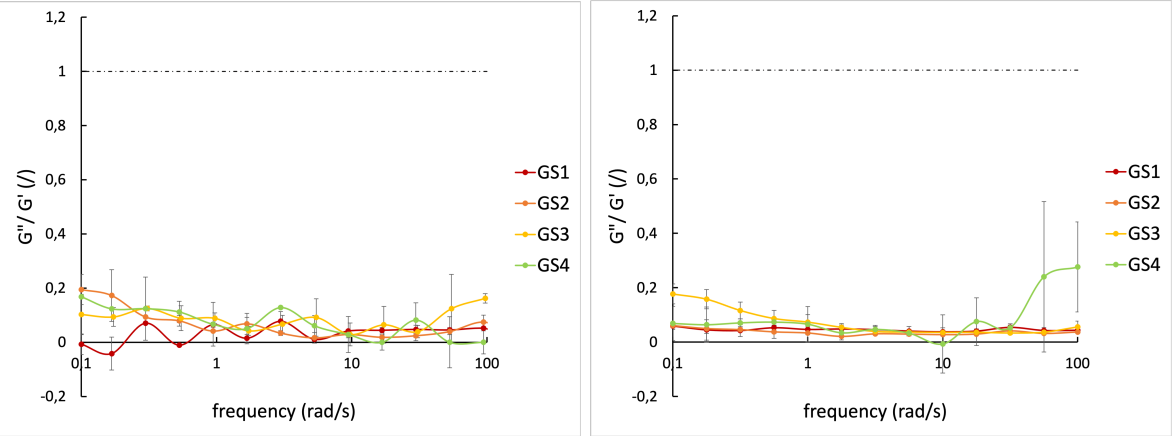

Figure 3.14: Damping factor obtained from FS tests for agarose gels prepared with agarose of different gel strengths at concentrations of 0.5% (left) and 1.0% (right)

Viscosity η

As already done for the influence of concentration, the viscosity of the gels was determined using data of the LVER of AS tests only, to obtain the steady viscosity. A bar chart representing the mean values of the viscosity along AS tests in the LVER for the different gels is shown in Figure 3.10. A clear tendency can be drawn: the viscosity of an agarose gel increases with the gel strength of the agarose.
In addition, it is worth noting that the influence of the concentration on viscosity is also confirmed as the viscosity is systematically higher for gels at 1% compared to 0.5% using the same gel type.

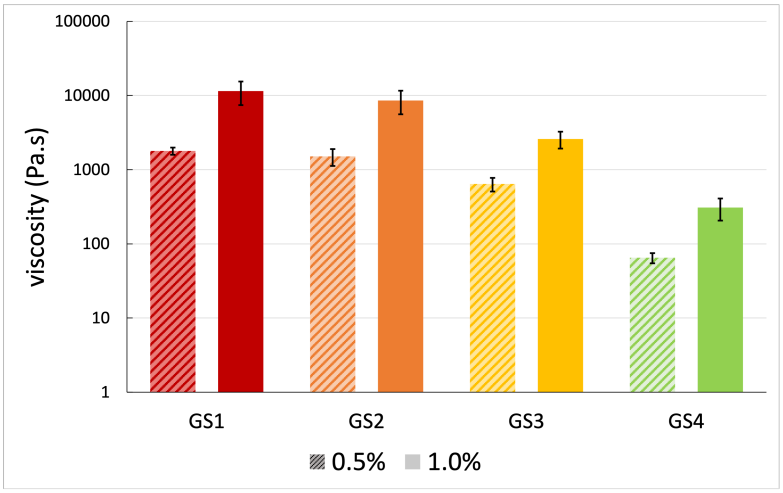

Figure 3.15: Viscosity obtained during mechanical tests for agarose gels prepared with agarose of different gel strengths at concentrations of 0.5% and 1.0%.

The viscosity means and the associated standard deviations are summarized in Table 3.8. It is worth noting that a quite large variability was observed for all gels, as the standard deviations are ranging for 10 to 35% of the associated mean value. This variation is even higher for the gels at 1% for which the standard deviation is around 30% of the mean viscosity for each gels. As mentioned earlier, the 1% gels are more rigid and prone to sample slippage, resulting in erroneous measurements. However, this does not justify the variability observed for

less concentrated gels. One can suppose that as the torque sensitivity of the rheometer causes inaccuracies for other properties and as the viscosity is related to the latter, the large deviation could originate from the equipment limitation.

	Viscosity (Pa.s)	
Agarose type	**Agarose concentration**	
	0.5%	1.0%
GS1	1789 ± 201	11449 ± 4009
GS2	1507 ± 387	8601 ± 3000
GS3	643 ± 136	2594 ± 670
GS4	65 ± 10	308 ± 102

Table 3.8: Summary of the steady viscosity obtained for agarose gels (0.5% and 1% w/v) prepared with agarose powders with different properties, namely gel strengths, calculated using the data obtained from AS tests in the LVER.

5 Conclusion of the chapter

In this chapter, the mechanical characterization of agarose gels prepared with agarose powders exhibiting different properties, i.e. gel strengths, and at different concentrations was achieved by means of rheology and DMA. Different tests were performed to get an insight on the behavior of such gels as a function of the applied shear strain or frequency. The storage and loss moduli, the damping factor and the viscosity were determined and the results were analyzed to better understand the influence of both the concentration and the gel strength on the hydrogel viscoelastic properties.

To sum up, for small amplitude deformations, an increase in concentration or in gel strength induces an increment in terms of moduli while the damping factor remains constant. This means that the gels become more rigid when increasing concentration or gel strength while the elastic dominance remains the same despite changes in composition. Except for the more rigid gel (3%_GS2), which displays a slight dependency on frequency, the gels properties are frequency independent, thus indicating a typical gel-like behavior. Still, the more rigid gel displays a gel-like behavior since the elastic dominance remains even though the moduli vary a little, which is mostly due to local relaxation in the gel in the low frequency domain, where dissipative modes can be activated since the time needed to relax is sufficient. During the FS, the damping factor always remains largely smaller than 1, once again highlighting the dominance of the elastic over viscous behavior. The viscosity follows the same trend as the moduli, it increases with concentration or gel strength.

It is worth noting that the rheology measurements were impaired in different ways. On the one hand the rheometer torque sensitivity was limiting to measure small torque, causing inaccuracy in all properties measurements, especially in soft gels. On the other hand, more rigid gels were prone to slippage which also caused noisy measurements. However, the general trend obtained are rather reliable despite the latter inaccuracies and are globally in accordance with the literature.

CHAPTER 4

Bacteria behavior in different agarose gels

This chapter aims to describe in details how we proceeded to determine the possible influence of agarose gelled culture media on *S. epidermidis* growth. In order to monitor bacterial growth, OD measurements but mostly fluorescence intensity were relied on. Moreover, microscopy methods, namely epifluorescence microscopy and CLSM, were used to observe the bacterial population from a morphological point of view to assess for viability but also growth mode. Finally, bacterial metabolic activity was investigated using AB assay.

1 Objective and strategy

As a reminder, the purpose of this work is to establish the link between the mechanical properties of different nutrient gelled media and the behavior of *S. epidermidis* bacteria. In order to understand the impact of the properties, different gelled media were prepared as already discussed in Chapter 3. Using the latter to culture bacteria, different parameters were monitored to get some insights on bacterial growth as well as their morphology and growth mode. Since this work is part of the project to design a patch to regulate skin dysbiosis, which is described in more details in Chapter 2, the bacterial parameters are monitored for *S. epidermidis* embedded in the agarose hydrogel.

In the first instance, the frozen bacteria were revived in liquid media and then concentrated in a NaCl solution for further reuse. This step is called bacterial culture. The bacteria were poured in nutrient broth and their growth was monitored based on OD measurements. Once the critical OD value was reached, the culture was stopped: the bacteria were concentrated by centrifugation and poured in a NaCl solution in order for the microorganisms to survive but not to proliferate anymore for further use. A suspension with glycerol was also prepared in order to cryo-preserve the culture bacteria and allow to revive them later, according to the same protocol, when fresh bacterial suspension is needed.

In the second instance, the growth of these bacteria obtained from the culture was assessed in gelled media. The bacteria were embedded to assess the behavior in conditions as similar as possible to the ones in the wells of

the patch. For this purpose, the fluorescence intensity was relied on. Indeed, the used bacteria were genetically engineered to express GFP through plasmid integration. As mentioned in Section 6.1 of Chapter 1, the fluorescence intensity is proportional to fluorophore concentration and thus growth was measured by measuring fluorescence intensity at a wavelength specific to GFP. To do so, a spectrometer was used to measure the fluorescence related to bacterial GFP in a 96-well microplate during 24 h to get a view on the time evolution of the bacteria in various media composition.

In the third instance, the morphology of the bacterial population and especially its growth mode were investigated using epifluorescence microscopy as well as CLSM. Taking images according to GFP wavelength enabled to spot if the bacteria tend to aggregate or not in the medium but also to assess a possible homogeneity in bacteria distribution.

Additionally, the metabolic activity of *S. epidermidis* bacteria was investigated using AB assay. The reduction of the blue resazurin to pink resorufin was measured using a spectrophotometer. However, as the bacteria used in this project are expressing a fluorophore, one first had to make sure the GFP fluorescence did not have any impact on the fluorescence measured to determine the amount of AB in its reduced form. After ascertaining that, the fluorescence related to the AB spectrum was measured using different agarose gels.

2 Materials

Bacteria: *S. epidermidis* strain engineered to express GFP in agar stab was kindly provided by Alexander Horswill and Jeffrey Kavanaugh (University of Colorado Denver - Anschutz Medical Campus, United State of America). It is a bacterial strain of *S. epidermidis* 1457 AH2983 that has been genetically engineered to express GFP thanks to plasmid integration and that does not form biofilms. The plasmid contains a resistance gene to chloramphenicol to select the bacteria expressing GFP. This bacterial strain is referred to as "GFP-*S. epidermidis*" in the present report.

Broth, antibiotics, sodium chloride and glycerol: Dehydrated Nutrient Broth (BD 234000) was purchased from BD Bioscience, chloramphenicol (C0378) and sodium chloride (S7653) were purchased from Sigma-Aldrich. Glycerol (10021083) was purchased from Thermo-Fisher Scientific.

Agaroses: As in the previous chapter, different agarose powders were purchased from Sigma Aldrich, their characteristics are summarized in Table 3.1 of Chapter 3.

AlamarBlue: AlamarBlue Cell Viability reagent (A50100) was purchased from ThermoFisher Scientific.

Water and other solutions: Milli-Q water, also known as ultrapure water, was obtained from a Merck Millipore system. It was characterized by a resistivity of 18.2 MΩ·cm.

3 Protocols

When working with bacteria, strict sterile conditions are necessary to avoid contamination by and/or of the bacteria. To that end, every handling should take place in a safety cabinet and every tools as well as solutions, tubes and

containers must be sterile or autoclave sterilized beforehand. Once a solution has been autoclaved, the container should never be opened outside of the cabinet to maintain sterility.

3.1 Bacterial culture

This step corresponded to the revival of the bacteria and their optional cryo-conservation afterwards. This experimental protocol took place in the following way.

1. **Preparation of a stock antibiotics solution:** In 10 mL of ethanol, 0.1 g of chloramphenicol was dissolved. The solution was stirred to dissolve the antibiotics while preventing exposure to light using aluminium foil.

2. **Preparation of the broth with antibiotics:** For the purpose of selecting only GFP-*S. epidermidis* which integrated the plasmid, chloramphenicol use was mandatory. First, 4 g of dehydrated nutrient broth was dissolved into 500 mL of ultrapure water. The solution was autoclaved. In the safety cabinet, 0.5 mL of the chloramphenicol stock solution was added to the broth and mixed gently.

3. **Preparation of the glycerol/water solution:** 100 mL of viscous glycerol and 100 mL of ultrapure water was poured in a bottle. The solution was mixed and agitated until homogenization was reached. The solution was sterilized by means of the autoclave.

4. **Preparation of the saline solution:** 4.38 g of NaCl was added to 500 mL of ultrapure water to obtain a final concentration of 15mM to match concentrations similar to the ones on the skin. The pH was adjusted to 6. The solution was sterilized by means of the autoclave.

5. **Preculture:** Two vented tubes were filled with 8 mL of autoclaved broth with antibiotics. From a tube containing cryo-preserved GFP-*S. epidermidis* 1457 AH2983 bacteria, a small piece of bacteria was collected by means of a loop and poured into each tube. The tubes were closed and the bacteria were dispersed in broth. The cap was slightly pulled to allow ventilation and the tubes were incubated at 37 °C at 180 rpm overnight.

6. **Culture:** In a sterile culture flask, 200 mL of fresh broth with chloramphenicol was added. The content of both vented tubes was poured in this flask and the bacteria were dispersed in the broth. The culture flask was incubated at 37 °C at 180 rpm. The spectrometer used was the Infinite 200 PRO plate reader (Tecan; serial number: 1810011954), in combination with the associated i-control software (Tecan). The OD was monitored by means of this spectrometer at a wavelength of 540 nm and the fluorescence intensity related to GFP expression was measured at excitation and emission wavelengths of respectively 488 and 515 nm. Cuvettes were used to measure the OD_{540} while fluorescence was monitored in a 96-well microplate. The first measurements were performed at 1-hour intervals but once the OD_{540} reached a value of 0.3, the measurements were performed closer together since the bacteria entered the exponential growth phase. Measurement were recorded until the culture reached a critical OD_{540} value of $\sim$0.45. The culture was stopped the following way: 40 mL of culture liquid was poured in four separate 50 mL centrifugation tubes and the latter were centrifuged at 4000 rpm for 5 minutes. The supernatant of each tube was discarded.

7. **Fresh bacteria suspension:** In one of the tubes centrifuged earlier, 20 mL of the 15 mM NaCl solution was added and the solution was vigorously agitated to disperse the bacteria pellet by shaking and vortexing. The solution was transferred into one of the other tubes containing bacteria and the bacteria were dispersed by vigorous agitation. The tube was centrifuged at 4000 rpm for 5 minutes and the supernatant was discarded.

5 mL of 15 mM NaCl solution was added to disperse the pellets and the solution was transferred into a 15 mL centrifugation tube. The bigger tube that was last centrifuged was rinsed three times with 2 mL of NaCl solution and the content was transferred to the 15 mL tube. Lastly, the 15 mL tube was centrifuged at 4000 rpm for 5 minutes and the supernatant was discarded. 8 mL of NaCl solution was added and the bacteria were dispersed by shaking vigorously and vortexing. *If the fresh suspension is not immediately needed, it can be stored in the refrigerator and be used up to one week after the culture.*

8. **Cryo-conservation:** In one of the tubes centrifuged at the end of the culture, 20 mL of broth with chloramphenicol was added and the tube was vigorously agitated to disperse the bacteria pellet. The content of this tube was transferred into the last tube obtained when stopping the culture. The tube was agitated vigorously to disperse the pellet and 20 mL of glycerol/water mix was added. The tube was agitated and stored in the freezer at -80 °C.

3.2 Medium preparation

The preparation of the media took place as already described in Section 3.1 in the previous chapter. Solutions ranging from 3% to 0.3% of agarose A9918 (GS2; gel strength $\geq$ 1000 g.cm^{-2} at 1%) were prepared as well as solutions at a concentration of either 0.5% or 1% for all agarose types. A9918 agarose was selected to prepare gels of various concentrations since it has a rather high gelling capacity, making it easy to cover a wide range of mechanical properties. Moreover, since it solidified rapidly at room temperature but not too much, its easy handling was also taken advantage of. Three solutions were prepared to assess concentration effect while four were prepared to assess gel strength effect.
Moreover, an additional 25 mL bottle was used to prepare 25 mL of liquid broth by mixing 0.2 g of dehydrated broth in 25 mL of ultrapure water and autoclaved together with the agarose media. An example of the set of media that were prepared for an experiment is presented in Table 4.1, media were named according to the same nomenclature as in Chapter 3.

Medium name	**Description**	**Weight (g) for 25 mL of medium**
3.0%_GS2	Agarose A9918 3.0%	0.75
0.5%_GS2	Agarose A9918 0.5%	0.125
0.3%_GS2	Agarose A9918 0.3%	0.075
1.0%_GS1	Agarose A0576 1.0%	0.25
1.0%_GS2	Agarose A9918 1.0%	0.25
1.0%_GS3	Agarose A4018 1.0%	0.25
1.0%_GS4	Agarose A5030 1.0%	0.25

Table 4.1: Summary table of the composition of the agarose gelled media used to perform bacterial assays.

3.3 Microplate preparation

As the gelled media solidified quite rapidly when cooled down, it was more appropriate to prepare the 96-well microplate before the autoclave cycle ended. In this purpose, the fresh bacteria suspension was taken out of the fridge and shaken to suspend the bacteria in the tube in the safety cabinet. Afterwards, 30 μL of the bacterial suspension was collected and poured in each well in which the culture was monitored. Five samples for each ster-

ilized media were used with bacteria while wells containing media without bacteria were used as negative controls. The remaining wells were filled with sterile water to avoid dehydration of the gels during the culture. In some experiments, the suspension was diluted 100 or 1000 times in sterile 15 mM NaCl solution and the same volume as for the initial suspension was added in the wells. This procedure allowed to get insight on the possible effect of initial bacteria concentration in agarose gelled media.

Once that was done and the gels were ready to be taken out of the autoclave, we proceeded with the more concentrated agarose gel, i.e. 3.0%_GS2, first as it was the one that solidifies the fastest. To facilitate the manipulation of this gel, we advise to cut the extremity of the collection tip to avoid any imprecision in the measured volume due to the adherence of the gel on the tip edges. First, the reference well (negative control) was filled with 200 μL of the hot 3.0%_GS2 solution. Second, 170 μL of this solution was added in each well with bacteria assigned to this gel. The filling process was reiterated with the other gels beginning with the more concentrated and strong gels and finishing with the liquid broth, to avoid gelation prior collection of the gels. An example of how to place the gels and bacteria in the microplate is proposed in Figure 4.1 considering the solutions presented in Table 4.1.

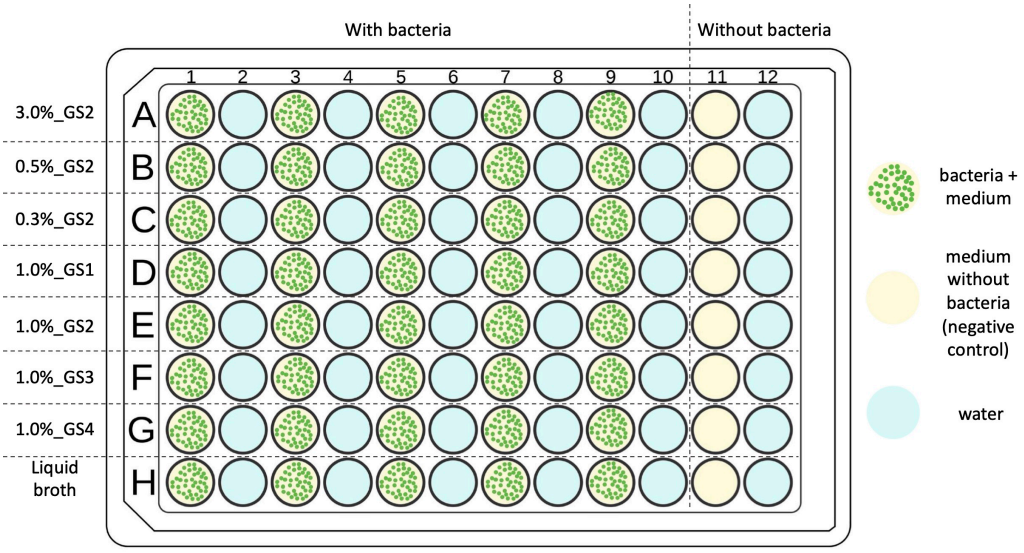

Figure 4.1: Description of the well plate used to perform bacterial assays.

3.4 Fluorescence spectroscopy

To assess bacterial growth, the microplate fluorescence intensity was measured for 24 h. For this purpose, the Infinite 200 PRO plate reader (Tecan; serial number: 1810011954) was used in combination with the associated i-control software (Tecan). Using this spectrophotometer, a 24 h cycle was performed during which the fluorescence intensity for an excitation wavelength of 488 nm and an emission wavelength of 515 nm was measured. The temperature within the spectrophotometer was kept at 37°C during the whole cycle so that the plate reader served as incubator. The gain of the fluorescence intensity was set to 75 dB to avoid intensity measurement saturation. The data were made available in the form of an Excel datasheet. These data were processed using Excel (Microsoft) and Igor (Wavemetrics) softwares.

3.5 Epifluorescence microscopy

As the bacteria express GFP, the Olympus IX71 inverted epifluorescence microscope was used to image bacterial population in the gels, using x20, x40 and x60 lenses. For this purpose, the bacteria were observed using the green channel either on glass slides or in the microplate. For this, small gel pieces were taken out of the plate using a spatula after spectrophotometer measurements and deposited on the glass slides and subsequently covered with glass coverslips, thinning as much as possible the gel containing embedded bacteria to ease microscopy observation. Some images were also taken using a LabTek (see Figure 4.2) as container for the gels, after incubation during 24 h at 37°C, prepared following the same protocol as for microplate filling.

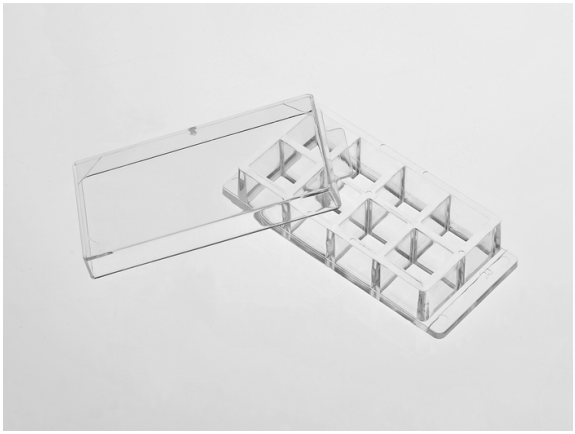

Figure 4.2: Labtek illustration[119]

3.6 Confocal laser scanning microscopy

To overcome the limitations related to epifluorescent microscopy as the sample were not liquid enough to not encounter blurring due to out-of-focus fluorescence, a confocal laser scanning microscope (CLSM) was used to get images with higher resolution and contrast by preventing the blur thanks to point-illumination. The green canal was also used during these microscopy measurements as well as a x60 objective. The samples were casted and observed in LabTek wells after 24 h of incubation. Z-stack imaging was performed to obtain 3D reconstructed images using Airyscan technology. This technology enables to increase even further the resolution compared to conventional 3D reconstruction. The Airyscan has a 32-channel detector array with a hexagonal array of micro lenses that act as a system of very small pinholes.[103]

3.7 Influence of GFP fluorescence on reduced AB fluorescence

To get information on the metabolic activity of GFP-*S. epidermidis* in various gelled media, AB reagent was chosen among the other molecules detailed in Section 6.3 of Chapter 1. However, as the bacterium used in this project fluoresces due to GFP expression, it was necessary to make sure the fluorescence measured to assess for AB reduction and thus bacterial metabolic activity was still reliable despite the presence of GFP. To this end, a bacterial culture was done in broth as described earlier until the OD reached ∼0.45 so that the bacteria were in the exponential growth phase. Part of the culture broth was subsequently diluted 100 times in fresh broth and 180 μL of the latter was poured in each well of a microplate. 20 μL of AB reagent was added in these wells and the microplate was incubated for 30 minutes in the dark. The fluorescence intensity related to the presence of the reduced form of AB reagent was measured ($\lambda_{excitation}$=530 nm, $\lambda_{emission}$=590 nm). Then, 200 μL of dilute culture broth was used as reference, and also incubated in a microplate and the fluorescence was measured in the same way. Finally the results obtained in the presence or the absence of AB reagent were compared.

3.8 AB assay

The gelled media prepared for this experiment were the same as the ones used to monitor bacterial growth. The seven gelled media are prepared according to the protocol introduced in the previous chapter and 25 mL liquid of broth was also prepared and autoclaved with the gel solutions. Just before the autoclave cycle came to an end,

the wells of a sterile microplate were filled with 27 μL of the 100 times diluted suspension of fluorescent bacteria. Dilution aims to avoid saturation of the intensity measured by the microplate reader. To those wells, 20 μL of AB reagent was added as well as to empty wells to serve as references (negative controls) for each tested medium. Once the gels were autoclaved, 153 μL of each gel was poured in the 5 wells attributed to this gel and 180 μL in the associated reference well. The remaining wells were filled with autoclaved water and the fluorescence intensity evolution was measured at 37 ° C during 24 h using the spectrophotometer. To measure the fluorescence related to AB reduction, $\lambda_{excitation}$ = 530 nm and $\lambda_{emission}$ = 590 nm were selected.

4 Results and discussion

In this section, the results obtained for bacterial behavior assessment are presented. In the first instance, the possible interference of GFP signal on AB fluorescence is investigated. In the second instance, bacterial behavior assessment per se is dealt with. First, the influence of the concentration of the agarose gel medium will be investigated, followed by the influence of its gel strength and concluding with general remarks.
In each of these two sections, the influence on growth measured by means of fluorescence spectroscopy is discussed, followed by morphological characterization of the bacteria as well as determination of their growth mode thanks to microscopy results. Finally, the possible effects of the mechanical properties of the medium on the metabolic activity of GFP-*S. epidermidis* populations are discussed.

4.1 Study of the possible interference of GFP signal on AB test

The results obtained when measuring the fluorescence related to resozurin presence, i.e. AB reduction (cfr. Section 6.3 of Chapter 1), are presented in Figure 4.3. As the fluorescence intensity measured in wells in the absence of AB reagent is zero along the whole measurement cycle, whereas it is not the case in the presence of the reagent, there is no interference of GFP on the measurement of the fluorescence intensity caused by the presence of the reduced form of AB. The use of AB to investigate the metabolic activity of fluorescent strains of GFP-*S. epidermidis* is thus possible and a priori reliable.

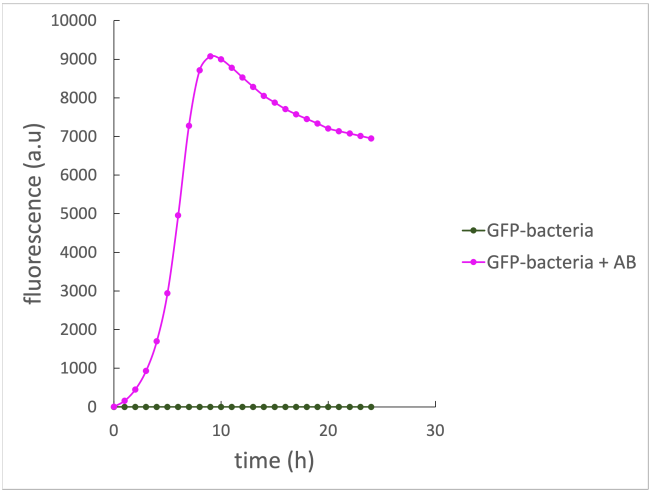

Figure 4.3: Variation of the fluorescence signal corresponding to alamarBlue (AB) reduction ($\lambda_{ex.}$ = 530 nm; $\lambda_{em.}$ = 590 nm) vs culture time, measured for GFP bacteria supplemented or not with AB reagent.

4.2 Influence of the agarose concentration

Bacterial growth

On the basis of the measurements obtained with the microplate reader, fluorescence intensity evolution is plotted using the mean value among similar wells, except for some outliers, for each concentration. The standard error is also computed to get insight on the variability upon measurement. In Figure 4.4, a typical example of the evolution of the fluorescence intensity vs culture time is shown. It is evaluated for agarose gels prepared with different concentrations of agarose GS2. Based on the graph, one can notice a trend: when decreasing the agarose concentration, the fluorescence intensity increases faster with time and the final fluorescence intensity reached after 24 h is higher in comparison to more concentrated gels. It is worth noting that the broth, which corresponds to a zero concentration of agarose, also follows the previous established trend.

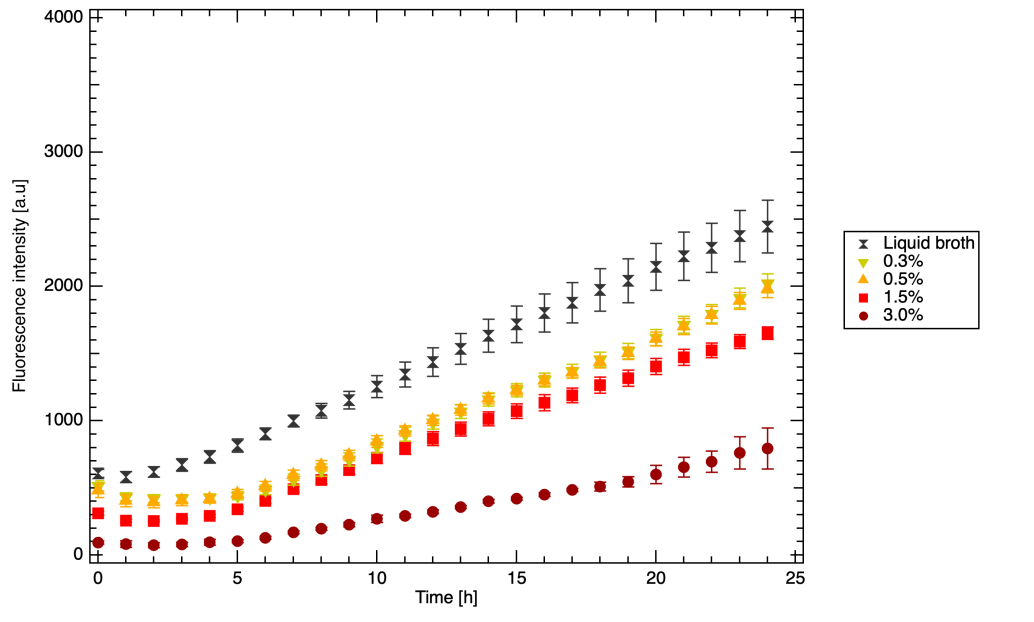

Figure 4.4: GFP Fluorescence intensity ($\lambda_{ex.}$: 488 nm; $\lambda_{em.}$: 515 nm) evolution of GFP-*S. epidermidis* in agarose (GS2) gelled media prepared with various agarose concentrations.

As it is deduced that the evolution of the fluorescence was either fast or slow depending on the concentration in comparison to gels prepared at a different agarose concentration, we look into the derivative of this evolution. In order to obtain a relatively smooth derivative, the curve is first interpolated and its derivative is calculated with Igor software. The parameters of the interpolation function are adapted each time to reach the best possible compromise between interpolation fidelity and noise in the associated derivative. An example of interpolation and the related derivation of the previous graph is available in the Appendix (Figure A.1) as well as a graph showing the fluorescence evolution over time for a different experiment day (Figure A.2). Moreover, the effect of bacteria concentration is assessed by dilution of the bacterial suspension used to seed the gel prior incubation and measurement in the spectrophotometer. In Figure 4.5, the evolution of the GFP fluorescence using bacterial suspensions with dilution factors of 1 or 100 as well as its derivative are shown. The derivative of the fluorescence intensity is referred to as 'fluorescence intensity rate', respectively 'rate' in this section. On the graph, the rates seem to first increase and then to become slightly unstable to finally stabilize around a certain rate value which is different for the different gelled media. The steady rate region is approximately reached after 5 h of culture. When considering the rate

values reached in the steady rate regime, the assumptions made earlier are confirmed: the rate is greater for less concentrated media whereas it is lower for more concentrated gels. This hypothetical trend seems valid whether the suspension is dilute or not. Moreover, the effect of the dilution of the bacterial suspension can also be highlighted: the initial fluorescence intensity is much lower for a lower bacterial concentration, which seems logical since for a low number of microorganisms, the amount of synthesized GFP is much smaller. Furthermore, the rate also seems to be influenced by the initial GFP-*S. epidermidis* concentration: the rate is smaller when a dilute suspension is used.

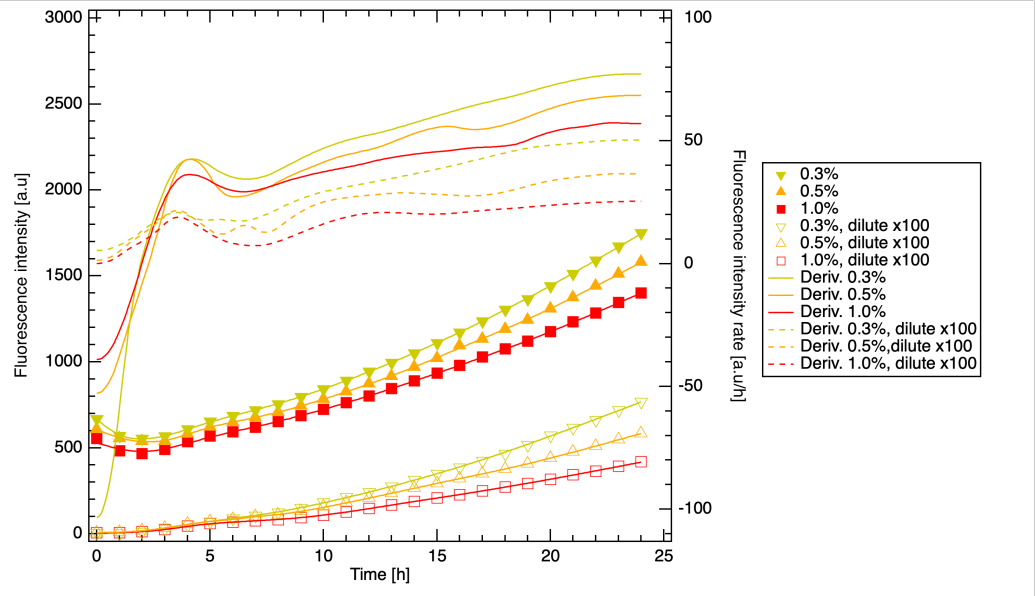

Figure 4.5: GFP fluorescence intensity ($\lambda_{ex.}$: 488 nm; $\lambda_{em.}$: 515 nm) evolution of dilute or undilute GFP-*S. epidermidis* grown in agarose (GS2) gelled media for various agarose concentrations and related fluorescence intensity rate (computed from derivatives of the fluorescence intensity vs time); dotted line stands for a suspension dilution factor 100 of the bacterial suspension, solid line stands for a dilution factor of 1.

Epifluorescence microscopy images

Epifluorescence microscope images were taken for two extreme agarose concentrations that were prepared to serve as the gelled culture media, i.e. 0.3% and 3.0% of agarose (GS2). Representative images of the bacterial populations observed after 24 h of culture in these two particular gels are presented in Figure 4.6. Gels were observed on glass slides using the x60 objective of the microscope and the bacterial suspension used to seed the gels was diluted 100 times to facilitate image capture. Indeed, a too large amount of bacteria induces a very high fluorescence intensity which makes it difficult to take images of satisfactory quality.

On the one hand, GFP-*S. epidermidis* bacteria growing in the lower concentration medium (0.3%) are shown in Figure 4.6(a). The presented image is reconstructed from various overlapping shots in order to capture a larger sample surface. Bacteria are rather dispersed in the medium and do not aggregate in a considerable way, being limited to aggregates of only a few cells. This behavior resembles the planktonic mode of growth that was mentioned earlier in the literature overview in Chapter 1.

On the other hand, bacteria growing in the more concentrated medium (3.0%) are presented in Figure 4.6(b). The

differences are quite marked between this image and the one analyzed here above. Indeed, in the less concentrated medium, the bacteria seem to grow in a planktonic way whereas they form huge aggregates in the 3.0% agarose gel, which resembles a biofilm growth mode more than a planktonic one. Larger images unfortunately cannot be obtained for this gel due to the green fluorescence background that hinders image reconstruction. Indeed, the bacteria that are out of focus and that fluoresce contribute to the image. This is notably due to the higher thickness of this sample. Indeed, the 3.0% gel is very rigid and even if great care was taken to ensure that the thickness between the glass slide and the cover slip is minimal, the sample was still too thick to avoid this blurring effect.

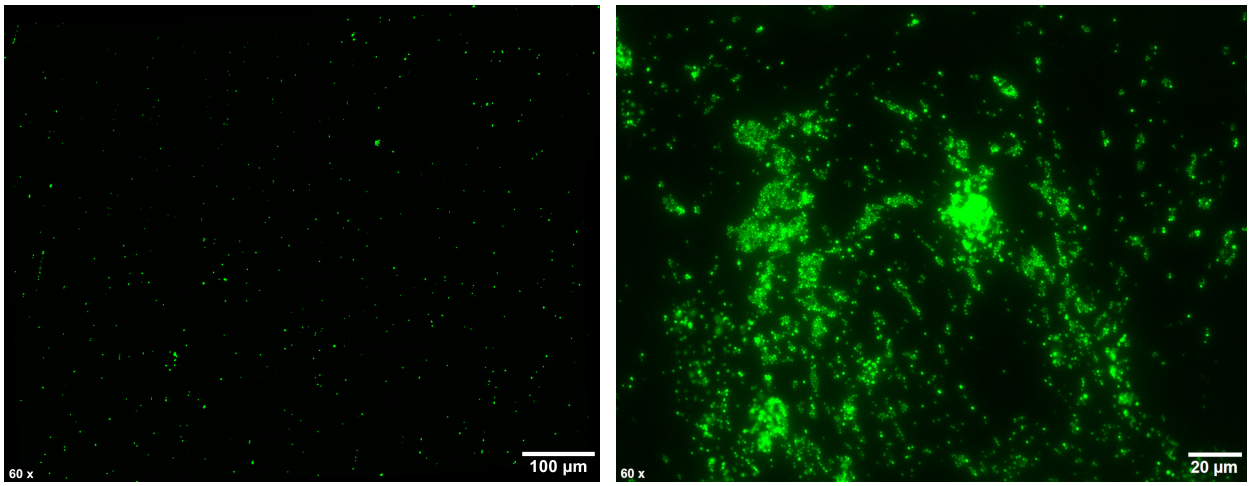

(a) 0.3% (b) 3.0%

Figure 4.6: Epifluorescence microscopy (Olympus IX71; x60 objective) images of GFP-*S. epidermidis* (dilution factor of the suspension: 100) grown for 24 h in 0.3% (left) and 3.0% (right) agarose (GS2) gelled media (observed on glass slides).

However, some behavioral heterogeneity is observed. Unfortunately, the use of glass slides to observe the gels inevitably involves the sampling of a piece of the gelled media and its subsequent crushing and thus deterioration. To be able to observe the bacteria grown in unaltered gel media, the wells of a microplate or a LabTek can be used. Moreover, it also allows to scan a larger sample portion since the observed object is not just a small gel piece anymore. LabTek is more suited to microscopy imaging since the bottom of the wells is specially designed to this end, in our case the bottom was a glass slide (borosilicate). Therefore, the images shown in Figure 4.7 are taken in LabTek wells for both of the considered medium concentrations. In Figure 4.7(a), some aggregates are forming in the 0.3% agarose medium. Even tough the rest of the image highlights the general planktonic behavior of the GFP-*S. epidermidis* population in this gel, some regions, especially the border of the wells, are exhibiting more or less aggregates. This sort of aggregate growth could be explained by the manner the bacterial suspension was poured in the LabTek. Indeed, the bacterial suspension forms a drop to minimize contact with the bottom surface of the LabTek. The bottom glass of the wells is probably treated to be hydrophobic and thus promote cell adhesion, possibly resulting in higher bacterial density in places where the drop formely was prior to gel casting. Moreover, bacterial cells are known to adhere readily on hydrophobic surfaces due to the nature of their envelope, which could also explain why aggregates form. On the contrary, single cells are observed in a great number in Figure 4.7(b) for a 3% agarose medium, even tough large aggregates are in large numbers. This variability in both media types highlights the fact that not one or the other growth is the only one to govern bacterial behavior but that more concentrated gels seem to drive towards biofilm growth more than less concentrated gels for which the growth is

more similar to the one in liquid media, namely planktonic growth.

Furthermore, it is worth noting that in all images, blur is caused by out of focus bacteria. This effect is predominantly disruptive for the analysis of images obtained using the most concentrated gels, probably due to the sample thickness as already mentioned for glass slides but also due to the tremendous fluorescence intensity of the 3D aggregates related to the out-focus bacteria that compose it, making it difficult to have images that are faithful to reality.

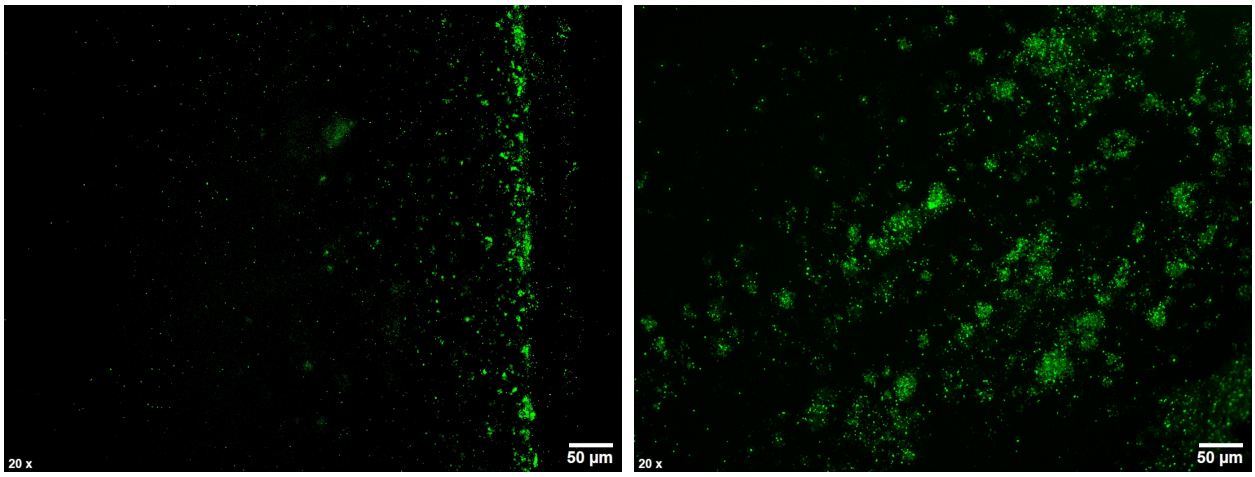

(a) 0.3% (b) 3.0%

Figure 4.7: Epifluorescence microscopy (Olympus IX71; x20 objective) images of GFP-*S. epidermidis* (dilution factor of the suspension: 100) grown for 24 h in 0.3% and 3.0% agarose (GS2) gelled media (observed in LabTek wells).

Furthermore, it is worth noting that in all images, blur is caused by out of focus bacteria. This effect is predominantly disruptive for the analysis of images obtained using the most concentrated gels, probably due to the sample thickness as already mentioned for glass slides but also due to the tremendous fluorescence intensity of the 3D aggregates related to the out-focus bacteria that compose it, making it difficult to have images that are faithful to reality.

Supplementary epifluorescence microscope images are available in the Appendix section.

CLSM images

CLSM allows to avoid the blurring effect encountered earlier using epifluorescence microscopy as bacteria out of focus are not contributing to the image anymore. Representative images of GFP-*S. epidermidis* population in 0.3% and 3.0% gelled culture media are shown in Figure 4.16, using 100 times dilute bacteria suspension. The samples were observed in LabTek wells.
On the one hand, bacteria growing in the lowest concentrated agarose gel (Figure 4.8(a)) exhibit the same behavior as deduced using the epifluorescence microscope: bacterial cells are rather dispersed and few aggregates composed of a few number of cells can be observed, the growth is rather similar to planktonic growth.
On the other hand, images in the higher concentration agarose also confirm the assumption made in the previous analysis: cells tend to aggregate in a much larger extent than for 0.3%, the growth mode tends to biofilm growth,

although free cells can still be spotted. Moreover, the fluorescence of the aggregates is very high. This phenomenon is problematic: when one wants to image single cells, saturation is observed for the aggregates when increasing the time exposure to be able to see free bacteria. Consequently, it is not possible to be sure that all planktonic cells in the plane are imaged properly because of this problem. Still, we can assess that more aggregates are forming in the more concentrated gel as compared to the less concentrated.

In summary, the deductions made with the previous observation technique are confirmed by CLSM images, that are of much better quality, allowing to get rid of blur.

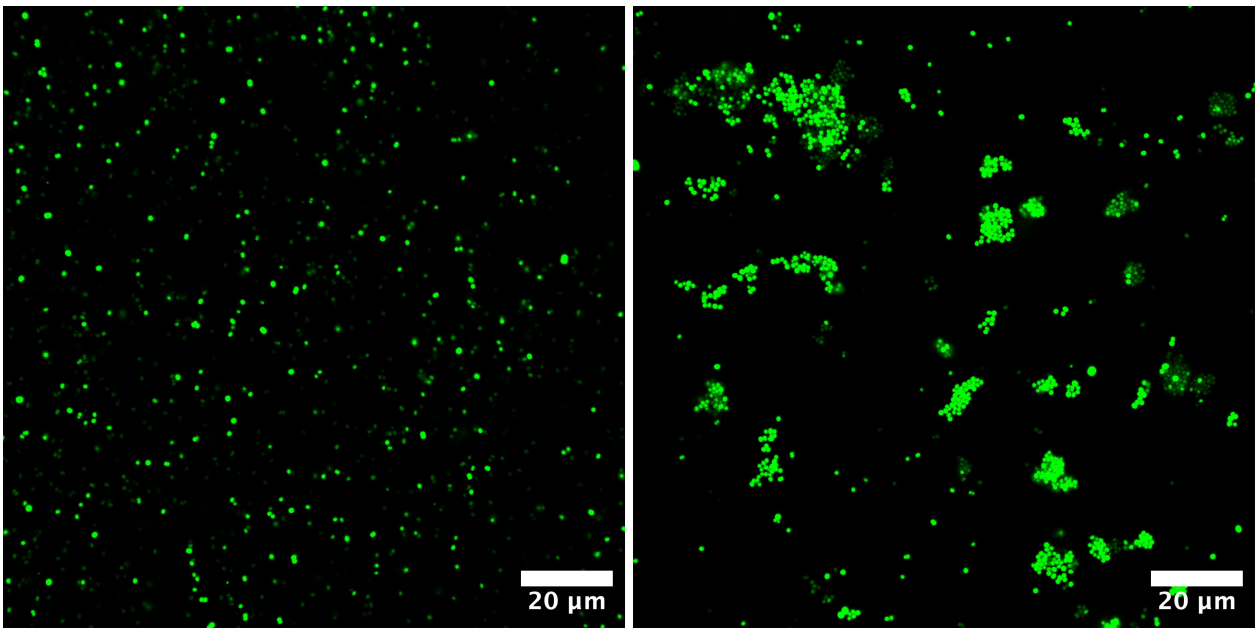

(a) 0.3% (b) 3.0%

Figure 4.8: CLSM images of GFP-*S. epidermidis* (dilution factor of the suspension: 100) grown for 24 h in 0.3% and 3.0% agarose (GS2) gelled media (observed in LabTek wells)

In addition, CLSM was also used to perform 3D observations of the samples, using 3D reconstructed images obtained thanks to the Airyscan technology. Projections of the obtained reconstructed 3D images taken in both gels are shown in Figure 4.9. The images were recorded starting from the bottom of the LabTek well up to a few micrometers above the bottom surface of the LabTek in the gel. The diffusion of GFP-*S. epidermidis* from the bottom surface where the suspension was poured initially, to the gel seems to be different, depending on the agarose concentration. Indeed, the bacteria grown in 0.3% medium (Figure 4.9(a)) are forming a more dispersed bacterial mat on the surface of support (bottom of the image) and seem to diffuse as single cells in the gel and subsequently form very small aggregates when growing or diffuse further in the medium. On the contrary, a very dense bacterial mat is present on the surface for 3% medium (Figure 4.9(b)) and some bacteria seem to have diffused and proliferate upon incubation to form bacteria clusters rather than to diffuse upon proliferation as it seemed to be the case for lower agarose concentration. These observations are in accordance with the ones previously made but also stress the importance importance of the way the bacteria are initially seeded in gelled media; they also help understand the blurring effect that was observed for epifluorescence microscopy, that is probably partly due to the presence of the mat when working with LabTeks or microplates.

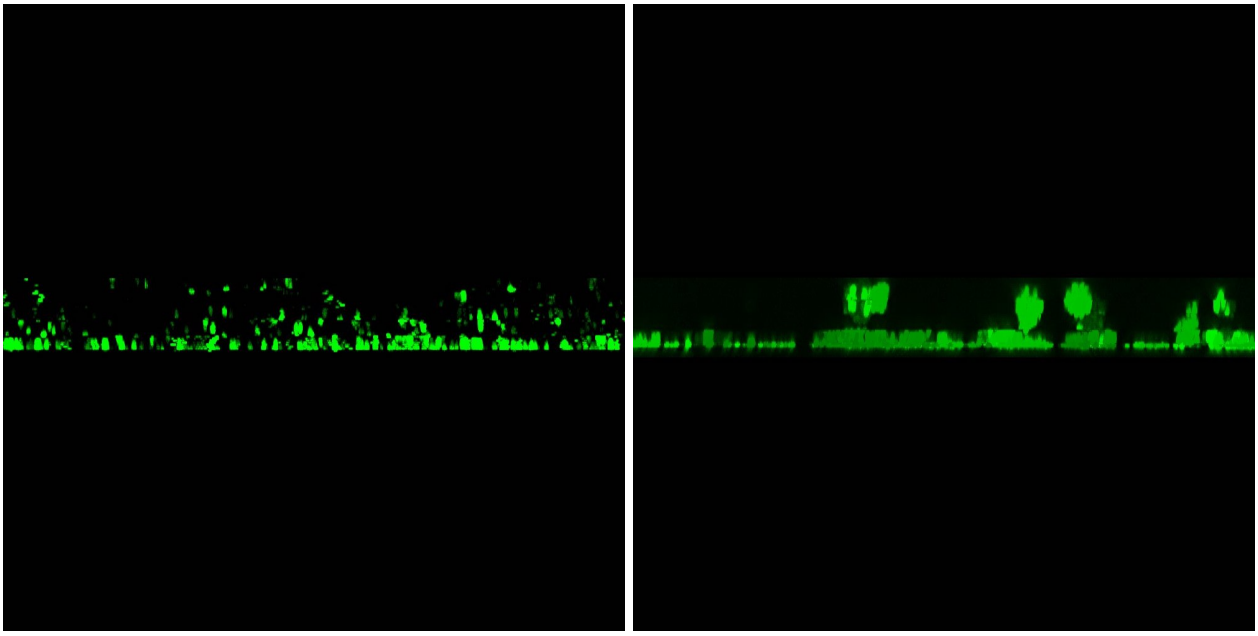

(a) 0.3% (b) 3.0%

Figure 4.9: Projections of z-stack obtained with CLSM (Airyscan) of GFP-*S. epidermidis* (dilution factor of the suspension: 100) grown for 24 h in 0.3% and 3.0% agarose (GS2) gelled media (observed in LabTek wells)

Metabolic activity

Since the presence of GFP does not interfere with the fluorescence intensity measured to account for AB reduction, AB assays were performed. When performing AB tests, the metabolic activity of GFP-*S. epidermidis* embedded in the gels was studied vs the culture time. For this, the AB reagent was added directly in the medium and the fluorescence of the sample was measured vs the time.

The experiment was repeated twice to ensure reliability. The evolution of the fluorescence intensity related to AB metabolization vs culture time is shown in Figure 4.10 for a gain of 75 dB. Two gains were used to measure fluorescence intensity (75 dB and 100 dB); however, for a gain of 100 dB, the microplate reader intensity measurement reached saturation which resulted in the abrupt stop of the curve at a fluorescence intensity of around 60 000 (see Appendix). No clear tendency can be identified on the graph, except for the fact that the fluorescence seems to be increasing faster in liquid broth in comparison with gelled media. This difference in terms of activity in liquid or gelled medium is most probably related to the dependence of the metabolic activity on the (bio)chemical composition of the medium. Since the composition is rather different when using agarose compared to liquid broth, it seems logical that a difference is observed. However, the agarose concentration seems to have no clear influence on the metabolic activity of GFP-*S. epidermidis*.

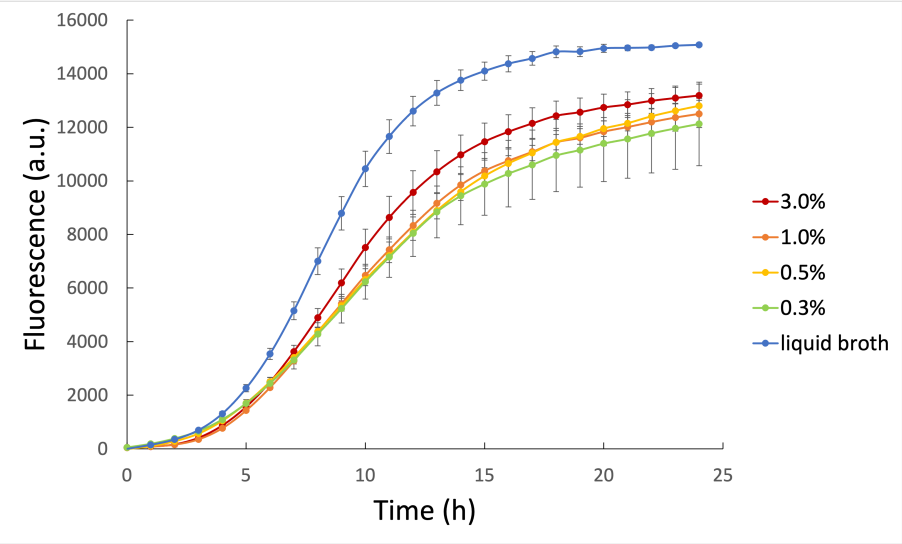

Figure 4.10: Fluorescence intensity ($\lambda_{ex.}$: 530 nm; $\lambda_{em.}$: 590 nm) evolution of GFP-*S. epidermidis* grown in agarose (GS2) gelled media supplemented with alamarBlue (AB) for various agarose concentrations to assess for metabolic activity by means of AB reduction and its detection; gain: 75 dB.

4.3 Influence of the gel strength

As a reminder, the gelled media discussed in this part of the chapter were prepared from different agarose gel powders, that have different properties including the gel strength they provide to the gels. The characteristics of these agarose gels are summarized in Table 3.1. All gels were prepared at the same concentration.

Bacterial growth

As already detailed above for the concentration influence, the means and standard errors were calculated and plotted to investigate bacterial growth in media with various agarose types with different gel strengths. The evolution of the fluorescence intensity related to GFP production of the bacterial strain is shown in Figure 4.11. First, it seems like bacteria in liquid medium grow much faster than in gelled media at first and that the growth rate decreases over time. Second, the fluorescence intensity reached after 24 h seems higher for the gels with a lower gel strength compared to the ones with higher gel strength. However the difference is much less marked as it was for concentration and the rate does not seem to vary much even when the properties of the gel vary. However, variability in the results has been observed as it will be discussed in the next section.

In Figure 4.12 are represented the fluorescence intensity evolution for either undilute or 100 times dilute bacterial suspension. The suspension was used to seed the gelled media prepared from different agarose powder at 1% w/v. On the graph, the trend resembles more the one exhibited by gels of different concentrations. Indeed, when the gel strength increases, the fluorescence rate as well as the maximal fluorescence decrease. Furthermore, the curve of the rate also follows a trend similar to the one observed in the previous section. Indeed, the rate tends to first increase to finally stabilize after a certain period of time ($\sim$ 5 h). The steady rate values for gelled media with a higher gel strength are lower compared to the rate of a gel with a smaller gel strength. Moreover, the same trend is observed even when the bacterial density is lowered, the rates are lower for dilute bacterial suspension in comparison to the situation where the former non diluted bacterial suspension is used to seed the gels. A supplementary graph is available in the Appendix section.

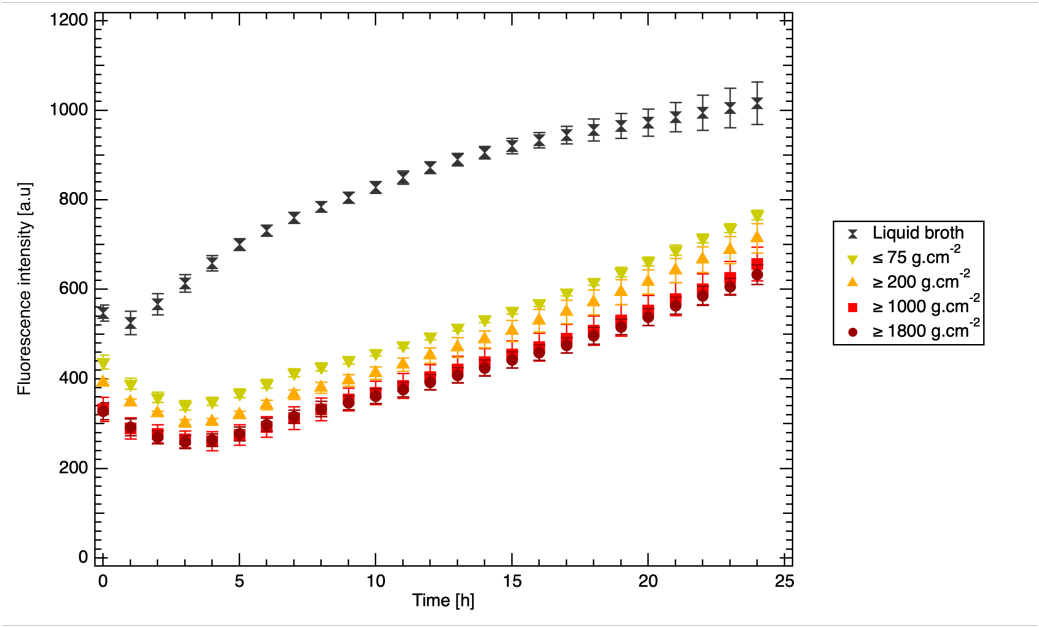

Figure 4.11: Fluorescence intensity ($\lambda_{ex.}$: 488 nm; $\lambda_{em.}$: 515 nm) evolution of GFP-*S. epidermidis* grown in agarose gelled media (1%) for agarose types with various gel strengths.

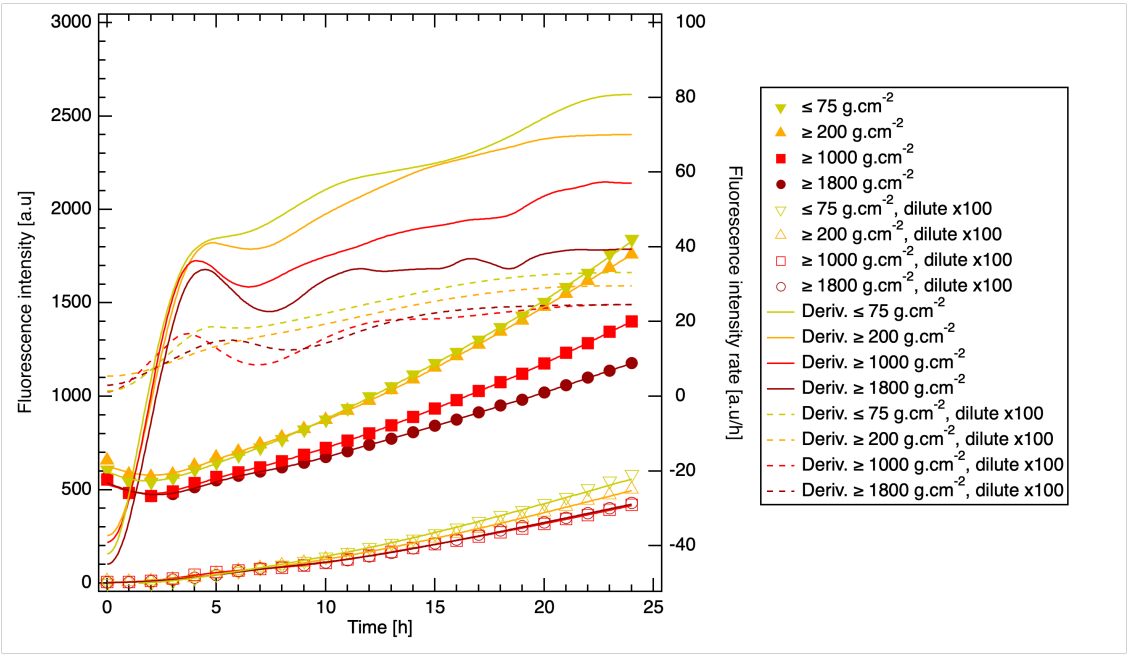

Figure 4.12: GFP fluorescence intensity ($\lambda_{ex.}$: 488 nm; $\lambda_{em.}$: 515 nm) evolution of dilute or undilute GFP-*S. epidermidis* grown in agarose gelled media (1%) for agarose types with various gel strengths and related fluorescence intensity rate (computed from derivatives of the fluorescence intensity vs time); dotted line stands for a suspension dilution factor 100 of the bacterial suspension, solid line stands for a dilution factor of 1.

Epifluorescence microscopy images

Images were taken for the agarose types exhibiting the two most different gel strengths, namely GS1 (gel strength $\geq$ 1800g.cm^{-2} for 1% w/v) and GS4 ($\geq$ 75g.cm^{-2} for 2% w/v). Representative images of the bacterial populations observed in these particular gels are presented in Figure 4.13. Bacteria were observed on glass slide using the x60 objective of the microscope and the suspension used to culture the cells was diluted 100 times to facilitate imaging capture.

On the one hand, GFP-*S. epidermidis* bacteria growing in the gelled medium with the smaller gel strength (GS4) (Figure 4.13(a)) seem to grow rather independently from one another though some aggregates of a few cells are also present but not prevalent. This growth mode is rather similar to the one encountered for planktonic bacteria in liquid media.
On the other hand, when grown in agarose gel with a higher gel strength (Figure 4.13(b)), bacteria tend to aggregate and form clusters. Even though some single bacteria persist, the majority grow as part of an aggregate, which moves away from a purely planktonic mode of growth.
It is once again worth noting that the fluorescence of the out of focus planes lowers the quality of the images taken by means of the epifluorescence microscope, probably caused by the thickness of the sample, especially for rigid gels such as the one used in Figure 4.13(b).

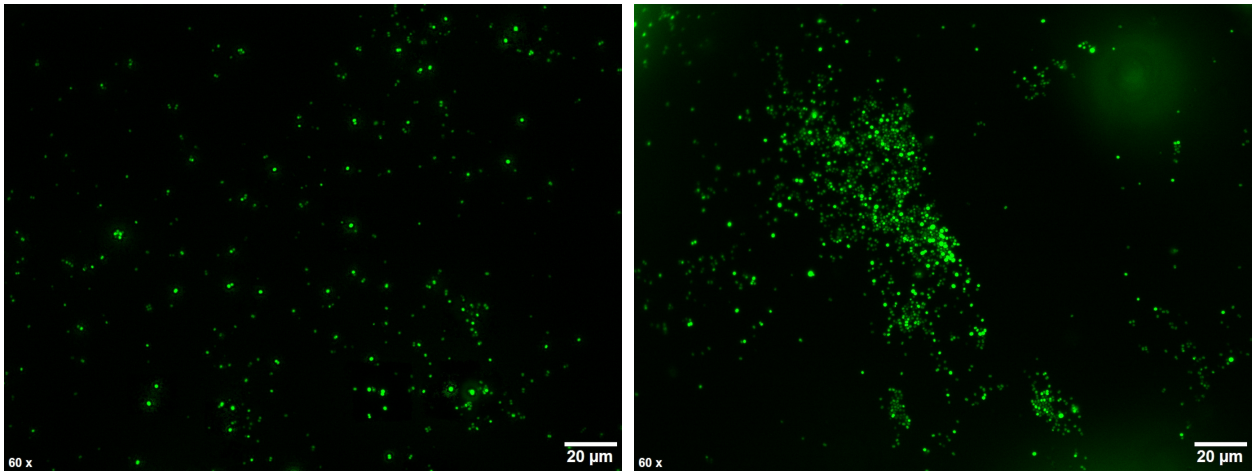

(a) Minimal gel strength (GS4). (b) Maximal gel strength (GS1).

Figure 4.13: Epifluorescence microscopy (Olympus IX71; x60 objective) images of GFP-*S. epidermidis* (dilution factor of the suspension: 100) grown for 24 h in agarose gelled media with either minimal or maximal gel strength (observed on glass slides).

Moreover, heterogeneity in bacteria cell distribution is observed for the stronger gel. Indeed, images taken at different places of the same sample give different read-outs as it is illustrated in Figure 4.14 for pictures taken with either x40 or x60 lenses. On the left image, much denser clusters are observed compared to the representative image shown here above, whereas the image on the right hand side of the figure demonstrates that there are almost no clusters in some areas, where the growth mode could at first be considered planktonic if the sample is not scanned further.

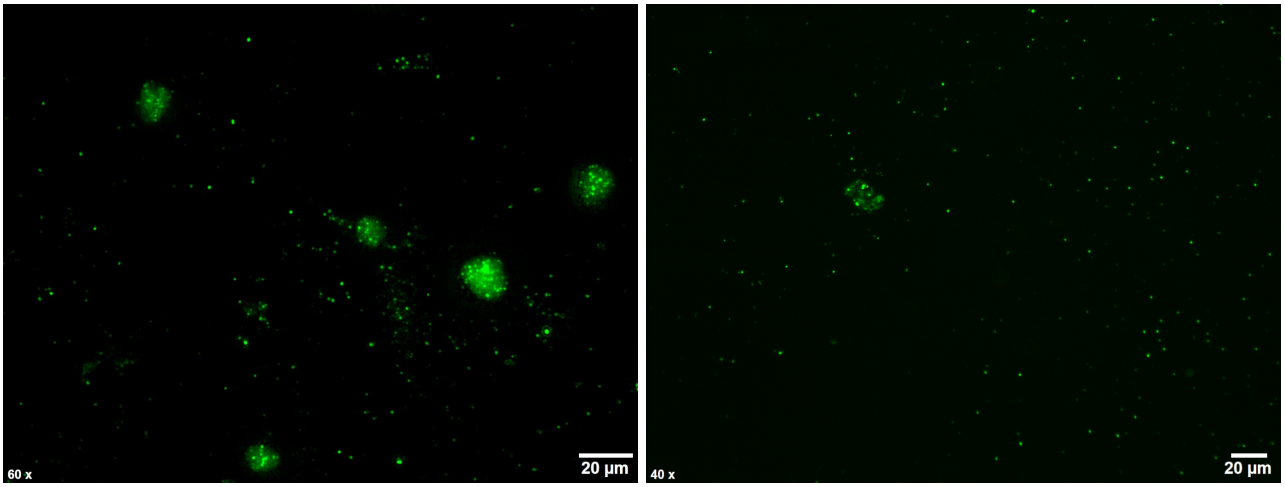

Figure 4.14: Epifluorescence microscopy (Olympus IX71; x60 (left) and x40 (right) objectives) images of GFP-*S. epidermidis* (dilution factor of the suspension: 100 (left) and 1 (right)) grown for 24 h in agarose gelled medium with maximal gel strength (observed on glass slides).

Nevertheless, heterogeneity in terms of growth mode was not detected for the softer gel. A reconstructed large image of the sample is indeed shown in Figure 4.15 and planktonic bacteria seems to dominate except for 1 aggregate on the right hand side of the image.

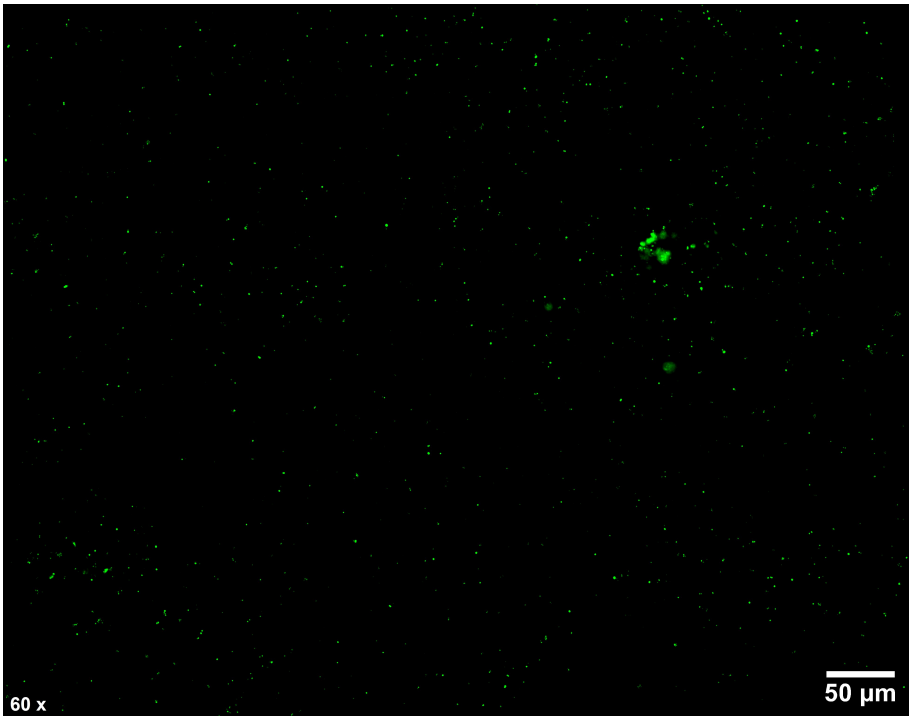

Figure 4.15: Epifluorescence microscopy (Olympus IX71; x60 objective) reconstructed large image of GFP-*S. epidermidis* (dilution factor of the suspension: 100) grown for 24 h in agarose gelled medium with minimal gel strength (observed on glass slides).

CLSM images

To get rid of the blurring effect related to the contribution of bacteria that are out of focus, CLSM images were taken. Representative images of GFP-*S. epidermidis* population grown for 24 h in gelled culture media with different gel strengths are shown in Figure 4.15, using 100 times dilute bacteria suspension in a LabTek. The agarose types used are the same as for the previous imaging technique.
On the one hand, bacteria growing in the softer agarose gel (Figure 4.16(a)) exhibit the same behavior as the one deduced using the epifluorescence microscope: bacterial cells are rather dispersed and few aggregates composed of a few number of cells can be observed, the growth is rather similar to planktonic growth.
On the other hand, growth images in the more rigid agarose gel also confirmed the observations made in the previous analysis: cells tend to aggregate in a much larger extent than in the softer gel. The growth mode tends to cluster growth, although some single cells are also growing in a planktonic fashion.

In summary, the deductions made with the previous observation technique are confirmed by CLSM images, that are of much better quality, allowing to get rid of blur.

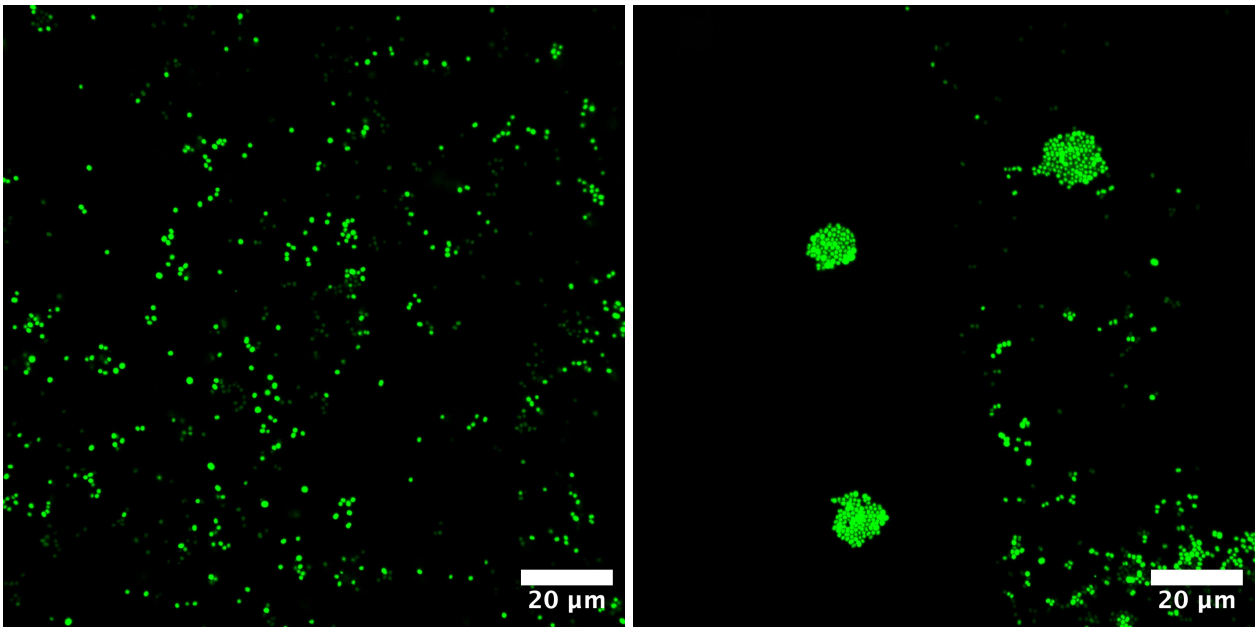

(a) Minimal gel strength (GS4). (b) Maximal gel strength (GS1).

Figure 4.16: CLSM images of GFP-*S. epidermidis* (dilution factor of the suspension: 100) grown for 24 h in agarose gelled media with either minimal (left) or maximal gel strength (right) (observed in LabTek wells).

Metabolic activity

Since GFP does not interfere with the fluorescence related to the reduced form of AB, this reagent is used to investigate the influence of the gel strength of agarose on the metabolic activity of GFP-*S. epidermidis*.

The experiment was repeated twice to ensure reliability. The evolution of the fluorescence intensity related to AB metabolization is shown in Figure 4.17 using a gain of 75 dB. As already done for the gels at various concentrations, two gains were used to measure the fluorescence intensity. However, for a gain of 100 dB, the

microplate reader reached saturation inducing that the curve stops abruptly at a fluorescence intensity of around 60 000 (see Appendix). On the graph, a trend can be highlighted: the higher the gel strength of the agarose, the slower the metabolization of AB. Indeed, the slope of the curve is the highest for the liquid culture medium and it decreases with increasing gel strength. Moreover, it seems like the fluorescence intensity reaches a plateau after some time. This plateau is reached once the reagent is completely reduced by the microorganism. Logically, this plateau is first reached by the medium providing the highest metabolization rate, namely the liquid broth, and is followed by the softer gels until the one with the highest gel strength finally reaches the plateau value.

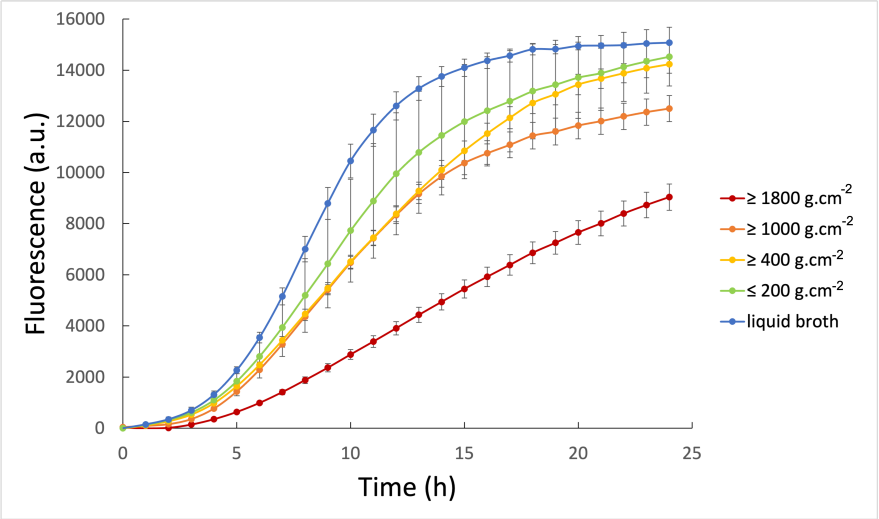

Figure 4.17: Fluorescence intensity ($\lambda_{ex.}$: 530 nm; $\lambda_{em.}$: 590 nm) evolution of GFP-*S. epidermidis* grown in agarose gelled media prepared with agarose powder of various gel strengths supplemented with alamarBlue (AB) to assess for metabolic activity by means of AB reduction and its detection; gain: 75 dB.

5 Conclusion of the chapter

In this chapter, the behavior of GFP-*S. epidermidis* bacteria was investigated in agarose gelled media by various means.

First the fluorescence related to the expression of GFP by the strain was used to determine the effects of the gel composition on bacterial growth. The increase of agarose concentration seems to slow down the growth of the microorganism and so does its gel strength. However, many variability was observed along experiment repetition, though the trend was generally conserved except for one gel or the other, with no clear repetition in these inaccuracies. When working with living material, the results are indeed more prone to variation even if the experimental conditions are kept as reproducible as possible during the whole process.

Second, the growth mode was observed using two different microscopy techniques. From the images obtained by means of the epifluorescence microscope, a trend has been established for both concentration and gel strength influence but since the image quality was hindered by the blurring effect of out of focus fluorescent microorganisms, CLSM was used to get rid of this negative effect. The trend formerly observed is confirmed by the latter: in media of low concentration or low gel strength, bacteria globally show a planktonic behavior whereas in the presence of high concentration or gel strength, GFP-*S. epidermidis* seems to adopt a biofilm growth, even if some single

bacteria still persist in the gelled media. Moreover, 3D images were taken for gels of different concentrations and highlight the presence of a bacterial mat on the bottom of the support where the suspension was deposited prior to gel casting. The diffusion of the bacteria across the gel also seem different depending on the gel concentration: the cells seem to diffuse as single cells in low concentration gels, whereas dense clusters are formed after diffusion of the first cells in concentrated agarose media.

Finally, the influence of the media composition on metabolic activity was investigated using AB reduction as an indicator. The fluorescence related to GFP expression was proved to cause no interference with the fluorescence related to the reduced form of AB reagent. The influence of agarose concentration and gel strength was this time different. On the one hand, it seemed like the concentration of gelling agent did not cause any changes in the metabolic activity, even though the fluorescence was higher in liquid broth in comparison to all prepared gels, which show a very similar behavior regardless of the agarose concentration. On the other hand, the gel strength of the used agarose seemed to affect the metabolic activity: indeed, the higher the gel strength, the slower the metabolization of AB seemed to take place. However, it is worth noting that the agarose types used in this project not only differ in terms of gel strength, but also in terms of chemical composition as well as potentially in terms of network microstructure. The reduction of AB could therefore be changed according to the medium composition if it reacts more with a particular agarose. In this view it is possible that the reduction is not representative of the metabolic activity and cannot be relied on to measure the latter.

CHAPTER 5

Summary and discussion

As a reminder the aim of this master thesis was to investigate the influence of the mechanical properties of different gelled culture media on the behavior of *S. epidermidis* populations. The use of the latter gels to grow bacteria is intended to allow for a better control on the bacteria behavior, namely their growth and their metabolic activity. The present chapter aims to establish the connection between the previous chapters, where the gels where firstly characterized from a mechanical point of view and secondly the bacterial behavior in the gelled media was investigated.

In Chapter 4, agarose concentration and gel strength were both proved to have an impact on the viscoelastic properties of the gels they form. Indeed, an increase in either gel strength or concentration induces an increase of the moduli as well as the viscosity. More specifically, the storage modulus G' accounts for the rigidity of the material when a shear deformation is applied. So to increase the stiffness of an agarose gel, one can simply increase the concentration and/or change agarose type to one showing a higher gel strength.

As already mentioned in Section 5.3 of Chapter 1, the stiffness of the hydrogel used to culture bacteria has been shown to play a role on the bacterial behavior. Based on the results of Chapter 4, the influence of the mechanical properties that can be suggested in the case of *S. epidermidis* in agarose gels is the following.

First, it seems like the stiffer the gel, the slower the bacterial growth since an increase in either concentration or gel strength implies a decrease of the growth rate. Consequently, the number of bacterial cells in a softer gels is greater that the one obtained in a stiffer gel, after the same incubation period. Second, stiffness seems to drive the growth towards biofilm mode. Both of these effects could be due to the ability of bacteria to sense changes in their environment, whether they are chemical, physical or of another nature, and to consequently adapt to it. This adaptation takes place thanks to differential gene expression induced by the sensing systems mentioned earlier.[78, 84, 94] Bacteria in biofilm growth mode are intended to provide a secure environment to reproduce slowly and survive whereas planktonic bacteria are designed to colonize new niches, not ensuring their long-term survival.[95] The switch between those two phenotypes may be induced by the nature of their surrounding environment.[78]

First, the diffusion in agarose of both cells and nutrients is hindered due to the network formed by the polymer bundles. This effect should be even more pronounced for agarose gels with a higher stiffness since the network is more dense and thus provides resistance to stress. Consequently, the rate of nutrient diffusion is impacted by the stiffness and gradients of nutrients can be observed in the gels which can also be sensed by the bacteria and induces a regulation in gene expression to favor one or the other growth mode depending on the nutrient availability.[78, 84] Moreover, as suggested in the work of Serwer et al. [76] for other bacteria (*E. Coli* and *Lysinibacillus*), clusters formation in more rigid environments could be explained by different means. Clustering could for instance promote growth since the cluster would provide a higher growth-derived force to counteract the forces applied by the gel fibers on the microorganisms. In the second instance, the irregular shape of the clusters could be due to the local variation of rigidity inside the gel: due to the presence of fibers, some places are more rigid than others, promoting the formation of immobilized clusters in some places and promoting the proliferation planktonically in softer areas. Furthermore, the presence of single bacteria even in rigid gels could be explained for two different reasons. First, a bacterium could have diffused, in the case at hand from the bottom of the support for example, and not replicate. Second, the migration of single cell from clusters post replication could also occur. This phenomenon could first originate from the nature of the near environment, which could be more favorable to planktonic growth. Migration could also be due to clustering-amplified forces generated by the combination of the forces of the bacteria to outgrow cells and drive towards the formation of new aggregates, starting from the released bacteria.
To sum up, clusters in rigid environments could be intended to maintain growth despite the physical constraint induced by the agarose network as well as the possible depletion in terms of nutrient related to diffusion limitation in some areas of the medium, and this despite the fact that the cells in biofilms exhibit a non optimal growth.
Nevertheless, even if the influence of the mechanical properties on the growth, i.e. the increase in cell number, seems to be proved, it is not the case considering the influence on metabolic activity. Indeed, the results obtained for the influence of the concentration and the one of the gel strength on the reduction of AB are different. Consequently, it is not possible to assert that the has an influence on the metabolic activity of the microorganism, within the tested concentration range at least. However, since the change in agarose type, which was formerly done to vary the gel strength of the medium, influences the metabolic activity, another parameter certainly comes into play by changing the cellular environment. This parameter could be related to the chemical composition or the structure formed by one or the other gel. The gels should be investigated further to determine the cause of this change in AB reduction. Since the fluorescence intensity only account for AB reduction, it is worth noting that it is possible that the metabolic activity of the bacteria remains unchanged and that the observed effects are due to interactions between agarose and the reagent, which would depend on the agarose type used to prepare the gelled medium. If such interactions exist, AB reduction would not be reliable to quantify the bacterial metabolic activity in agarose gels prepared using different agarose powders.

In conclusion, this work showed that the mechanical, i.e. viscoelastic properties, of the culture gel medium influence the bacterial behavior of *S. epidermidis*, in terms of growth rate but also of growth mode, probably inducing a switch in gene expression of the microorganism, which could be beneficial in the framework of future applications such as the the bacterial patch used to restore healthy skin that was mentioned earlier in this report.

In the future, these results will be used in the design of the previously mentioned patch engineered by our laboratory. Indeed, the growth and eventually the metabolic activity of the bacteria embedded in the wells of the construct could be controlled by fine tuning the mechanical properties of the gelled media in order to achieved optimal growth kinetics.

CHAPTER 6

Improvements and prospects

Despite the fact that the results obtained during this master thesis are quite convincing, many things are still to come. Firstly, some improvements could be implemented to further optimize the protocols and consequently the quality of the obtained results. Moreover, many other parameters could be investigated to better understand the influence of the mechanical properties on the behavior of *S. epidermidis*.

1 Improvements

Different aspects of both the mechanical characterization as well as the study of bacterial growth and metabolic activity could be improved further in the following way.

First, the use of a rheometer with a better torque sensitivity could be considered to get rid of the variation obtained upon repetition of the experiments due to this limitation. Moreover, the use of striated plate or disposable plate scratched with sandpaper could be interesting to test for rheology measurements, in order to further improve the adherence between the sample and the plates. In this way, more rigid gels could also be tested using rheology whereas it was not the case here, i.e. for the most concentrated gel. Furthermore, it would be very interesting to test some agarose gels using both DMA and rheology to cross-check the results obtained from one or the other technique and ensure their reliability. This could be achieved using the previously mentioned improvement, that would broaden the range of concentrations that could be tested by rheological means.

Second, adaptation of the protocols to get insight on the bacterial behavior are necessary to get rid of the bias that still persists in the present work. Indeed, bacteria should not be in contact with the bottom surface of the microplate or the LabTek. Actually, the bacterial mat observed on CLSM images could be partially or entirely due to the way the bacteria were poured in the first place. A better way to proceed would be to pour in the wells a first layer of gel, then add the bacteria suspension and finally cover it with a second layer of gel, so that bacteria would be sandwiched in the gel. Using this protocol, the growth of bacteria would be exclusively related to the growth behavior as such and not influenced by the interaction between cells and solid substrate anymore.

2 Prospects

To deepen the understanding of the influence of agarose properties on *S. epidermidis*, several aspects could be explored in the future.

In the first instance, since it has not been identified during this master thesis, the influence of the agarose nature on the reduction of AB and on the metabolic activity of the cells should be investigated further. Indeed it would be of great interest to determine if the nature of the agarose influences only the chemical reaction on which the metabolic activity assay relies or if the activity is really impacted. In order to do so, the different agarose types should be characterized further to understand in what way they differ from one another, may it be on a microstructural point of view, physico-chemical composition or other parameters that could impact both the reduction in itself or the metabolism of the microorganism. Other techniques could also be considered to assess metabolic activity, for instance one of the other techniques introduced in Chapter 1.
Furthermore, it would be interesting to investigate the influence of agarose concentration on the microstructure of the network. It would allow to precisely determine in which way the concentration impacts the bacterial behavior. Indeed, concentration variation induces many different changes in the materials, which could themselves be the origin of particular behaviors observed in a bacterial population, rather than concentration as such. For instance, the pore size distribution varies as a function of concentration and could per se influence the way the bacterial population behaves.
Additionally, since gene expression is influenced by the cellular environment, it would be particularly interesting to investigate the influence of gelled medium composition. Genomic regulation as well as secretome studies would be especially relevant to understand which changes the mechanical and/or chemical properties of agarose gels can induce in terms of gene expression and molecules secretion.

In the second instance, it would be relevant to investigate the evolution of the population of GFP-*S. epidermidis* in the gels over time by means of microscopy. Time-lapse images of the cultured bacteria in solid media could be captured in an incubation chamber under the microscope objective, whether it is epifluorescence microscope or CLSM. Prior knowledge could be gained first using epifluorescence microscopy and then confirmed by confocal microscopy later on to get better quality images. In this way, the diffusion of the bacteria in the gel could be assessed to better understand how clusters form in a better way.

Finally, some investigations related to more specific applications could be implemented. As a reminder, this work is part of a more global project concerning the engineering of a patch containing encapsulated *S. epidermidis* bacteria to fight against the development of skin pathologies, namely acne vulgaris. As mentioned at the end of Section 2.1 of Chapter 1, *S. epidermidis* possesses an antimicrobial action against *C. acnes*, whose abnormal proliferation in anaerobic conditions causes acne vulgaris. This antimicrobial action relies on the fermentation of glycerol to produce short chain fatty acids of *S. epidermidis* in anaerobic conditions, i.e. in acne lesions. In particular, succinic acid, which was shown to limit *C. acnes* overgrowth, seem of critical importance in this regulation process. Therefore, optimizing the synthesis of those fatty acids of interest by means of medium optimization would be of great interest for such novel therapeutic option. Finally, this application is just one example of the spectrum of possibilities offered by *S. epidermidis*. Its use could be broaden in many ways, to regulate the action of other commensals but also possibly to fight against pathogenic colonization.

APPENDIX A

Fluorescence intensity: bacterial growth

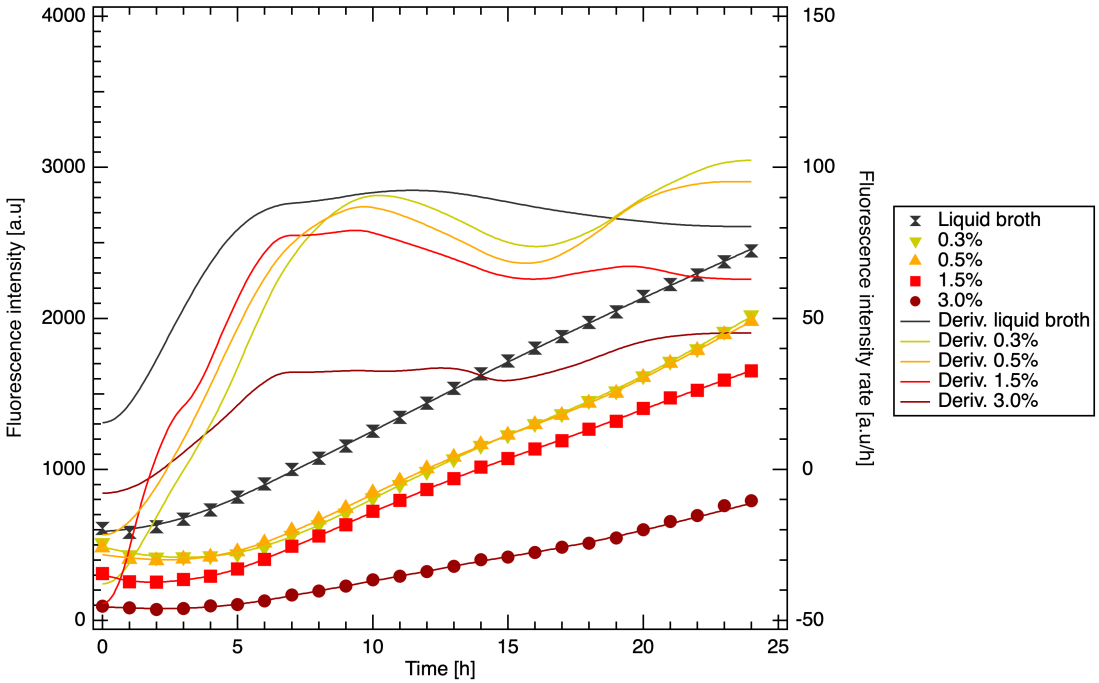

Figure A.1: GFP fluorescence intensity ($\lambda_{ex.}$: 488 nm; $\lambda_{em.}$: 515 nm) evolution of dilute or undilute GFP-*S. epidermidis* grown in agarose (GS2) gelled media for various agarose concentrations and related fluorescence intensity rate (computed from derivatives of the fluorescence intensity vs time); dotted line stands for a suspension dilution factor 100 of the bacterial suspension, solid line stands for a dilution factor of 1.(link to the related Section)

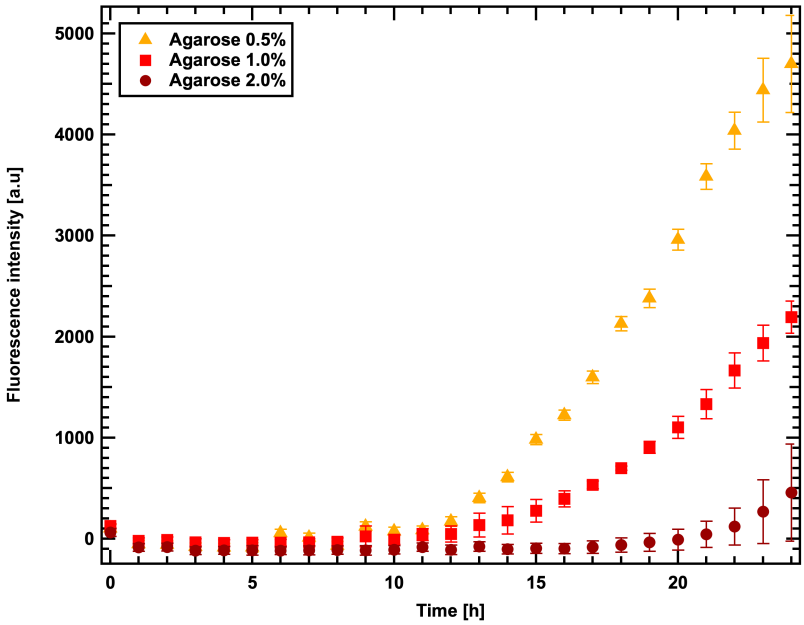

Figure A.2: GFP Fluorescence intensity ($\lambda_{ex.}$: 488 nm; $\lambda_{em.}$: 515 nm) evolution of GFP-*S. epidermidis* in agarose (GS2) gelled media prepared with various agarose concentrations (dilution factor: 1000) (link to the related Section)

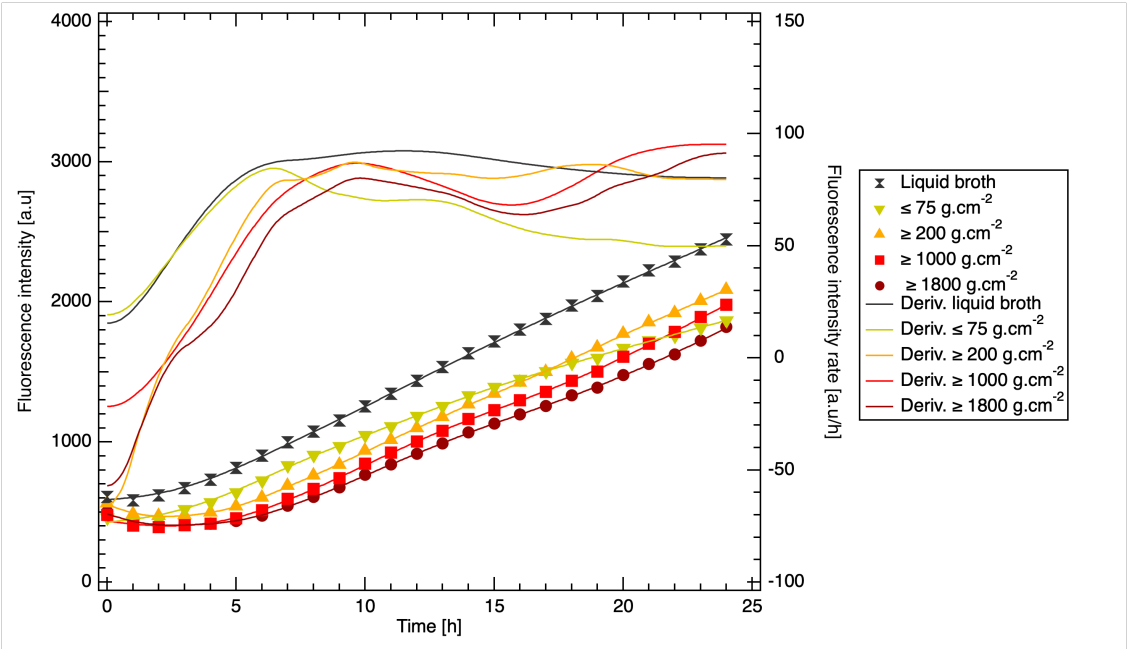

Figure A.3: Fluorescence intensity ($\lambda_{ex.}$: 488 nm; $\lambda_{em.}$: 515 nm) and fluorescence intensity rate of *S. epidermidis* in agarose gelled media for agarose types with various gel strengths.(link to the related Section)

APPENDIX B

Epifluorescence microscopy

Return to the related section using this link.

1 0.3% agarose (GS2) gelled medium

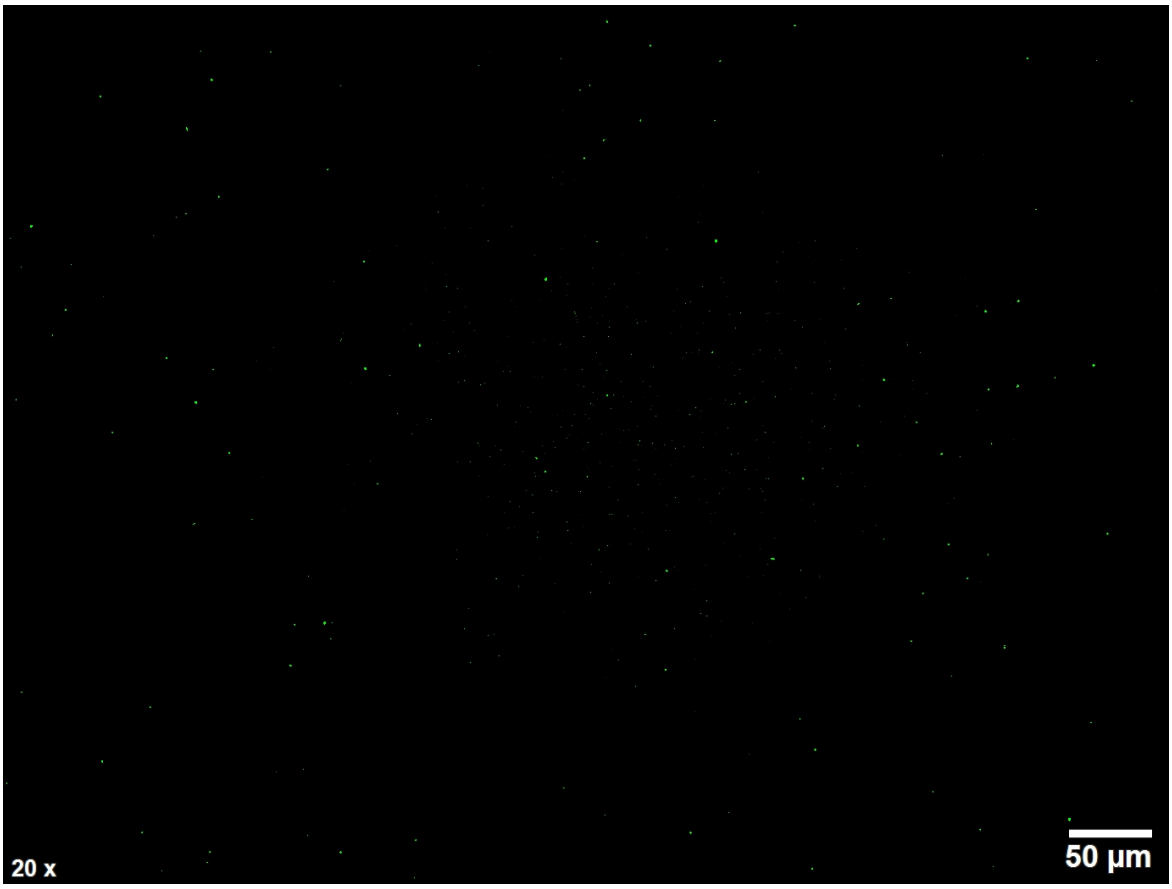

Figure B.1: Epifluorescence microscopy (Olympus IX71; x20 objective) image of GFP-*S. epidermidis* (dilution factor of the suspension: 100) grown for 24 h in a 0.3% agarose (GS2) gelled medium (observed in LabTek wells).

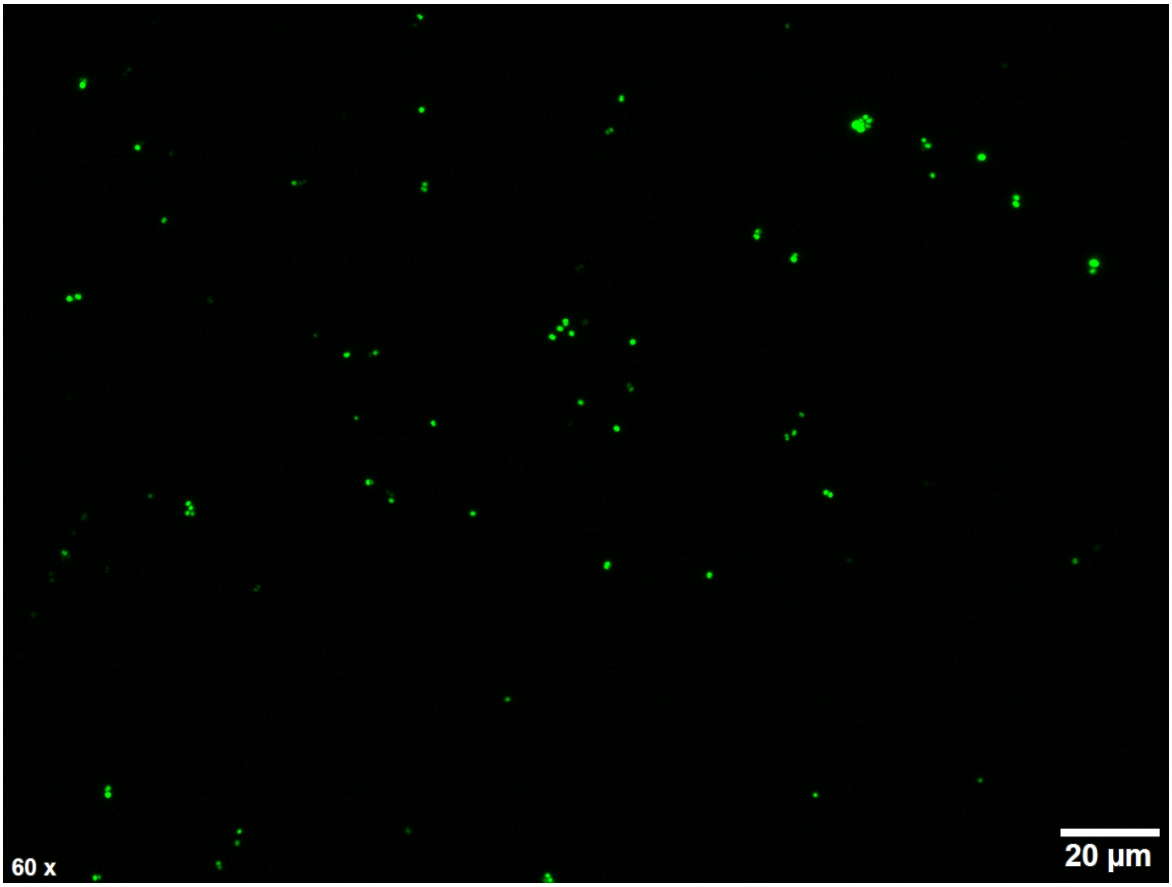

Figure B.2: Epifluorescence microscop (Olympus IX71; x60 objective) image of GFP-*S. epidermidis* (dilution factor of the suspension: 100) grown for 24 h in a 0.3% agarose (GS2) gelled medium (observed on glass slides).

2 3.0% agarose (GS2) gelled medium

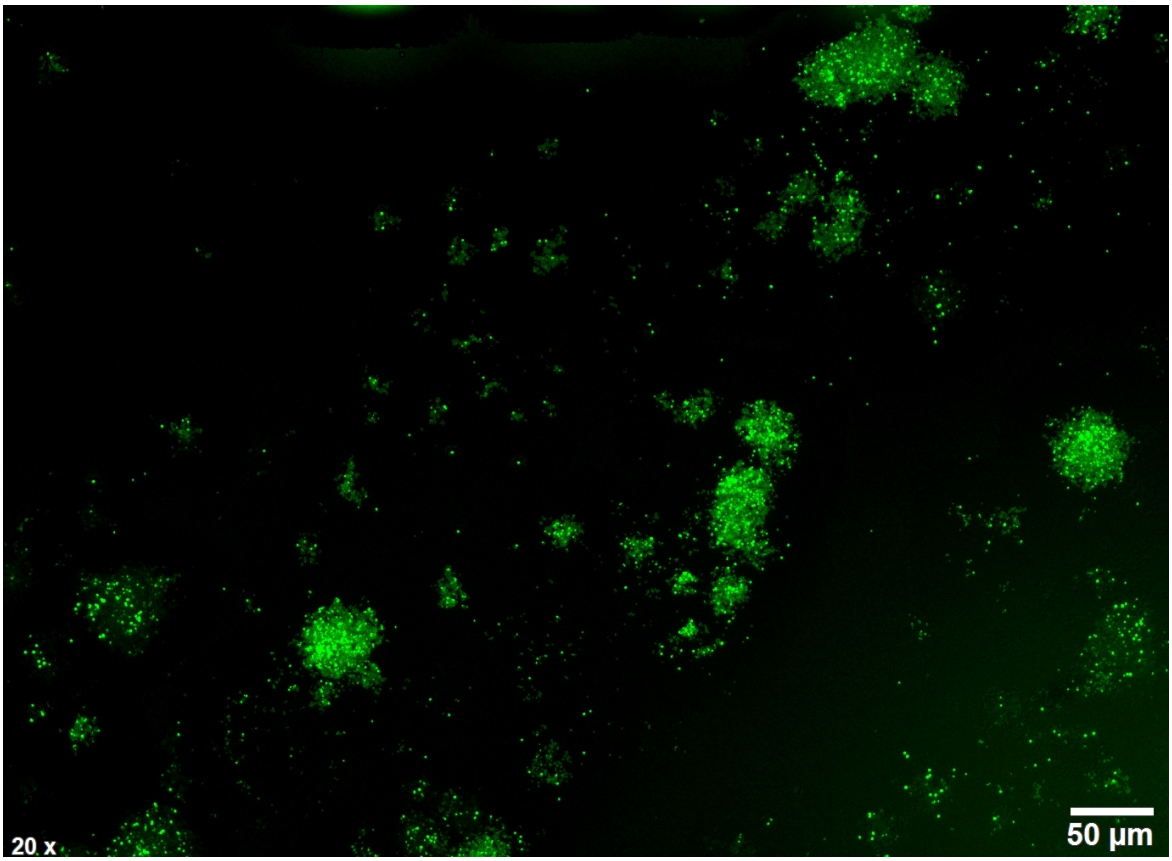

Figure B.3: Epifluorescence microscopy (Olympus IX71; x20 objective) image of GFP-*S. epidermidis* (dilution factor of the suspension: 100) grown for 24 h in a 3.0% agarose (GS2) gelled medium (observed in LabTek wells).

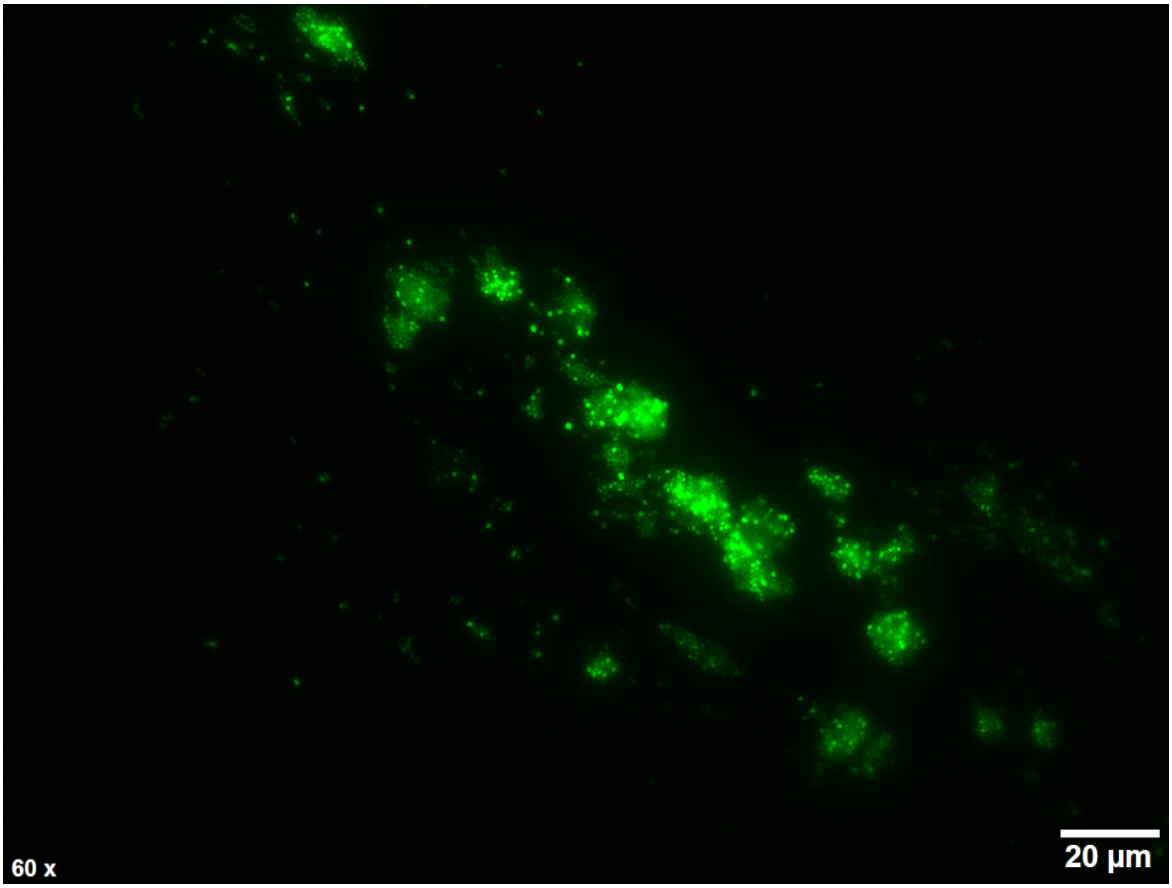

Figure B.4: Epifluorescence microscopy (Olympus IX71; x60 objective) image of GFP-*S. epidermidis* (dilution factor of the suspension: 100) grown for 24 h in a 3.0% agarose (GS2) gelled medium (observed on glass slides).

APPENDIX C

AB reduction to assess metabolic activity of GFP-*S. epidermidis*

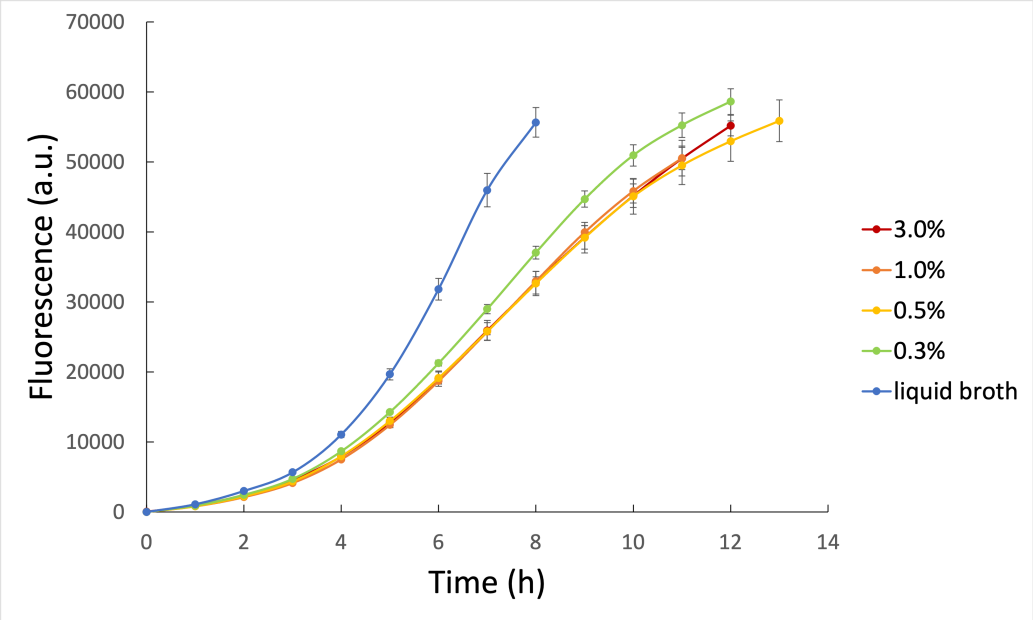

Figure C.1: Fluorescence intensity ($\lambda_{ex.}$: 530 nm; $\lambda_{em.}$: 590 nm) evolution of GFP-*S. epidermidis* grown in agarose (GS2) gelled media supplemented with alamarBlue (AB) for various agarose concentrations to assess for metabolic activity by means of AB reduction and its detection; gain: 100 dB. (link to the related Section)

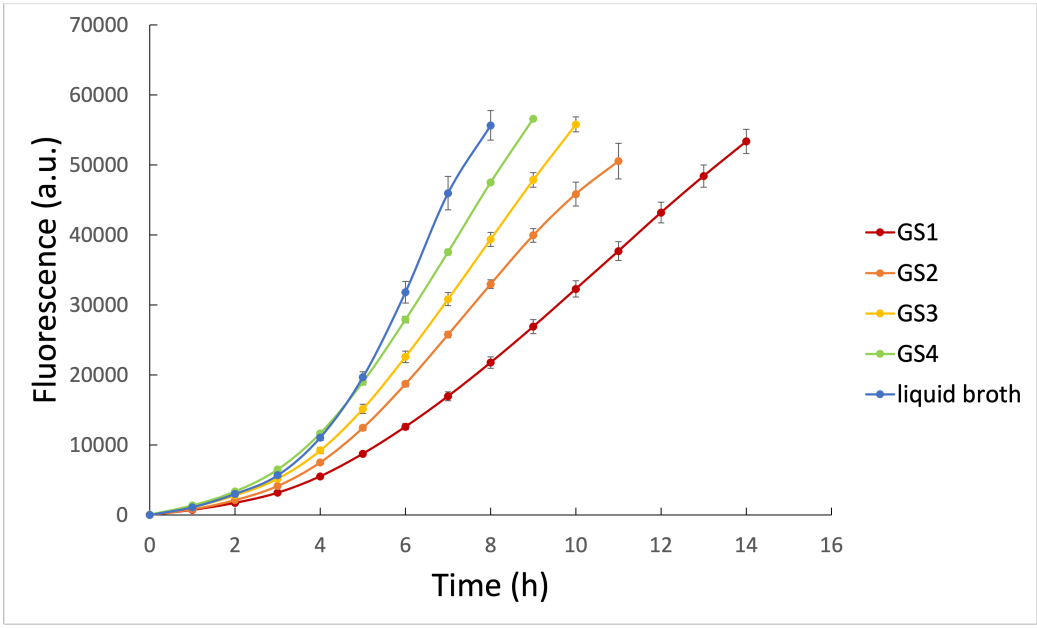

Figure C.2: Fluorescence intensity ($\lambda_{ex.}$: 530 nm; $\lambda_{em.}$: 590 nm) evolution of GFP-*S. epidermidis* grown in agarose gelled media prepared with agarose powder of various gel strengths supplemented with alamarBlue (AB) to assess for metabolic activity by means of AB reduction and its detection; gain: 100 dB.(link to the related Section)

Bibliography

[1] N. Fyhrquist, A. Salava, P. Auvinen, and A. Lauerma, "Skin Biomes," *Current Allergy and Asthma Reports*, vol. 16, no. 5, p. 40, 2016, ISSN: 1529-7322, 1534-6315. DOI: 10.1007/s11882-016-0618-5. (visited on 04/10/2022) (cit. on pp. 1, 4–6).

[2] M. Fournière, T. Latire, D. Souak, M. G. J. Feuilloley, and G. Bedoux, "Staphylococcus epidermidis and Cutibacterium acnes: Two Major Sentinels of Skin Microbiota and the Influence of Cosmetics," *Microorganisms*, vol. 8, no. 11, p. 1752, 2020, ISSN: 2076-2607. DOI: 10.3390/microorganisms8111752. (visited on 04/10/2022) (cit. on pp. 1, 4).

[3] L. B. Nørreslet, T. Agner, and M.-L. Clausen, "The Skin Microbiome in Inflammatory Skin Diseases," *Current Dermatology Reports*, vol. 9, no. 2, pp. 141–151, 2020, ISSN: 2162-4933. DOI: 10.1007/s13671-020-00297-z. (visited on 04/10/2022) (cit. on pp. 1, 4–6).

[4] A. L. Byrd, Y. Belkaid, and J. A. Segre, "The human skin microbiome," *Nature Reviews Microbiology*, vol. 16, no. 3, pp. 143–155, 2018, ISSN: 1740-1526, 1740-1534. DOI: 10.1038/nrmicro.2017.157. (visited on 04/10/2022) (cit. on pp. 1, 5, 6).

[5] P. Chen, G. He, J. Qian, Y. Zhan, and R. Xiao, "Potential role of the skin microbiota in Inflammatory skin diseases," *Journal of Cosmetic Dermatology*, vol. 20, no. 2, pp. 400–409, 2021, ISSN: 1473-2130, 1473-2165. DOI: 10.1111/jocd.13538. (visited on 04/10/2022) (cit. on pp. 1, 5, 6).

[6] C. Callewaert, N. Knödlseder, A. Karoglan, M. Güell, and B. Paetzold, "Skin microbiome transplantation and manipulation: Current state of the art," *Computational and Structural Biotechnology Journal*, vol. 19, pp. 624–631, 2021, ISSN: 20010370. DOI: 10.1016/j.csbj.2021.01.001. (visited on 04/10/2022) (cit. on pp. 1, 5, 6).

[7] B. Dréno, "The microbiome, a new target for ecobiology in dermatology," *European Journal of Dermatology*, vol. 29, no. 1, pp. 15–18, 2019. DOI: 10.1684/ejd.2019.3535 (cit. on pp. 1, 5, 6).

[8] Y. Wang, S. Kuo, M. Shu, J. Yu, S. Huang, A. Dai, A. Two, R. L. Gallo, and C.-M. Huang, "Staphylococcus epidermidis in the human skin microbiome mediates fermentation to inhibit the growth of Propionibacterium acnes: Implications of probiotics in acne vulgaris," *Applied Microbiology and Biotechnology*, vol. 98, no. 1, pp. 411–424, 2014, ISSN: 0175-7598, 1432-0614. DOI: 10.1007/s00253-013-5394-8. (visited on 04/11/2022) (cit. on pp. 1, 7, 9).

[9] M. Otto, "Staphylococcus epidermidis — the 'accidental' pathogen," *Nature Reviews Microbiology*, vol. 7, no. 8, pp. 555–567, 2009, ISSN: 1740-1526, 1740-1534. DOI: 10.1038/nrmicro2182. (visited on 04/11/2022) (cit. on pp. 1, 6–9).

[10] J.-P. Claudel, N. Auffret, M.-T. Leccia, F. Poli, S. Corvec, and B. Dréno, "Staphylococcus epidermidis: A Potential New Player in the Physiopathology of Acne?" *Dermatology*, vol. 235, no. 4, pp. 287–294, 2019, ISSN: 1018-8665, 1421-9832. DOI: 10.1159/000499858. (visited on 04/11/2022) (cit. on pp. 1, 6, 7).

[11] N. Kandemir, W. Vollmer, N. S. Jakubovics, and J. Chen, "Mechanical interactions between bacteria and hydrogels: An experimental and modelling approach," Ph.D. dissertation, Newcastle University, Dec. 2018. [Online]. Available: http://www.nature.com/articles/s41598-018-29269-x (visited on 04/17/2022) (cit. on pp. 2, 9, 22–24, 42).

[12] G. Wijesinghe, A. Dilhari, B. Gayani, N. Kottegoda, L. Samaranayake, and M. Weerasekera, "Influence of Laboratory Culture Media on in vitro Growth, Adhesion, and Biofilm Formation of Pseudomonas aeruginosa and Staphylococcus aureus," *Medical Principles and Practice*, vol. 28, no. 1, pp. 28–35, 2019, ISSN: 1011-7571, 1423-0151. DOI: 10.1159/000494757. (visited on 04/27/2022) (cit. on pp. 2, 23).

[13] J. Müller, A. C. Jäkel, J. Richter, M. Eder, E. Falgenhauer, and F. C. Simmel, "Bacterial Growth, Communication, and Guided Chemotaxis in 3D-Bioprinted Hydrogel Environments," *ACS Applied Materials & Interfaces*, vol. 14, no. 14, 2022, ISSN: 1944-8244, 1944-8252. DOI: 10.1021/acsami.1c20836. (visited on 04/28/2022) (cit. on pp. 2, 22, 23).

[14] L. Yahia, "History and Applications of Hydrogels," *Journal of Biomedical Sciencies*, vol. 04, no. 02, 2015, ISSN: 2254609X. DOI: 10.4172/2254-609X.100013. (visited on 04/13/2022) (cit. on pp. 2, 9–12, 21, 22).

[15] J. L. Martínez, "Short-sighted evolution of bacterial opportunistic pathogens with an environmental origin," *Frontiers in Microbiology*, vol. 5, 2014, ISSN: 1664-302X. DOI: 10.3389/fmicb.2014.00239. (visited on 06/01/2022) (cit. on p. 5).

[16] S. Kleinschmidt, F. Huygens, J. Faoagali, I. U. Rathnayake, and L. M. Hafner, "Staphylococcus epidermidis as a cause of bacteremia," *Future Microbiology*, vol. 10, no. 11, pp. 1859–1879, 2015, ISSN: 1746-0913, 1746-0921. DOI: 10.2217/fmb.15.98. (visited on 04/11/2022) (cit. on pp. 6–9).

[17] M. Sabaté Brescó, L. G. Harris, K. Thompson, B. Stanic, M. Morgenstern, L. O'Mahony, R. G. Richards, and T. F. Moriarty, "Pathogenic Mechanisms and Host Interactions in Staphylococcus epidermidis Device-Related Infection," *Frontiers in Microbiology*, vol. 8, p. 1401, 2017, ISSN: 1664-302X. DOI: 10.3389/fmicb.2017.01401. (visited on 04/11/2022) (cit. on pp. 6–9).

[18] A. E. Namvar, S. Bastarahang, N. Abbasi, G. S. Ghehi, S. Farhadbakhtiarian, P. Arezi, M. Hosseini, S. Z. Baravati, Z. Jokar, and S. G. Chermahin, "Clinical characteristics of Staphylococcus epidermidis: A systematic review," *GMS Hygiene and Infection Control; 9(3):Doc23; ISSN 2196-5226*, 2014. DOI: 10.3205/DGKH000243. (visited on 04/11/2022) (cit. on pp. 6, 8, 9).

[19] M. M. Brown and A. R. Horswill, "Staphylococcus epidermidis—Skin friend or foe?" *PLOS Pathogens*, vol. 16, no. 11, K. A. Kline, Ed., e1009026, 2020, ISSN: 1553-7374. DOI: 10.1371/journal.ppat.1009026. (visited on 04/11/2022) (cit. on pp. 6, 7).

[20] G. Christensen and H. Brüggemann, "Bacterial skin commensals and their role as host guardians," *Beneficial Microbes*, vol. 5, no. 2, pp. 201–215, 2014, ISSN: 1876-2883, 1876-2891. DOI: 10.3920/BM2012.0062. (visited on 04/12/2022) (cit. on p. 8).

[21] A. Sagar, *Staphylococcus Epidermidis - An Overview*, Oct. 2020. [Online]. Available: https://microbenotes.com/staphylococcus-epidermidis/ (cit. on p. 9).

[22] *Biosafety level*, Page Version ID: 1080690513, Apr. 2022. [Online]. Available: https://en.wikipedia.org/w/index.php?title=Biosafety_level&oldid=1080690513 (visited on 04/17/2022) (cit. on p. 9).

[23] F. Ullah, M. B. H. Othman, F. Javed, Z. Ahmad, and H. M. Akil, "Classification, processing and application of hydrogels: A review," *Materials Science and Engineering: C*, vol. 57, pp. 414–433, 2015, ISSN: 09284931. DOI: 10.1016/j.msec.2015.07.053. (visited on 04/13/2022) (cit. on pp. 9, 10, 12).

[24] Y. S. Zhang and A. Khademhosseini, "Advances in engineering hydrogels," *Science*, vol. 356, no. 6337, eaaf3627, 2017, ISSN: 0036-8075, 1095-9203. DOI: 10.1126/science.aaf3627. (visited on 04/13/2022) (cit. on pp. 9–12).

[25] W. A. Laftah, S. Hashim, and A. N. Ibrahim, "Polymer Hydrogels: A Review," *Polymer-Plastics Technology and Engineering*, vol. 50, no. 14, pp. 1475–1486, 2011, ISSN: 0360-2559, 1525-6111. DOI: 10.1080/03602559.2011.593082. (visited on 04/13/2022) (cit. on pp. 10–12).

[26] I. Yazici and O. Okay, "Spatial inhomogeneity in poly(acrylic acid) hydrogels," *Polymer*, vol. 46, no. 8, pp. 2595–2602, 2005, ISSN: 00323861. DOI: 10.1016/j.polymer.2005.01.079. (visited on 06/01/2022) (cit. on p. 10).

[27] M. L. Oyen, "Mechanical characterisation of hydrogel materials," *International Materials Reviews*, vol. 59, no. 1, pp. 44–59, 2014, ISSN: 0950-6608, 1743-2804. DOI: 10.1179/1743280413Y.0000000022. (visited on 04/14/2022) (cit. on pp. 11, 13–15).

[28] A. Singh, P. Sharma, V. Garg, and G. Garg, "Hydrogels: A review," *International Journal of Pharmaceutical Sciences Review and Research*, vol. 4, pp. 97–105, Sep. 2010 (cit. on p. 11).

[29] L. Li, J. M. Scheiger, and P. A. Levkin, "Design and Applications of Photoresponsive Hydrogels," *Advanced Materials*, vol. 31, no. 26, p. 1 807 333, 2019, ISSN: 0935-9648, 1521-4095. DOI: 10.1002/adma.201807333. (visited on 06/01/2022) (cit. on p. 12).

[30] M. Azeera, S. Vaidevi, and K. Ruckmani, "Characterization Techniques of Hydrogel and Its Applications," in *Cellulose-Based Superabsorbent Hydrogels*, M. I. H. Mondal, Ed., Cham: Springer International Publishing, 2018, pp. 1–24, ISBN: 9783319765730. DOI: 10.1007/978-3-319-76573-0_25-1. (visited on 05/02/2022) (cit. on pp. 12, 15).

[31] J. Menczel and R. Prime, *Thermal Analysis of Polymers: Fundamentals and Applications*. Wiley, 2009, ISBN: 9780471769170. [Online]. Available: https://books.google.lu/books?id=qEuQDwAAQBAJ (cit. on pp. 12, 14).

[32] T. K. Meyvis, B. G. Stubbe, M. J. Van Steenbergen, W. E. Hennink, S. C. De Smedt, and J. Demeester, "A comparison between the use of dynamic mechanical analysis and oscillatory shear rheometry for the characterisation of hydrogels," *International Journal of Pharmaceutics*, vol. 244, no. 1-2, pp. 163–168, 2002, ISSN: 03785173. DOI: 10.1016/S0378-5173(02)00328-9. (visited on 04/14/2022) (cit. on pp. 13, 14).

[33] *Young's modulus*, Page Version ID: 1083006359, Apr. 2022. [Online]. Available: https://en.wikipedia.org/w/index.php?title=Young%27s_modulus&oldid=1083006359 (visited on 06/01/2022) (cit. on p. 13).

[34] D. O. Freytes, J. Martin, S. S. Velankar, A. S. Lee, and S. F. Badylak, "Preparation and rheological characterization of a gel form of the porcine urinary bladder matrix," *Biomaterials*, vol. 29, no. 11, pp. 1630–1637, 2008, ISSN: 01429612. DOI: 10.1016/j.biomaterials.2007.12.014. (visited on 05/16/2022) (cit. on p. 13).

[35] S. K. Kaliappan, "Characterization of physical properties of polymers using AFM force-distance curves," Ph.D. dissertation, Universität Siegen, Oct. 2007 (cit. on pp. 13–15).

[36] E. Van Ruymbeke, "LMAPR2019 - Polymer Science and Engineering: Viscoelasticity (Lecture 2) (UCLouvain)," available at: https://moodle.uclouvain.be/pluginfile.php/302947/mod_resource/content/1/Lecture_2_viscoelastic_properties_2021.pdf, 2021 (cit. on pp. 13, 16).

[37] A. Jonas, "LMAPR2019A - Polymer Science and Engineering : Physics (UCLouvain)," 2020 (cit. on p. 14).

[38] S. Carrà, F. Chiozza, F. Curto, and M. Ferraioli, "Rheology to understand operational parameter, as a predictive method to avoid off specifications and maximizing the packaging proce," *Annual transactions of the nordic rheology society*, vol. 23, pp. 135–142, 2015 (cit. on p. 15).

[39] D. K. Baby, "Chapter 9 - Rheology of hydrogels," in *Rheology of Polymer Blends and Nanocomposites*, ser. Micro and Nano Technologies, S. Thomas, C Sarathchandran, and N. Chandran, Eds., Elsevier, 2020, pp. 193–204, ISBN: 978-0-12-816957-5. DOI: 10.1016/B978-0-12-816957-5.00009-4 (cit. on pp. 15, 16).

[40] I. Kwiecień and M. Kwiecień, "Application of Polysaccharide-Based Hydrogels as Probiotic Delivery Systems," *Gels*, vol. 4, no. 2, p. 47, 2018, ISSN: 2310-2861. DOI: 10.3390/gels4020047. (visited on 04/14/2022) (cit. on p. 16).

[41] A. Hayashi, K. Kinoshita, and S. Yasueda, "Studies of the Agarose Gelling System by the Fluorescence Polarization Method. III.," *Polymer Journal*, vol. 12, no. 7, pp. 447–453, 1980, ISSN: 0032-3896, 1349-0540. DOI: 10.1295/polymj.12.447. (visited on 04/14/2022) (cit. on pp. 16, 17).

[42] F. B. A. Descallar and S. Matsukawa, "Change of network structure in agarose gels by aging during storage studied by NMR and electrophoresis," *Carbohydrate Polymers*, vol. 245, 2020, ISSN: 01448617. DOI: 10.1016/j.carbpol.2020.116497. (visited on 04/14/2022) (cit. on pp. 16–19, 21).

[43] P. Serwer, "Agarose gels: Properties and use for electrophoresis," *Electrophoresis*, vol. 4, no. 6, pp. 375–382, 1983, ISSN: 0173-0835, 1522-2683. DOI: 10.1002/elps.1150040602. (visited on 04/14/2022) (cit. on pp. 16–19).

[44] R. Lapasin and S. Pricl, *Rheology of Industrial Polysaccharides: Theory and Applications*. Boston, MA: Springer US, 1995, ISBN: 9781461359159 9781461521853. DOI: 10.1007/978-1-4615-2185-3. (visited on 04/15/2022) (cit. on pp. 16, 17).

[45] N. Ichinose and H. Ura, "Concentration dependence of the sol-gel phase behavior of agarose-water system observed by the optical bubble pressure tensiometry," *Scientific Reports*, vol. 10, no. 1, 2020, ISSN: 2045-2322. DOI: 10.1038/s41598-020-58905-8. (visited on 04/14/2022) (cit. on p. 16).

[46] S. Hjertén, "Agarose as an anticonvection agent in zone electrophoresis," *Biochimica et Biophysica Acta*, vol. 53, no. 3, pp. 514–517, 1961, ISSN: 00063002. DOI: 10.1016/0006-3002(61)90210-4. (visited on 06/01/2022) (cit. on p. 17).

[47] M. Duckworth and W. Yaphe, "The structure of agar," *Carbohydrate Research*, vol. 16, no. 1, pp. 189–197, 1971, ISSN: 00086215. DOI: 10.1016/S0008-6215(00)86113-3. (visited on 04/14/2022) (cit. on pp. 17, 19).

[48] Y. Zhang, X. Fu, D. Duan, J. Xu, and X. Gao, "Preparation and characterization of agar, agarose, and agaropectin from the red alga Ahnfeltia plicata," *Journal of Oceanology and Limnology*, vol. 37, no. 3, pp. 815–824, 2019, ISSN: 2096-5508, 2523-3521. DOI: 10.1007/s00343-019-8129-6. (visited on 05/23/2022) (cit. on p. 17).

[49] Raheem Tabet, *Evaluation Of Agarophytes*, Jan. 2014. [Online]. Available: https://raheemtabet.wordpress.com/2014/01/29/evaluation-of-agarophytes/ (visited on 04/15/2022) (cit. on p. 17).

[50] Lonza, *BenchGuide SourceBook - Appendix B: Agarose Physical Chemistry*. [Online]. Available: https://www.google.com/url?sa=t&rct=j&q=&esrc=s&source=web&cd=&cad=rja&uact=8&ved=2ahUKEwiB06O6nJb3AhWFGuwKHTF3AHoQFnoECAoQAQ&url=http%3A%2F%2Fwww.lonzabio.jp%2Fcatalog%2Fpdf%2Fpd%2FPD029.pdf&usg=AOvVaw3podqdfZa7hmqyAFRw4wP0 (visited on 04/15/2022) (cit. on pp. 18–21).

[51] J. Stellwagen and N. C. Stellwagen, "Internal Structure of the Agarose Gel Matrix," *The Journal of Physical Chemistry*, vol. 99, no. 12, 1995, ISSN: 0022-3654, 1541-5740. DOI: 10.1021/j100012a054. (visited on 04/14/2022) (cit. on p. 18).

[52] M. Ramzi, C. Rochas, and J.-M. Guenet, "Phase Behavior of Agarose in Binary Solvents," *Macromolecules*, vol. 29, no. 13, pp. 4668–4674, 1996, ISSN: 0024-9297, 1520-5835. DOI: 10.1021/ma9600062. (visited on 04/15/2022) (cit. on p. 18).

[53] C. Rochas, A. Brulet, and J.-M. Guenet, "Thermally reversible Gelation of Agarose in Water/Dimethyl Sulfoxide Mixtures," *Macromolecules*, vol. 27, no. 14, pp. 3830–3835, 1994, ISSN: 0024-9297, 1520-5835. DOI: 10.1021/ma00092a023. (visited on 04/15/2022) (cit. on p. 18).

[54] Sigma Aldrich, *Product Information: Agarose*, Mar. 2022. [Online]. Available: https://www.sigmaaldrich.com/deepweb/assets/sigmaaldrich/product/documents/936/001/a9952pis.pdf (cit. on pp. 18, 20, 33, 34).

[55] P. L. Indovina, E. Tettamanti, M. S. Micciancio-Giammarinaro, and M. U. Palma, "Thermal hysteresis and reversibility of gel–sol transition in agarose–water systemsa)," *The Journal of Chemical Physics*, vol. 70, no. 6, pp. 2841–2847, 1979, ISSN: 0021-9606, 1089-7690. DOI: 10.1063/1.437817. (visited on 04/15/2022) (cit. on p. 18).

[56] B. Dai and S. Matsukawa, "Elucidation of gelation mechanism and molecular interactions of agarose in solution by 1H NMR," *Carbohydrate Research*, vol. 365, pp. 38–45, 2013, ISSN: 00086215. DOI: 10.1016/j.carres.2012.10.005. (visited on 04/14/2022) (cit. on pp. 19, 21).

[57] C. Chen, X. Li, D. Zhao, Y. Li, H. Shi, G. Ma, and Z. Su, "Precise control of agarose media pore structure by regulating cooling rate," *Journal of Separation Science*, vol. 40, no. 22, pp. 4467–4474, 2017, ISSN: 16159306. DOI: 10.1002/jssc.201700546. (visited on 04/14/2022) (cit. on p. 19).

[58] M. Ghebremedhin, S. Seiffert, and T. A. Vilgis, "Physics of agarose fluid gels: Rheological properties and microstructure," *Current Research in Food Science*, vol. 4, pp. 436–448, 2021, ISSN: 26659271. DOI: 10.1016/j.crfs.2021.06.003. (visited on 04/15/2022) (cit. on pp. 19–21, 33).

[59] T. Morita, T. Narita, S.-a. Mukai, M. Yanagisawa, and M. Tokita, "Phase behaviors of agarose gel," *AIP Advances*, vol. 3, no. 4, p. 042 128, 2013, ISSN: 2158-3226. DOI: 10.1063/1.4802968. (visited on 04/16/2022) (cit. on p. 19).

[60] M. Bertasa, A. Dodero, M. Alloisio, S. Vicini, C. Riedo, A. Sansonetti, D. Scalarone, and M. Castellano, "Agar gel strength: A correlation study between chemical composition and rheological properties," *European Polymer Journal*, vol. 123, p. 109 442, 2020, ISSN: 00143057. DOI: 10.1016/j.eurpolymj.2019.109442. (visited on 04/16/2022) (cit. on pp. 20, 35, 40).

[61] M. Maaloum, N. Pernodet, and B. Tinland, "Agarose gel structure using atomic force microscopy: Gel concentration and ionic strength effects," *Electrophoresis*, vol. 19, no. 10, pp. 1606–1610, 1998, ISSN: 0173-0835, 1522-2683. DOI: 10.1002/elps.1150191015. (visited on 04/14/2022) (cit. on pp. 20, 21).

[62] P. Zarrintaj, S. Manouchehri, Z. Ahmadi, M. R. Saeb, A. M. Urbanska, D. L. Kaplan, and M. Mozafari, "Agarose-based biomaterials for tissue engineering," *Carbohydrate Polymers*, vol. 187, pp. 66–84, 2018, ISSN: 01448617. DOI: 10.1016/j.carbpol.2018.01.060. (visited on 04/17/2022) (cit. on p. 21).

[63] P. A. H. M. Wijnen and M. P. van Dieijen-Visser, "Capillary Electrophoresis of Serum Proteins. Reproducibility, Comparison with Agarose Gel Electrophoresis and a Review of the Literature," *Clinical Chemistry and Laboratory Medicine*, vol. 34, no. 7, 1996, ISSN: 1434-6621, 1437-4331. DOI: 10.1515/cclm.1996.34.7.535. (visited on 04/17/2022) (cit. on p. 21).

[64] K. D. Cole and B. Åkerman, "The Influence Of Agarose Concentration In Gels On The Electrophoretic Trapping Of Circular Dna," *Separation Science and Technology*, vol. 38, no. 10, pp. 2121–2136, 2003, ISSN: 0149-6395, 1520-5754. DOI: 10.1081/SS-120021616. (visited on 04/14/2022) (cit. on p. 21).

[65] M. Khodadadi Yazdi, A. Taghizadeh, M. Taghizadeh, F. J. Stadler, M. Farokhi, F. Mottaghitalab, P. Zarrintaj, J. D. Ramsey, F. Seidi, M. R. Saeb, and M. Mozafari, "Agarose-based biomaterials for advanced drug delivery," *Journal of Controlled Release*, vol. 326, pp. 523–543, 2020, ISSN: 01683659. DOI: 10.1016/j.jconrel.2020.07.028. (visited on 04/17/2022) (cit. on p. 21).

[66] M. Rinaudo, "Main properties and current applications of some polysaccharides as biomaterials," *Polymer International*, vol. 57, no. 3, pp. 397–430, 2008, ISSN: 09598103, 10970126. DOI: 10.1002/pi.2378. (visited on 04/17/2022) (cit. on p. 22).

[67] M. Lufton, O. Bustan, B.-h. Eylon, E. Shtifman-Segal, T. Croitoru-Sadger, A. Shagan, A. Shabtay-Orbach, E. Corem-Salkmon, J. Berman, A. Nyska, and B. Mizrahi, "Living Bacteria in Thermoresponsive Gel for Treating Fungal Infections," *Advanced Functional Materials*, vol. 28, no. 40, 2018, ISSN: 1616301X. DOI: 10.1002/adfm.201801581. (visited on 04/28/2022) (cit. on p. 22).

[68] Y. Dong, Z. Zhang, Y.-Y. Deng, and Y. Wang, "Immobilization of Nitrifying Bacteria in Waterborne Polyurethane Hydrogel for Removal of Ammonium Nitrogen from Wastewater," in *2009 3rd International Conference on Bioinformatics and Biomedical Engineering*, 2009, pp. 1–4. DOI: 10.1109/ICBBE.2009.5162924 (cit. on p. 22).

[69] E. J. Stewart, M. Ganesan, J. G. Younger, and M. J. Solomon, "Artificial biofilms establish the role of matrix interactions in staphylococcal biofilm assembly and disassembly," *Scientific Reports*, vol. 5, no. 1, 2015, ISSN: 2045-2322. DOI: 10.1038/srep13081. (visited on 04/27/2022) (cit. on p. 22).

[70] C. Bienaimé, J.-N. Barbotin, and J.-E. Nava-Saucedo, "How to build an adapted and bioactive cell microenvironment? A chemical interaction study of the structure of Ca-alginate matrices and their repercussion on confined cells: Adapted and Bioactive Cell Microenvironment," *Journal of Biomedical Materials Research Part A*, vol. 67A, no. 2, pp. 376–388, 2003, ISSN: 15493296. DOI: 10.1002/jbm.a.10487. (visited on 04/27/2022) (cit. on p. 22).

[71] J. P. Park, M. Do, S. H. Hong, J. Ryu, D. Kang, K. Rho, J. H. Ahn, and H. Lee, "BIOMOSAIC Film: Artificial Biofilms with Catalytic and Self-Sealing Properties," *Advanced Materials Interfaces*, vol. 6, no. 18, 2019, ISSN: 2196-7350, 2196-7350. DOI: 10.1002/admi.201900379. (visited on 04/27/2022) (cit. on pp. 22, 23).

[72] T. R. Garrett, M. Bhakoo, and Z. Zhang, "Bacterial adhesion and biofilms on surfaces," *Progress in Natural Science*, vol. 18, no. 9, pp. 1049–1056, 2008, ISSN: 10020071. DOI: 10.1016/j.pnsc.2008.04.001. (visited on 04/27/2022) (cit. on pp. 22, 23).

[73] M. Strathmann, T. Griebe, and H.-C. Flemming, "Agarose hydrogels as EPS models," *Water Science and Technology*, vol. 43, no. 6, pp. 169–175, 2001, ISSN: 0273-1223, 1996-9732. DOI: 10.2166/wst.2001.0367. (visited on 06/03/2022) (cit. on pp. 22, 23).

[74] V. Kostenko, H. Ceri, and R. J. Martinuzzi, "Increased tolerance of *Staphylococcus aureus* to vancomycin in viscous media," *FEMS Immunology & Medical Microbiology*, vol. 51, no. 2, pp. 277–288, 2007, ISSN: 09288244, 1574695X. DOI: 10.1111/j.1574-695X.2007.00300.x. (visited on 04/28/2022) (cit. on pp. 22–24).

[75] B. Pabst, B. Pitts, E. Lauchnor, and P. S. Stewart, "Gel-Entrapped Staphylococcus aureus Bacteria as Models of Biofilm Infection Exhibit Growth in Dense Aggregates, Oxygen Limitation, Antibiotic Tolerance, and Heterogeneous Gene Expression," *Antimicrobial Agents and Chemotherapy*, vol. 60, no. 10, pp. 6294–6301, 2016, ISSN: 0066-4804, 1098-6596. DOI: 10.1128/AAC.01336-16. (visited on 04/27/2022) (cit. on p. 22).

[76] P. Serwer, B. Hunter, and E. T. Wright, "Cell–gel interactions of in-gel propagating bacteria," *BMC Research Notes*, vol. 11, no. 1, p. 699, 2018, ISSN: 1756-0500. DOI: 10.1186/s13104-018-3811-x. (visited on 04/27/2022) (cit. on pp. 22, 23, 71).

[77] M. Strathmann, T. Griebe, and H.-C. Flemming, "Artificial biofilm model - a useful tool for biofilm research," *Applied Microbiology and Biotechnology*, vol. 54, no. 2, pp. 231–237, 2000, ISSN: 0175-7598, 1432-0614. DOI: 10.1007/s002530000370. (visited on 04/27/2022) (cit. on p. 22).

[78] H. H. Tuson, L. D. Renner, and D. B. Weibel, "Polyacrylamide hydrogels as substrates for studying bacteria," *Chem. Commun.*, vol. 48, no. 10, pp. 1595–1597, 2012, ISSN: 1359-7345, 1364-548X. DOI: 10.1039/C1CC14705F. (visited on 04/28/2022) (cit. on pp. 22, 23, 70, 71).

[79] M. C. Gutiérrez, Z. Y. García-Carvajal, M. Jobbágy, L. Yuste, F. Rojo, C. Abrusci, F. Catalina, F. del Monte, and M. L. Ferrer, "Hydrogel Scaffolds with Immobilized Bacteria for 3D Cultures," *Chemistry of Materials*, vol. 19, no. 8, pp. 1968–1973, 2007, ISSN: 0897-4756, 1520-5002. DOI: 10.1021/cm062882s. (visited on 04/27/2022) (cit. on p. 22).

[80] Z. Ming, L. Han, M. Bao, H. Zhu, S. Qiang, S. Xue, and W. Liu, "Living Bacterial Hydrogels for Accelerated Infected Wound Healing," *Advanced Science*, vol. 8, no. 24, 2021, ISSN: 2198-3844, 2198-3844. DOI: 10.1002/advs.202102545. (visited on 04/27/2022) (cit. on p. 22).

[81] E. Zhao, H. Liu, Y. Jia, T. Xiao, J. Li, G. Zhou, J. Wang, X. Zhou, X.-J. Liang, J. Zhang, and Z. Li, "Engineering a photosynthetic bacteria-incorporated hydrogel for infected wound healing," *Acta Biomaterialia*, vol. 140, pp. 302–313, 2022, ISSN: 17427061. DOI: 10.1016/j.actbio.2021.12.017. (visited on 04/28/2022) (cit. on p. 22).

[82] J. Blacutt, Z. Lan, E. M. Cosgriff-Hernandez, and V. D. Gordon, "Quantitative confocal microscopy and calibration for measuring differences in cyclic-di-GMP signalling by bacteria on biomedical hydrogels," *Royal Society Open Science*, vol. 8, no. 1, p. 201 453, 2021, ISSN: 2054-5703. DOI: 10.1098/rsos.201453. (visited on 04/28/2022) (cit. on pp. 22–24).

[83] N. Kandemir, W. Vollmer, N. S. Jakubovics, and J. Chen, "Mechanical interactions between bacteria and hydrogels," *Scientific Reports*, vol. 8, no. 1, p. 10 893, 2018, ISSN: 2045-2322. DOI: 10.1038/s41598-018-29269-x. (visited on 04/27/2022) (cit. on pp. 22, 23).

[84] H. H. Tuson and D. B. Weibel, "Bacteria–surface interactions," *Soft Matter*, vol. 9, no. 17, p. 4368, 2013, ISSN: 1744-683X, 1744-6848. DOI: 10.1039/c3sm27705d. (visited on 04/27/2022) (cit. on pp. 22, 70, 71).

[85] T. Huq, A. Khan, R. A. Khan, B. Riedl, and M. Lacroix, "Encapsulation of Probiotic Bacteria in Biopolymeric System," *Critical Reviews in Food Science and Nutrition*, vol. 53, no. 9, pp. 909–916, 2013, ISSN: 1040-8398, 1549-7852. DOI: 10.1080/10408398.2011.573152. (visited on 04/27/2022) (cit. on p. 22).

[86] P. Stewart, L. Grab, and J. Diemer, "Analysis of biocide transport limitation in an artificial biofilm system," *Journal of Applied Microbiology*, vol. 85, no. 3, pp. 495–500, 1998, ISSN: 1364-5072, 1365-2672. DOI: 10.1046/j.1365-2672.1998.853529.x. (visited on 04/30/2022) (cit. on p. 23).

[87] K. M. Salli and A. C. Ouwehand, "The use of in vitro model systems to study dental biofilms associated with caries: A short review," *Journal of Oral Microbiology*, vol. 7, no. 1, 2015, ISSN: null. DOI: 10.3402/jom.v7.26149. (visited on 04/30/2022) (cit. on p. 23).

[88] K. Rasmussen and K. Østgaard, "Adhesion of the marine bacterium Pseudomonas sp. NCIMB 2021 to different hydrogel surfaces," *Water Research*, vol. 37, no. 3, pp. 519–524, 2003, ISSN: 00431354. DOI: 10.1016/S0043-1354(02)00306-8. (visited on 04/27/2022) (cit. on p. 23).

[89] A. Krumm, *Measure microbial growth using the „OD600"*. [Online]. Available: https://www.bmglabtech.com/measure-microbial-growth-using-the-od600/ (visited on 05/02/2022) (cit. on pp. 24–26).

[90] F. Widdel, "Theory and measurement of bacterial growth," *Di dalam Grundpraktikum Mikrobiologie*, vol. 4, no. 11, pp. 1–11, 2007 (cit. on pp. 24, 25).

[91] Orbit Biotech, *Bacterial growth curve*, en-US, Apr. 2018. [Online]. Available: https://orbitbiotech.com/bacterial-growth-curve-generation-time-lag-phase-log-phase-exponential-phase-decline-phase/ (visited on 05/02/2022) (cit. on p. 25).

[92] *Nephelometer*, Page Version ID: 1082723323, Apr. 2022. [Online]. Available: https://en.wikipedia.org/w/index.php?title=Nephelometer&oldid=1082723323 (visited on 05/03/2022) (cit. on p. 26).

[93] *Nephelometry (medicine)*, Page Version ID: 1071081099, Feb. 2022. [Online]. Available: https://en.wikipedia.org/w/index.php?title=Nephelometry_(medicine)&oldid=1071081099 (visited on 05/03/2022) (cit. on p. 26).

[94] K. K. Jefferson, "What drives bacteria to produce a biofilm?" *FEMS Microbiology Letters*, vol. 236, no. 2, pp. 163–173, 2004, ISSN: 03781097. DOI: 10.1111/j.1574-6968.2004.tb09643.x. (visited on 05/13/2022) (cit. on pp. 26, 70).

[95] E. Hernández-Jiménez, R. del Campo, V. Toledano, M. T. Vallejo-Cremades, A. Muñoz, C. Largo, F. Arnalich, F. García-Rio, C. Cubillos-Zapata, and E. López-Collazo, "Biofilm vs. planktonic bacterial mode of growth: Which do human macrophages prefer?" *Biochemical and Biophysical Research Communications*, vol. 441, no. 4, pp. 947–952, 2013, ISSN: 0006291X. DOI: 10.1016/j.bbrc.2013.11.012. (visited on 05/12/2022) (cit. on pp. 26, 70).

[96] P. N. Skandamis and S. Jeanson, "Colonial vs. planktonic type of growth: Mathematical modeling of microbial dynamics on surfaces and in liquid, semi-liquid and solid foods," *Frontiers in Microbiology*, vol. 6, 2015, ISSN: 1664-302X. DOI: 10.3389/fmicb.2015.01178. (visited on 05/12/2022) (cit. on p. 26).

[97] C. D. Hickey, J. J. Sheehan, M. G. Wilkinson, and M. A. E. Auty, "Growth and location of bacterial colonies within dairy foods using microscopy techniques: A review," *Frontiers in Microbiology*, vol. 6, 2015, ISSN: 1664-302X. DOI: 10.3389/fmicb.2015.00099. (visited on 05/13/2022) (cit. on p. 26).

[98] R. Zimmermann, "Estimation of Bacterial Number and Biomass by Epifluorescence Microscopy and Scanning Electron Microscopy," in *Microbial Ecology of a Brackish Water Environment*, W. D. Billings, F. Golley, O. L. Lange, J. S. Olson, and G. Rheinheimer, Eds., vol. 25, Berlin, Heidelberg: Springer Berlin Heidelberg, 1977, pp. 103–120, ISBN: 9783642667930 9783642667916. DOI: 10.1007/978-3-642-66791-6_10. (visited on 05/13/2022) (cit. on p. 26).

[99] *Fluorescence microscope*, Page Version ID: 1071543912, Feb. 2022. [Online]. Available: https://en.wikipedia.org/w/index.php?title=Fluorescence_microscope&oldid=1071543912 (visited on 05/13/2022) (cit. on pp. 26, 27).

[100] J. W. Lichtman and J.-A. Conchello, "Fluorescence microscopy," *Nature Methods*, vol. 2, no. 12, pp. 910–919, 2005, ISSN: 1548-7091, 1548-7105. DOI: 10.1038/nmeth817. (visited on 05/13/2022) (cit. on pp. 26, 27).

[101] D. J. Webb and C. M. Brown, "Epi-Fluorescence Microscopy," in *Cell Imaging Techniques*, D. J. Taatjes and J. Roth, Eds., vol. 931, Totowa, NJ: Humana Press, 2012, pp. 29–59, ISBN: 9781627030557 9781627030564. DOI: 10.1007/978-1-62703-056-4_2. (visited on 05/13/2022) (cit. on pp. 26, 27).

[102] ThermoFisher, *Epifluorescence Microscope Basics - US*. [Online]. Available: //www.thermofisher.com/us/en/home/life-science/cell-analysis/cell-analysis-learning-center/molecular-probes-school-of-fluorescence/imaging-basics/fundamentals-of-fluorescence-microscopy/epifluorescence-microscope-basics.html (visited on 05/13/2022) (cit. on p. 27).

[103] A. D. Elliott, "Confocal Microscopy: Principles and Modern Practices," *Current Protocols in Cytometry*, vol. 92, no. 1, 2020, ISSN: 1934-9297, 1934-9300. DOI: 10.1002/cpcy.68. (visited on 05/13/2022) (cit. on pp. 27, 55).

[104] *Confocal microscopy*, Page Version ID: 1086309029, May 2022. [Online]. Available: https://en.wikipedia.org/w/index.php?title=Confocal_microscopy&oldid=1086309029 (visited on 05/13/2022) (cit. on p. 27).

[105] F. Mokobi, *Confocal Microscope- Definition, Principle, Parts, Types, Labeled Diagram, Applications*, Nov. 2021. [Online]. Available: https://microbenotes.com/confocal-microscope/ (visited on 05/13/2022) (cit. on p. 27).

[106] Eastern Cereal and Oilseed Research Centre, M. Kaláb, A.-F. Yang, and D. Chabot, "Conventional Scanning Electron Microscopy of Bacteria," *infocus Magazine*, pp. 42–61, 2008, ISSN: 17504740. DOI: 10.22443/rms.inf.1.33. (visited on 05/14/2022) (cit. on pp. 27, 28).

[107] *Scanning electron microscope*, Page Version ID: 1087145870, May 2022. [Online]. Available: https://en.wikipedia.org/w/index.php?title=Scanning_electron_microscope&oldid=1087145870 (visited on 05/13/2022) (cit. on p. 28).

[108] D Fotiadis, "Imaging and manipulation of biological structures with the AFM," *Micron*, vol. 33, no. 4, pp. 385–397, 2002, ISSN: 09684328. DOI: 10.1016/S0968-4328(01)00026-9. (visited on 06/01/2022) (cit. on p. 28).

[109] M. E. Núñez, M. O. Martin, P. H. Chan, L. K. Duong, A. R. Sindhurakar, and E. M. Spain, "Atomic Force Microscopy of Bacterial Communities," in *Methods in Enzymology*, vol. 397, Elsevier, 2005, pp. 256–268, ISBN: 9780121828028. DOI: 10.1016/S0076-6879(05)97015-8. (visited on 06/01/2022) (cit. on p. 28).

[110] Y. Dufrêne, "LBRNA2202-Nanobiotechnologies: Lecture Slides (UCLouvain)," 2021 (cit. on p. 28).

[111] A. Villarino, O. M. Bouvet, B. Regnault, S. Martin-Delautre, and P. A. Grimont, "Exploring the frontier between life and death in Escherichia coli: Evaluation of different viability markers in liveand heat- or UV-killed cells," *Research in Microbiology*, vol. 151, no. 9, pp. 755–768, 2000, ISSN: 09232508. DOI: 10.1016/S0923-2508(00)01141-4. (visited on 05/11/2022) (cit. on p. 29).

[112] ThermoFisher, *LIVE/DEAD® BacLight Bacterial Viability Kits - Product information*, 2004 (cit. on p. 29).

[113] ——, *BacLightTM RedoxSensorTM CTC Vitality Kit - Product Information*, 2005 (cit. on p. 29).

[114] N. Parthuisot, P. Catala, K. Lemarchand, J. Baudart, and P. Lebaron, "Evaluation of ChemChrome V6 for bacterial viability assessment in waters," *Journal of Applied Microbiology*, vol. 89, no. 2, pp. 370–380, 2000, ISSN: 1364-5072, 1365-2672. DOI: 10.1046/j.1365-2672.2000.01126.x. (visited on 05/11/2022) (cit. on p. 29).

[115] ThermoFisher, *alamarBlue Assay - product Sheet* (cit. on p. 30).

[116] J. O'Brien, I. Wilson, T. Orton, and F. Pognan, "Investigation of the Alamar Blue (resazurin) fluorescent dye for the assessment of mammalian cell cytotoxicity: Resazurin as a cytotoxicity assay," *European Journal of Biochemistry*, vol. 267, no. 17, pp. 5421–5426, 2000, ISSN: 00142956. DOI: 10.1046/j.1432-1327.2000.01606.x. (visited on 05/11/2022) (cit. on p. 30).

[117] H. A. Barnes, "A review of the slip (wall depletion) of polymer solutions, emulsions and particle suspensions in viscometers: Its cause, character, and cure," *Journal of Non-Newtonian Fluid Mechanics*, vol. 56, no. 3, pp. 221–251, 1995, ISSN: 03770257. DOI: 10.1016/0377-0257(94)01282-M. (visited on 05/16/2022) (cit. on p. 36).

[118] Mettler Toledo, *STARe thermal analysis system, operating instructions to the DMA/SDTA861e module*. CH-8630 Schwerzenbach, Switzerland: Mettler Toledo, 2005. [Online]. Available: https://manualzz.com/doc/27672168/dma-861-manual (cit. on pp. 37, 38).

[119] *8 Well chambered cover Glass with #1.5 high performance cover glass | Cellvis*. [Online]. Available: https://www.cellvis.com/_8-well-chambered-cover-glass-with-number-1.5-high-performance-cover-glass_/product_detail.php?product_id=60 (visited on 06/01/2022) (cit. on p. 55).

UNIVERSITÉ CATHOLIQUE DE LOUVAIN
École polytechnique de Louvain
Rue Archimède, 1 bte L6.11.01, 1348 Louvain-la-Neuve, Belgique | **www.uclouvain.be/epl**